Universidad de Navarra

Facultad de Ciencias

Effect of hypoxia on caveolin-1 expression, caveolae structure and insulin signaling

Maider Varela Guruceaga

Universidad de Navarra

Facultad de Ciencias

Effect of hypoxia on caveolin-1 expression, caveolae structure and insulin signaling

Memoria presentada por Dª Maider Varela Guruceaga para aspirar al grado de Doctor por la Universidad de Navarra.

El presente trabajo ha sido realizado bajo nuestra dirección en el Departamento de Bioquímica y Genética y autorizo su presentación ante el Tribunal que lo ha de juzgar.

Pamplona, 12 de diciembre de 2016.

Dr. Carlos de Miguel Vázquez

Dr. Fermín Milagro Yoldi

Este trabajo ha sido realizado gracias a la financiación de la Asociación de Amigos de la Universidad de Navarra (Beca predoctoral 2012-2016) además de la Línea Especial de “Nutrition, Obesity and Health” de la Universidad de Navarra (LE/97) y los proyectos CIBERobn y Nutrigenio (Ref. AGL2013-45554-R, MINECO, Gobierno de España)

“Hermoso es lo que vemos. Más hermoso es lo que sabemos.
Pero mucho más hermoso es lo que no conocemos”

Niels Steensen

“Beautiful is what we see. More beautiful is what we know. But
much more beautiful is what we do not know”

Niels Steensen

A mis padres

A mis hermanas

A mis abuelos

A Diego

AKNOWLEDGMENTS

Me parece increíble éste momento. ¡Estoy acabando mi tesis! Nunca olvidaré cuando empecé mi carrera en Venezuela y admiraba a los estudiantes de doctorado que más tarde se convirtieron en mi modelo a seguir. Han sido muchos los que han apoyado y compartido conmigo este camino duro, pero también lleno de experiencias increíbles que me han hecho crecer y ser mejor persona y profesional.

En primer lugar, agradezco a la Universidad de Navarra y a la Facultad de Ciencias por abrirme sus puertas y darme la oportunidad de hacer el máster y posteriormente el doctorado en ella. Ha sido una gran experiencia que me ha fortalecido mucho, con lo cual, ¡muchas gracias!

Muchas gracias a la Asociación de Amigos de la Universidad de Navarra, por depositar su confianza en mí y concederme la beca pre-doctoral para la realización de este trabajo. Sin duda alguna hubiese sido imposible llevarlo a cabo sin su apoyo. Por otro lado, tengo que agradecer a la EMBO por concederme la beca que me permitió realizar mi estancia en el extranjero y poder optar al doctorado internacional.

A mis directores de tesis, el Dr. Carlos de Miguel y el Dr. Fermín Milagro. A ustedes les debo un agradecimiento especial por aceptarme en su grupo para llevar a cabo este trabajo y cumplir este gran objetivo profesional. Gracias por dirigir este trabajo y siempre plantearme retos que me han enseñado a ser independiente en mi trabajo y desarrollar mi criterio científico. Sé que son herramientas, sin duda, indispensables para mi futuro próximo. Gracias Carlos por siempre estar disponible para mí, por tu comprensión y por preocuparte por mí en todos los buenos y malos momentos de la tesis y también personales a lo largo de estos años. Gracias Fermín por tu increíble apoyo, por venir siempre a buscarme con una solución o unas palabras de aliento para continuar trabajando cuando me he sentido perdida y frustrada. Muchas gracias a los dos por escuchar mis opiniones y mis ideas, sé que a veces he sido demasiado insistente, pero les aseguro que siempre ha sido con las ganas de mejorar el trabajo.

Gracias a todos los que forman parte del departamento de Bioquímica y Genética por acogerme tan bien desde el primer día. A los profesores: María Jesús Lopez Zabalza, Juan José Martinez Irujo, Eduardo Ansorena, Guillermo Zalba, María Iraburu y Silvia Cenoz. A Marijose y a los que son o han sido doctorandos durante estos años, Aitor, Javier, Alvaro, Antonia, Sara, todos los alumnos de TFG y másteres. Realmente han hecho que me sintiera como en casa desde que llegue del otro lado del mundo. Muchas gracias a todos por los momentos compartidos a lo largo de este trabajo y por amenizar este proceso.

Esta tesis me deja también grandes amistades para toda la vida. Gracias a los que se han convertido en mi segunda familia. María Martínez, no hay palabras suficientes para darte las gracias por todo lo que hemos vivido juntas. Gracias por tu apoyo

incondicional tanto a nivel técnico como personal. Por tu gran energía y positivismo. Es lo que sin duda necesita todo doctorado durante la tesis. No sé qué hubiese hecho sin ti. A Marina, por ser mi ejemplo profesional, por escucharme siempre con atención y poder tener discusiones científicas de nivel, por tus increíbles gastro-consejos y por ayudarme a descubrir esta hermosa ciudad que se ha convertido en mi hogar. Sin duda tu amistad es una de las mejores cosas que me deja este trabajo. A Ali, porque a pesar de que estuviste poco tiempo en el departamento, dejaste tu gran huella. Muchas gracias por ser mi amiga y espero poder verte más a menudo. A Gabriel, porque realmente has sido mi colega latino en este proceso de hacer la tesis. Por tus consejos científicos y no científicos y por ayudarme a desahogar todos los momentos no tan buenos. No sabes cuanta ayuda me has dado. Después de esto, te espera una visita por Estocolmo. A Amaia, por darme un ejemplo de valentía, fortaleza e integridad que a este mundo le viene tan bien, por escucharme siempre. Te mereces una gran tesis y estoy segura de que lo vas a conseguir. Mucho ánimo para lo que te queda, no es fácil, pero ten presente que después de superar esto, seguro que podemos con todo. A Paulo, por tu gran apoyo para muchos experimentos, por siempre mostrarte tan colaborador y por tu amistad en estos años de doctorado. Te deseo muchísima suerte en la recta final y que logres lo que te propongas. ¡¡Mil gracias familia!! Espero que no pase mucho tiempo hasta que podamos reencontrarnos todos con una buena copa de vino por estas calles.

I have to write a special thanks to all the people who work on *Le laboratoire Stress oxydant et pathologies métaboliques* (SOPAM). A big thanks to Dr. Soazig Le Lay, for your confidence on my work, for your closeness and for giving me the amazing opportunity to stay at your lab and to learn from a great researcher like you. Thanks to the heads of the lab, Dr. Ramaroson Andriantsitohaina and Dr. Maria del Carmen Martinez and all the Ph.D students, engineer and other staff for accepting me and make me feel like one of you. It has been an important and productive experience about scientific collaboration and reminds me how much I enjoy this work. Thank you very much!

Gracias a mi segundo departamento, ciencias de la alimentación y fisiología, por ser tan majos y acogerme siempre como una más. Agradezco especialmente al Dr. Alfredo Martinez Hernandez por permitirme formar parte del Centro de Investigación en Nutrición. A todos los demás miembros del centro porque, aunque es verdad que trabajamos en espacios diferentes, eso no fue un problema para que me brindaran ayuda o simplemente un "¿qué tal vas?". Especialmente quiero agradecer a Ana Lorente, por la paciencia que has tenido enseñándome los entresijos del ChIP y compartiendo mucho la frustración que conlleva muchas veces trabajar con mis adipocitos dándome ánimos y mostrando siempre una sonrisa.

Quiero agradecer también a los que me inspiraron para conseguir esta meta, al laboratorio de neuropéptidos. A la Dra. Anita Stern, por enseñarme que la búsqueda

del saber es uno de los oficios más bonitos y esenciales para el desarrollo de una sociedad y la clave para un futuro mejor. A la Dra. Chary por mostrarme el lado amable y positivo de dedicarle tantas horas y esfuerzo a este trabajo. Al Dr. Carlos Ciangherotti, gracias porque siempre creíste en mí y por enseñarme a que siempre puedes hacer un mejor trabajo. Gracias porque sin ustedes, no hubiese descubierto esta profesión que tanto me gusta y que me ha traído tantas cosas buenas.

Gracias a los mejores roomates del mundo mundial. A Santi por tu infinita paciencia escuchando toda clase de problemas con el western blot aunque no entendieras del todo y A Marcos por tu apoyo técnico y ayudarme en momentos de estrés. Quiero que sepan que siempre lo he apreciado mucho y que han sido grandes amigos.

Por último, pero no menos importante, quiero darle gracias infinitas a mi familia, porque sin ellos hubiese sido imposible llegar hasta aquí.

Gracias a mi familia de Portalondo, su apoyo ha sido incalculable para mí. No hay forma de que yo pueda devolverles toda su ayuda. Gracias por recibirme como un miembro más de la familia sin siquiera conocerme. Por estar siempre ahí, sobre todo en los inicios, cuando me sentía desubicada en un lugar que no era el mío, ustedes estuvieron ahí para hacerme sentir como en casa de amama. Debo de dar un agradecimiento muy especial a Arantza y a Gurutz porque su apoyo y preocupación fue muchas veces fundamental no sólo al inicio, sino también al final de toda esta etapa. Por el apoyo que también le han dado a mi familia en este momento tan crítico. No tengo mucho más que estas palabras para darles las gracias infinitas por todo.

Como no agradecer a mis padres, a quienes va dedicada esta tesis porque sin lugar a dudas, este trabajo hubiese sido impensable si ustedes no hubiesen buscado siempre el mejor futuro para mí. Especial agradecimiento a mi mamá, porque has estado para apoyarme en todos los momentos de mi vida y este no ha sido la excepción. Por resistir como una campeona tantos años de infinita distancia y diferencia horaria. A amama y aitona, otras personas fundamentales para todos mis avances y logros en esta vida. ¡Ustedes son mis segundos padres! Y por eso esta tesis lleva también su nombre. A mis increíbles hermanas, porque creo que tengo a las mejores!. Porque las dos son un ejemplo a seguir de esfuerzo, trabajo duro y fortaleza. Gracias Karenina por emocionarte siempre por mis aciertos y defenderme y apoyarme en los desaciertos. Gracias Vicky, porque tu apoyo, sobretodo en esta recta final ha sido incalculable para mí. No se preocupen chicas que algún día seremos muy grandes. De eso no tengo ninguna duda.

Este último párrafo quiero dedicárselo a mi fiel compañero en todo este trabajo, a mi chico, mi mejor amigo, mi mejor consejero, mi científico favorito, mi vida entera. Sólo tú sabes bien lo que he trabajado por esto, y por todos los buenos y malos momentos que he pasado. Nunca me imaginé que la decisión de cruzar el charco por perseguir una gran meta me iba a conducir además a conocer a la persona con la que espero

construir un gran futuro. Gracias por hacer de estos años de trabajo una emocionante y hermosa aventura que volvería a repetir a tu lado sin pensarlo. ¡Te amo!

A todos los que he nombrado y a los que no, ¡GRACIAS TOTALES!

LIST OF ABBREVIATIONS

Adipoq	Adiponectin
ARNT	Aryl hydrocarbon nuclear translocator
AS160	Akt substrate of 160 kDa
BCA	Bicinchoninic acid
BMI	Body mass index
C/EBP	CCAAT/enhancer binding proteins
Cav-1	Caveolin-1
Cav-2	Caveolin-2
Cav-3	Caveolin-3
CBS	Calf bovine serum
COPD	Chronic obstructive pulmonary disease
COX-1	Cyclooxygenase-1
CSD	Caveolin scaffolding domain
ChIP	Chromatin immunoprecipitation
Dex	Dexamethasone
DPBS	Dulbecco's Phosphate-Buffered Saline
EGF	Epidermal growth factor
EHD2	EH-domain containing 2
EM	Electron microscopy
EMSA	Electrophoretic mobility shift assay
Eno2	Enolase-2
eNOS	Endothelial nitric oxide synthase
FBS	Fetal bovine serum
FFA	Free fatty acid
FRET	Fluorescence energy transfer
GDP	Guanosine diphosphate
GH	Growth hormone
Ghrh	Growth hormone releasing hormone
GLUT1	Glucose transporter type 1
GLUT3	Glucose transporter type 3

GLUT4	Glucose transporter type 4
GSVs	GLUT4 storage vesicles
GTP	Guanosine triphosphate
HAoEC	Human aortic endothelial cells
HES	Drosophila hairy/Enhancer of split
HIF-1	Hypoxia inducible factor-1
HRE	Hypoxia response element
IBMX	Isobutilmethylxanthine
IGF-1	Insulin-like growth factor-1
IGF-1R	Insulin-like growth factor 1 receptor
IF	Immunofluorescence
IH	Intermittent hypoxia
IL-6	Interleukin-6
IL-8	Interleukin-8
IR	Insulin receptor
IRβ	Beta subunit of insulin receptor
IRE1	Inositol-requiring protein 1
IRS-1	Insulin receptor substrate 1
LPL	Lipoprotein lipase
MCP-1	Monocyte chemoattractant protein-1
MIF	Macrophage migration inhibitory factor
MMP2	Matrix metalloproteinase-2
mTOR	Mammalian target of rapamycin
MURC	Muscle related coiled-coil protein
NO	Nitric oxide
NRF-1	Nuclear respiratory factor 1
ORO	Oil red O
OSA	Obstructive sleep apnea
PAI-1	Plasminogen activator inhibitor-1
PBS	Phosphate-buffered saline
PDK-1	3-phosphoinositide dependent protein kinase-1

PERK	Protein kinase RNA-like endoplasmic reticulum kinase
PGC-1α	Peroxisome proliferator-activated receptor gamma coactivator 1-α
PHD	Prolyl hydroxylases
PI3K	Phosphoinositide-dependent kinase-1
Pik3r1	Phosphoinositide-3-kinase regulatory subunit 1
Pik3r3	Phosphoinositide-3-kinase regulatory subunit 3
PIP2	Phosphatidylinositol-4,5- bisphosphate
PIP3	Phosphatidylinositol-3,4,5- trisphosphate
PKB/Akt	Protein kinase B
PMSF	Phenylmethanesulfonyl fluoride
PPARγ	Peroxisome proliferator-activated Receptor γ
PTRF	Polymerase I and transcript release factor
q.s.	"quantum sufficit"/quantity required
RT-PCR	Real-Time Polymerase Chain Reaction
SA-β-gal	Senescence-associated beta-galactosidase
SDPR	Serum deprivation response
SDS-PAGE	Sodium dodecyl sulfate polyacrylamide gel electrophoresis
SOD	Superoxide dismutase
Sort1	Sortilin-1
SRBC	Sdr-related gene product that binds to c-kinase
TNF-α	Tumor necrosis factor-α
TSS	Transcription starting site
UPR	Unfolded protein response
VEGF	Vascular endothelial growth factor
VHL	Von Hippel-Lindau protein
WHO	World Health Organization
Xbp1	X-box binding protein

TABLE OF CONTENTS

INTRODUCTION

INTRODUCTION

1. Obesity

1.1. Definition

World Health Organization (WHO) defines obesity as abnormal or excessive fat accumulation being usually estimated by body mass index (BMI), which is the ratio of weight over height expressed in kilograms per square meter (Després, 2012). The excessive fat accumulation is often produced by an imbalance between the food intake and the energy expenditure due to detrimental lifestyle changes, and it could be influenced by genetic and epigenetic predisposition (Hurt et al., 2011; Sellayah et al., 2014; Speakman, 2013).

1.2. Prevalence

Obesity is recognized as a growing public health problem in both, developed and developing countries (Speakman, 2013), and is a causal factor in a number of metabolic and endocrine disorders, including metabolic syndrome, cardiovascular disease, type 2 diabetes, bone and joint dysfunctions, and some forms of cancer (Sellayah et al., 2014). The worldwide prevalence of obesity nearly doubled between 1980 and 2008 (Barja-Fernández et al., 2014). In 2014, 39% of adults were overweight and 13% were obese, which has driven WHO to consider obesity the world epidemic of 21st century (Barja-Fernández et al., 2014).

When fat accumulation is excessive, a large number of associated comorbidities are developed (i.e., type 2 diabetes, obstructive sleep apnea, hypertension, atherosclerosis and hyperlipidemias), increasing morbidity and mortality (Sellayah et al., 2014; Wells, 2012; Williams et al., 2015). In fact, obesity and its related health problems represent an important burden to the healthcare system worldwide. Recent estimation calculated that roughly $150 billion are spent per year as a direct consequence of this disease together with the social impact and emotional distress associated (Sellayah et al., 2014; Wyatt et al., 2006).

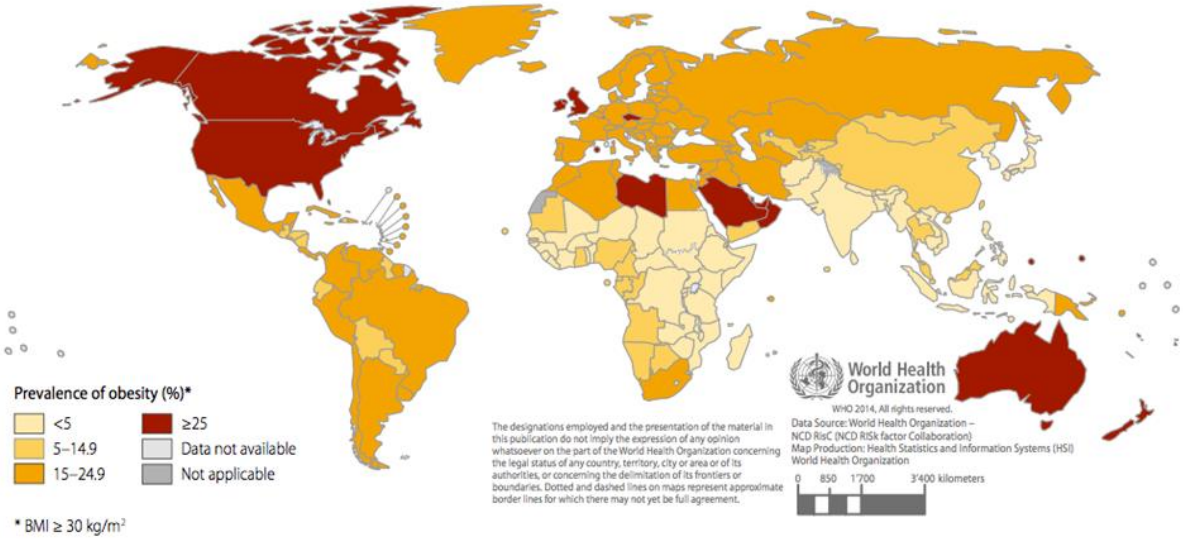

Figure I1. Age-standardized prevalence of obesity in men aged 18 years and over (BMI ≥30 kg/m2). Global status report on NCDs 2014. World Health Organization.

In order to reduce the prevalence of obesity and the associated comorbidities, several strategies at both levels, public health and clinical, have been developed with modest success (Holdsworth et al., 2013; Wells, 2012) . This situation could be due, in part, to the poor understanding of the physiological mechanism involved in the regulation of energy homeostasis (Barja-Fernández et al., 2014; Wells, 2012).

It has been well established that one of the most important mechanisms leading to the comorbidities associated with obesity, including type 2 diabetes and cardiovascular diseases is the appearance of insulin resistance (Ginsberg, 2000; Qatanani and Lazar, 2007). In addition to this, there is also ample evidence of a reduction in the oxygen supply in obese adipose tissue, which is usually accompanied by an inflammatory process. These two conditions contribute to the development of insulin resistance and all the complications linked to obesity (Ye, 2009).

2. Insulin resistance

2.1. Introduction

Insulin is an anabolic hormone released by the pancreatic β-cells which exerts its primary action in skeletal and cardiac muscle, adipose tissue and liver. Insulin plays

important roles in development, growth, cell differentiation, lipid and protein metabolism, glucose homeostasis and nitric oxide (NO) synthesis (Low Wang et al., 2004; Sesti, 2006).

Insulin resistance is classically defined as a significantly diminished responsiveness of target cells to normal circulating levels of insulin (Henry, 2003; Mlinar et al., 2007). As a consequence, a compensatory hyperinsulinemia is needed to maintain glucose and lipid homeostasis (Mlinar et al., 2007). Nevertheless, when insulin secreted by pancreas is insufficient to compensate for insulin resistance, circulating glucose concentration rises until it produces a sustained hyperglycemia (Bailey, 2005). Both, insulin resistance and resulting hyperglycemia have deleterious effects in the organism. Hyperglycemia is responsible of the microvascular complications of type 2 diabetes (diabetic retinopathy, loss of vision, and nephropathy), whereas insulin resistance increases cardiovascular risks leading to one of the most significant causes of death (Bailey, 2005; Klein, 1995).

The development of insulin resistance, as well as obesity, is dependent of genetic and environmental factors including food intake, reduced physical activity, aging and the administration of drugs (Lopes et al., 2016; Mlinar et al., 2007). Therefore, obesity is an important condition that predisposes for insulin resistance. It has been calculated that around 23% of people with a BMI<25 kg/m2 develop insulin resistance, whereas 48.7% of overweight patients appear to be insulin resistant and the incidence of this condition reaches up to 66.3% in obese patients (Govers, 2015).

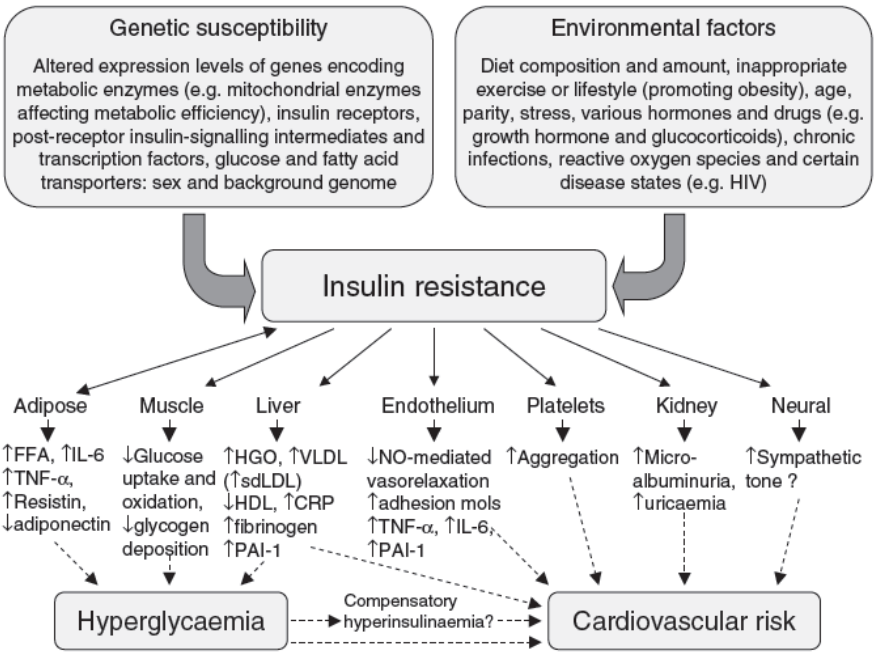

Figure I2. Causes and effects of insulin resistance. Insulin resistance can develop through genetic or environmental factors, commonly mixtures of both, giving rise to disturbances of nutrient metabolism and varying cardiovascular risks. CRP, C-reactive protein; FFA, free fatty acids; HGO, hepatic glucose output; HIV, human immunodeficiency virus; IL-6, interleukin-6; PAI-1, plasminogen activator inhibitor-1; sdLDL, small dense low-density lipoprotein; TNF-α, tumor necrosis factor-α; VLDL, very-low-density lipoprotein (Bailey, 2005).

2.2. Insulin signaling

Insulin signaling pathway regulates glucose entry in adipocytes and skeletal muscle cells and gluconeogenesis in the liver. This process is mediated by the translocation of the facilitative glucose transporter GLUT4 to the plasma membrane, allowing the uptake of glucose into the cell. Insulin actions represent the first step for the energy storage and synthesis of lipids, proteins and carbohydrates.

Under fasting condition, when circulating insulin levels are low, GLUT4 is sequestered in vesicles in the cytoplasm and only a small percentage of this protein is located in the plasma membrane. When carbohydrates are ingested, insulin is secreted by the pancreas and binds to the insulin receptor (IR), triggering the signaling cascade that ends with GLUT4 translocation (Wilcox, 2005).

IR is a heterotetrameric complex composed by two extracellular α-subunits and two intracellular β-subunits with tyrosine kinase activity linked by disulphide bonds. Circulating insulin, through its direct interaction with the α-subunit, induces the

activation of the intrinsic tyrosine kinase activity of the β-subunit. This results in the autophosphorylation of the receptor in specific tyrosine residues (Y1158, Y1162, Y1163), followed by the recruitment of several substrates including Insulin Receptor Substrates (IRS-1 and IRS-2) (Hubbard, 1997). Tyrosine phosphorylation of IRSs by IR induces the exposure of hidden recognition sites, producing the recruiting of additional molecules that contain Src homology 2 (SH2) domains, including phosphatidylinositol 3-kinase (PI3K), which is a heterodimer comprised of a regulatory subunit, P85, and a catalytic subunit, P110 (Jiménez et al., 2002; Di Zazzo et al., 2014). When PI3K is located in close proximity to the plasma membrane and, therefore, to its lipid substrates, the inhibitory role of P85 is reduced and P110 converts phosphatidylinositol-4,5-bisphosphate (PIP2) to phosphatidylinositol 3,4,5 trisphosphate (PIP3) at the plasma membrane (Choi et al., 2002; Liu et al., 2009). PIP3 acts as a second messenger recruiting PDK1 and protein kinase B (PKB/Akt) (Liu et al., 2009). In these circumstances, PDK1 activates PKB/Akt by phosphorylation and after several subsequent phosphorylation steps of various downstream proteins, GLUT4 transporter is finally translocated to the plasma membrane allowing glucose uptake from the extracellular space (Christian K.Roberts, Andrea L.Hevener, 2014; Liu et al., 2009).

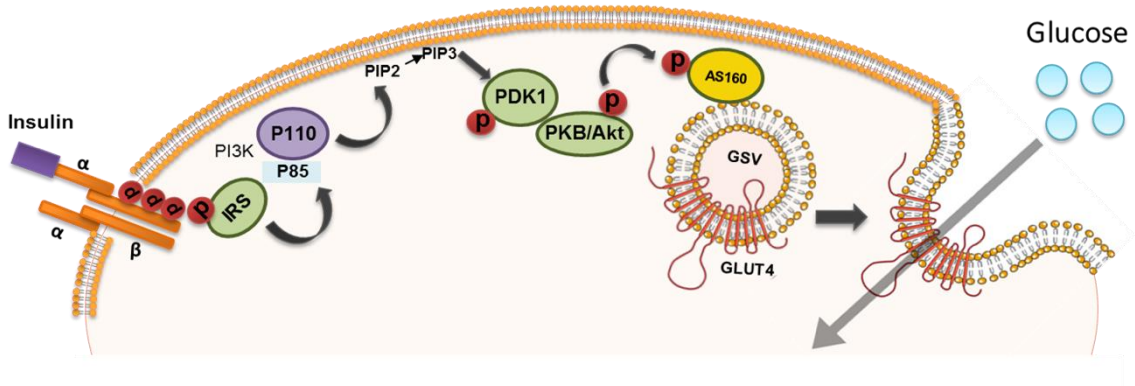

Figure I3. PI3K-dependent insulin signaling. Insulin activates the insulin receptor, which phosphorylates and recruits substrate adaptors such as the IRS family of proteins. Tyrosine-phosphorylated IRS then displays binding sites for numerous signaling partners. Among them, PI3K has a major role in insulin function, mainly via the activation of the Akt/PKB. AS160 is rapidly phosphorylated by Akt/PKB leading to GLUT4 translocation to the plasma membrane to allow the entrance of glucose.

GLUT4 belongs to a family of glucose transporter isoforms (GLUTs), constituted by 12 transmembrane domains, which catalyze the facilitative diffusion transport of hexoses across the plasma membrane. Particularly, in absence of insulin, GLUT4 is essentially located in intracellular compartments called GLUT4-storage vesicles (GSVs) (Bruno et al., 2016).

Recent evidence indicates that translocation of GLUT4 to the plasma membrane induced by insulin is regulated by Rab-GTPase proteins, which play an important role in the vesicle transport process (Huang and Czech, 2007). Recently, multiple members of this family of proteins including RAB10, RABA4 and RAB5 have been found in GSVs (Bruno et al., 2016). Classically, Rabs function as molecular switches; when GTP is bound Rab is active, whereas hydrolysis of GTP to GDP inactivates this protein.

AS160 is one of the major proteins of the Rab-GTPase family that has been involved in the regulation of GLUT4 translocation. AS160 is a putative target of Akt at Thr642 and in multiple serine residues. Unlike the classic mechanism of activation-inactivation of the Rab-GTPase protein family, AS160 is shown to be regulated by phosphorylation (Sano, 2003). Nonphosphorylated AS160 bound to GSVs inhibits GLUT4 trafficking and translocation to the plasma membrane. However, insulin stimulation results in the rapid phosphorylation of AS160 and its dissociation from GSVs, leading to a significant increase in GLUT4 translocation (Christian K.Roberts, Andrea L.Hevener, 2014; Tan et al., 2012).

3. Hypoxia

Oxygen is necessary at a molecular level for most metabolic processes (Trayhurn, 2014). The cell exposure to oxygen could vary depending on the tissue, from 16% in the pulmonary alveoli to less than 6% in other organs of the body (Semenza, 2001). Cell oxygen levels are rigorously regulated primarily by mitochondrial oxidative phosphorylation and oxygen delivery by erythrocytes through capillary networks (Hagen et al., 2003; Taylor, 2008). The alteration of oxygen homeostasis due to an increase in oxygen demand and the insufficient supply of this molecule by the capillary networks induce a hypoxia situation in the tissue (Fridlyand and Philipson, 2006).

Hypoxia has been pointed as a crucial feature in the pathophysiology of heart disease, cancer, obesity, cerebrovascular disease and chronic lung disease, which represent important causes of mortality in western countries (Losso and Bawadi, 2005; Semenza, 2001).

3.1. Hypoxia signaling pathways

Since oxygen is an essential factor required for metabolism, including the production of ATP, metazoans have evolved multiple mechanisms in order to adapt and survive periods of hypoxia (Kaelin and Ratcliffe, 2008; Zepeda et al., 2013).

3.1.1. Hypoxia-inducible factor signaling

The primary signaling pathway activated by hypoxia is driven by the hypoxia-inducible factor (HIF) family of proteins. HIFs are basic helix-loop-helix transcription factors that function as heterodimers consisting of two subunits, an oxygen sensitive α-subunit and a constitutively expressed β-subunit (HIF-1β), also known as the aryl hydrocarbon receptor nuclear translocator (ARNT) (Deng et al., 2016; Lee et al., 2011).

Conversely to β-subunit, three α-subunits have been described—HIF-1α, HIF-2α, and HIF-3α. HIF-1α has received the most attention and is considered as the master regulator of oxygen homeostasis (Glück et al., 2015; Trayhurn, 2014). Under normoxia condition, HIF-1α subunit is hydroxylated by activated prolyl hydroxylases (PHDs). As a result, HIF-1α is bound to the tumour suppressor Von Hippel–Lindau (VHL) protein. This interaction causes HIF-1α to become ubiquitylated and targeted to the proteasome, where it is degraded (Harris, 2002). At low oxygen concentrations, PHDs are inactivated, preventing HIF-1α from being degraded. HIF-1α is therefore accumulated in the nucleus, where it associates to the HIF-1β subunit. This complex activates gene transcription by binding to specific HIF-responsive elements (HREs) present in target genes (Glück et al., 2015).

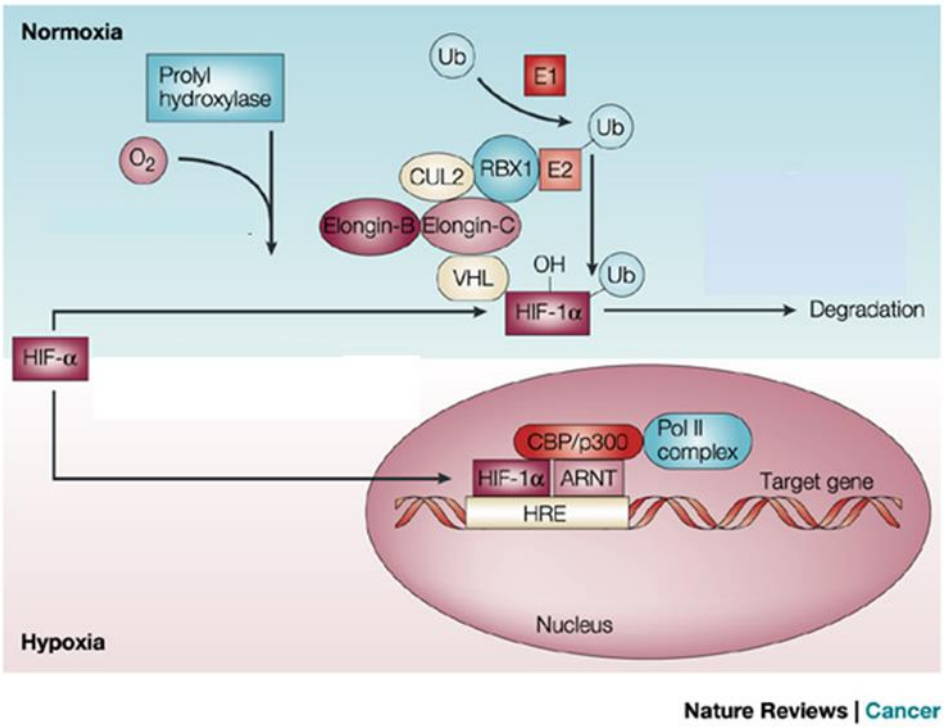

Figure I4. HIF-1 signaling pathway. In the presence of oxygen (O_2), prolyl hydroxylase modifies hypoxia-inducible transcription factor (HIF)-1α, allowing it to interact with the Von Hippel–Lindau (VHL) complex. VHL is part of a larger complex that includes elongin-B, elongin-C, CUL2, RBX1 and an ubiquitin-conjugating enzyme (E2). This complex, together with an ubiquitin-activating enzyme (E1), mediates the ubiquitylation (Ub) of HIF-1α and subsequent proteasome degradation. In the absence of oxygen, prolyl hydroxylase cannot modify HIF-1α, and the protein remains stable. Stabilized HIF-1α is translocated to the nucleus, where it interacts with cofactors such as aryl hydrocarbon receptor nuclear translocator (ARNT), CBP/p300 and the DNA polymerase II (Pol II) complex to bind to hypoxia-responsive element (HREs) and activate transcription of target genes. Figure adapted from: Harris, 2002.

HIF-1 regulates more than 100 different genes involved in a multiplicity of cellular processes, including glucose utilization, inflammation, extracellular matrix (ECM) metabolism, and apoptosis (Trayhurn, 2014; Zepeda et al., 2013).

More recently, two HIF-1 independent pathways have been related to the cellular response to hypoxia inducing important effects in gene expression: the mammalian target of rapamycin (mTOR) pathway and the unfolded protein response (UPR) (Wouters and Koritzinsky, 2008).

3.1.2. mTOR signaling pathway

mTOR is a ubiquitous serine/threonine kinase that stimulates proliferation and survival under stress. To achieve this objective, two interacting complexes, mTORC1 and

mTORC2, promote the transcription of genes involved in carbohydrate metabolism and lipogenesis, enhance protein translation, and inhibit autophagy (Perl, 2015). Arsham and colleagues showed that brief incubation of HEK293 cells in hypoxia (1.5% O_2) prevented the phosphorylation of mTOR and its effectors: 4E-BP1, p70S6K, rpS6, and eIF4G (Arsham et al., 2003). Through this HIF-1 independent mechanism, hypoxia induced protein synthesis and reduced the autophagy and apoptosis process (Arsham et al., 2003).

3.1.3. Unfolded protein response (UPR)

The unfolded protein response (UPR) is an adaptive response initiated by reticulum stress. UPR signaling is initiated by three ER-transmembrane transducers: PERK (PKR-like ER kinase), inositol-requiring protein 1 (IRE1) and ATF6 (Ruiz de Galarreta et al., 2016). The UPR controls multiple downstream processes, including production, maturation and degradation of proteins, cell metabolism and cell death.

Recently, it has been demonstrated in human diploid fibroblasts and transformed cells that incubation in anoxia or hypoxia (1% O_2) led to phosphorylation of PERK and its substrate, eIF2α. This effect was correlated with a decrease in the rates of protein synthesis and was independent of the function of HIF-1 (Koumenis et al., 2002). Phosphorylation of eIF2α was also increased in several cell lines obtained from normal or cancer tissues after culture in hypoxic atmosphere (Koritzinsky et al., 2007; Wouters and Koritzinsky, 2008).

In addition, it has been shown that hypoxia is able to activate IRE1, increasing the splicing rate and the transcription of X-box binding protein (XBP1). XBP1-deficient cells present a reduced capacity to survive in a hypoxic microenvironment, indicating the importance of this pathway to the adaptation to hypoxic microenvironment (Romero-Ramírez et al., 2004).

3.2. Hypoxia in obesity

It has been well established that, in obesity, there exists hypertrophy (increase of cell size) and hyperplasia (increase in the number of cells) of adipocytes, which enlarge the mass of adipose tissue. Considering the adipose tissue expansion, it was proposed that white fat depots show hypoxic areas leading to the establishment of the inflammatory

response observed in the tissue. This hypothesis has been supported in part by evidence, indicating that the limited vascularization of the adipose tissue in obesity is insufficient to maintain normal oxygen levels throughout the organ (Trayhurn, 2014; Trayhurn and Wood, 2004; Yin et al., 2009). Consistent results indicate that fasting and postprandial blood flow in adipose tissue is decreased in obese insulin-resistant versus lean insulin-sensitive subjects (Goossens and Blaak, 2015; Karpe et al.). Another argument to support the development of hypoxia in obese adipose tissue is that the diameter of hypertrophic adipocytes (150-200 µM) could exceed the normal diffusion distance of oxygen across tissues (100-200 µM) (Goossens and Blaak, 2015; Trayhurn, 2014). In this context, partial pressure of oxygen of almost zero has been reported at only 100 µM from blood vessels in some tissues (Brahimi-Horn and Pouysségur, 2007).

All these observations represent important evidences, but do not really demonstrate that hypoxia occurs in the obese adipose tissue. In this sense, several key *in vivo* studies have been performed to determine the real O_2 levels in adipose tissue using pimonidazole hydrochloride staining, which forms a colored adduct in hypoxic tissues. These experiments have shown that weight gain in ob/ob, KKAy (type 2 diabetes model), and dietary-induced obese mice, induced the development of hypoxia in parametrial and epididymal white adipose tissue (Hosogai et al., 2007; Rausch et al., 2008; Ye et al., 2007). Moreover, the expression of hypoxia-responsive genes, including HIF-1α (*Hif1a*), GLUT1 (*Slc2a1*), leptin (*Lep*), plasminogen activator inhibitor-1 (PAI-1 or *Serpine1*), matrix metalloproteinase-2 (*Mmp2*) and adrenomedullin (*Adm*), were upregulated in white adipose tissue of ob/ob mice and diet-induced obese mice compared to normal mice (Hosogai et al., 2007; Rausch et al., 2008; Ye et al., 2007). The lactate production was determined in white adipose tissue of high-fat diet fed mice and KKAy mice and showed an important increase of 1.7- and 1.5-fold higher than those of normal-diet fed mice and control, respectively (Hosogai et al., 2007). There are also studies using a needle-type fiber optic O_2 sensor allowing the quantification of pO_2. Ye J and colleagues have demonstrated markedly lower levels of O_2 in epididymal and retroperitoneal adipose tissue in obese mouse models compared to lean mice. More precisely, pO_2 was reduced threefold in the first such study: 15.2 versus 47.9 mm Hg (Ye et al., 2007).

Taken together, there is substantial evidence that the hypertrophy of adipocytes and the subsequent fat depot expansion result in the development of hypoxia in the tissue. This situation is involved in the dysfunction of adipocytes and the related metabolic diseases derived from obesity.

3.3. Hypoxia and adipocyte dysfunction

3.3.1. Secretory pattern of adipokines

The effects of hypoxia on the expression of specific adipokines have been determined by several groups. Lolmede and colleagues showed that the exposure of mouse 3T3-F442A adipocytes to a low O_2 tension (5%) resulted in increased expression and release of leptin, vascular endothelial growth factor (VEGF), matrix metalloproteinase-2 (MMP2) and -9 (MMP9), compared to the cells cultured in normoxia condition (Lolmède et al., 2003). The second major hormone released by adipocytes is adiponectin, which has important functions as insulin sensitizer and as anti-inflammatory. It has been shown that adiponectin is downregulated after 12 hours of hypoxia (1% O_2) in murine 3T3-L1 adipocytes (Chen et al., 2006; Hosogai et al., 2007). Moreover, adipocyte-specific HIF-1α knock-out mice increase the expression of adiponectin in contrast to the wild-type mice (Jiang et al., 2013). Since adiponectin is an important hormone which induces insulin response and anti-inflammatory effects in adipocytes, this evidence has a particular significance since low plasma levels of adiponectin are associated with the development of obesity-related insulin resistance and cardiovascular disease (Kadowaki et al., 2006). Similar effects in the leptin and adiponectin production induced by hypoxia have been observed in human adipocytes. Taken together, these results indicate that reduction in pO_2 is the primary mechanism for the rise in the production of leptin and for the downregulation of adiponectin (Trayhurn, 2014).

Besides leptin and adiponectin, other major inflammation-related adipokines have been shown to be modulated by hypoxia. The protein serum amyloid A (SAA)-3, which is also released by mature adipocytes and induces tumor necrosis factor-α (TNF-α), IL-6, IL-8 and monocyte chemotactic protein-1 (MCP-1) release, is increased in 3T3-L1 adipocytes incubated in hypoxia (1% O_2) (De Oliveira et al., 2013). Furthermore, the

expression and secretion of FIAF/angiopoietin-like protein 4, IL-6, macrophage migration inhibitory factor (MIF) and VEGF, are stimulated by hypoxia in human adipocytes (Wang et al., 2007).

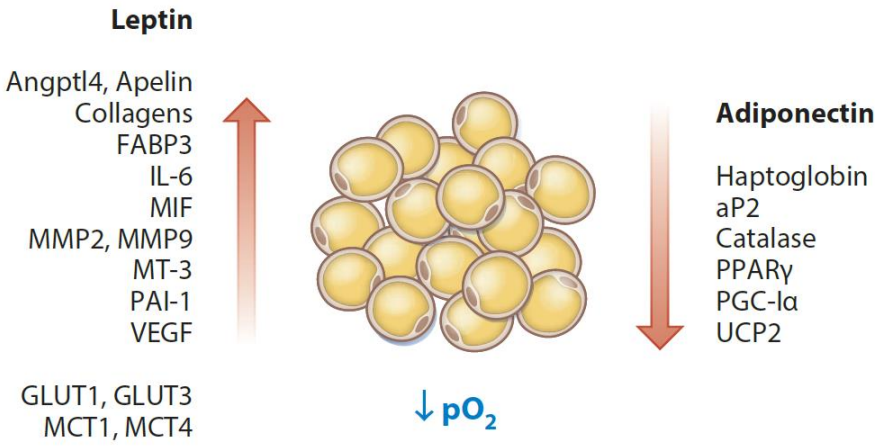

Figure I5. **Effects of hypoxia on the expression of key genes in human adipocytes** (↑ increased, ↓ decreased expression). Genes encoding both adipokines and proteins involved in general cellular metabolism are shown. Angptl3, angiopoietin-like protein 3; FABP3, fatty acid binding protein 3; GLUT, glucose transporter; IL-6, interleukin-6; MCT, monocarboxylate transporter; MMP, matrix metalloproteinase; pO2, oxygen partial pressure; PAI, plasminogen activator inhibitor; PGC, peroxisome proliferator-activated receptor-gamma coactivator; PPAR, peroxisome proliferator-activated receptor; UCP2, uncoupling protein-2; VEGF, vascular endothelial growth factor. Figure from: Trayhurn, 2014.

3.3.2. Lipid oxidation and oxidative metabolism

It is known that lipid oxidation and lipolysis are among the most prominent pathways modulated by hypoxia in adipocytes. Hashimoto and colleagues found that modest hypoxia (5% O_2) decreased the size of lipid droplets and lipid storage, increased basal lipolysis and augmented fatty acid release in 3T3-L1 adipocytes (Hashimoto et al., 2013). Moreover, experiments made in human adipocytes showed that hypoxia inhibits lipogenesis and induces basal lipolysis probably due to inhibition of hexosamine biosynthesis (O'Rourke et al., 2013).

On the other hand, hypoxia has been shown to downregulate the expression of important genes involved in mitochondrial metabolism and oxidative phosphorylation. In renal carcinoma cells lacking the VHL tumor suppressor, HIF-1 negatively regulates mitochondrial biogenesis and O_2 consumption (Zhang et al., 2007). In 3T3-L1 adipocytes, hypoxia (2% O_2) decreases ATP production, NADH dehydrogenase activity, mitochondrial membrane potential, and expression of mitochondria-related genes including *NRF-1*, *PGC-1α*, *COX1* and *SOD*. Microarrays studies also demonstrate that hypoxia downregulates genes related to oxidative metabolism (Mazzatti et al., 2012).

3.3.3. Glucose utilization

One of the main metabolic consequences of hypoxia is a shift towards anaerobic metabolism, which induces a change in the glucose mobilization mechanism.

It has been demonstrated that GLUT1, a facilitative glucose transporter independent of insulin, is a direct target of HIF-1 and is presumed to be the main transporter responsible for basal glucose uptake (Hayashi et al., 2004). Experiments in human SGBS-differentiated adipocytes showed that hypoxia (1% O_2) for up to 24 h resulted in significant increases in GLUT1 (9.2-fold), GLUT3 (9.6-fold peak at 8 h), and GLUT5 (8.9-fold) mRNA levels compared to adipocytes maintained in normoxia (21% O_2) (Wood et al., 2007). This result is consistent with the strong increase (6-fold) detected in basal glucose uptake measured by 2-deoxyglucose uptake assay after 24 hours of hypoxia in human adipocytes (Wang et al., 2007). Furthermore, recent evidence suggests that basal glucose uptake is also enhanced in adipocytes as an acute response to hypoxia (Lu et al., 2016).

Glucose uptake in adipocytes is mainly regulated by insulin. In normoxia, insulin induces a 10-fold increase in glucose transport in 3T3-L1 differentiated adipocytes. However, incubation of murine adipocytes in hypoxia for 16 hours shows inhibited insulin-induced glucose transport. Protein expression of GLUT4 was not altered in this experiment (Regazzetti et al., 2009).

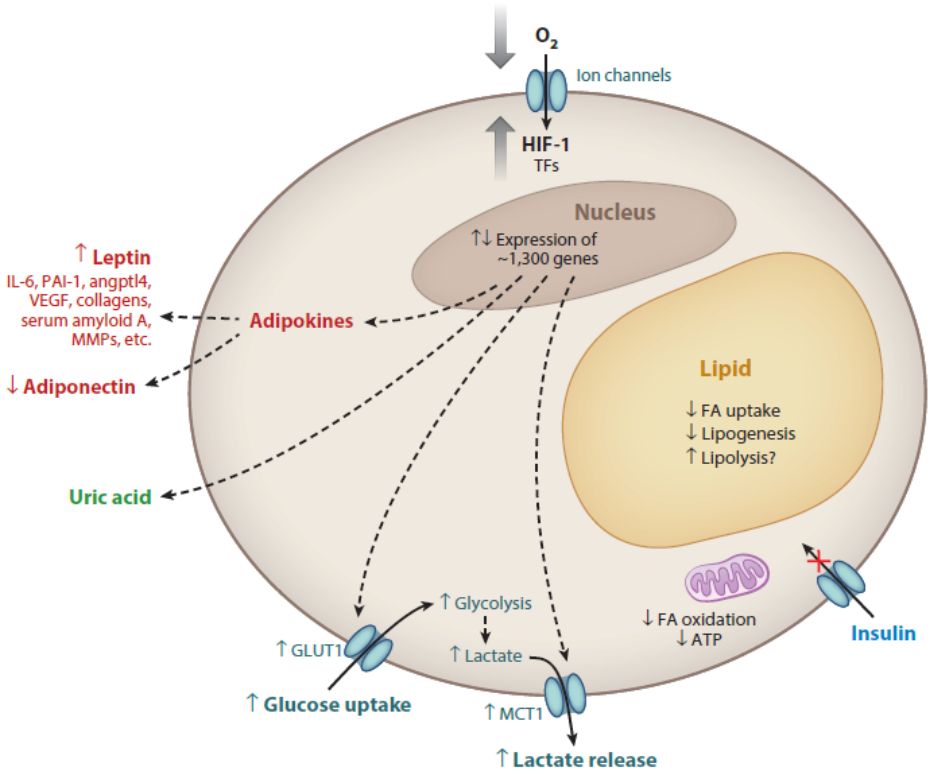

Figure I6. Schematic illustration of the major effects of hypoxia on key functions of white adipocytes. Solid arrows indicate direct pathways; dashed arrows indicate that multiple steps are involved. Angptl3, angiopoietin-like protein 3; ATP, adenosine triphosphate; FA, fatty acid; GLUT, glucose transporter; HIF, hypoxia-inducible factor; IL-6, interleukin-6; MCT, monocarboxylate transporter; MMPs, matrix metalloproteinases; PAI, plasminogen activator inhibitor; TFs, transcription factors (in addition to HIF-1); VEGF, vascular endothelial growth factor. Figure from: Trayhurn, 2014.

3.3.4. Lactate production

Lactate is the end product of anaerobic glycolysis. The increased glucose utilization due to the enhanced basal glucose uptake by adipocytes in response to hypoxia implies that the production and release of this metabolite rises significantly (Lolmède et al., 2003). This effect was also observed in white adipose tissue of an animal model of obesity (Hosogai et al., 2007). In the obese adipose tissue, it has been observed that up to 70% of the glucose utilized by adipocytes is metabolized to lactate, establishing a direct relation between the proportion of glucose that is converted to lactate and fat cell size (DiGirolamo et al., 1992).

Recent evidence also suggests that lactate is more than a metabolic product of glycolysis and may behave as a signaling molecule involved in the inflammatory response and the induction of insulin resistance in skeletal muscle cells (Choi et al., 2002; Samuvel et al., 2009).

3.4. Insulin resistance and other metabolic disturbances related to hypoxia

Dysregulation of adipocyte function as a consequence of hypoxia, discussed previously, promotes the appearance of insulin resistance, which may finally induce the development of type 2 diabetes. The reduced levels of adiponectin in hypoxic adipose tissue and the rise in the release of the pro-inflammatory cytokine IL-6 by low oxygen concentration constitute a mechanism by which insulin sensitivity is impaired (Wang et al., 2007).

A further hypoxia effect that promotes insulin resistance in adipose tissue is the reduced activity showed by the insulin-induced glucose transporter, GLUT4. The exposure of adipocytes to prolonged hypoxia (48 hours) induced downregulation of the GLUT4 gene (*Slc2a4*) (Wood et al., 2009). Moreover, the glucose uptake induced by insulin and measured by 2-deoxyglucose assay is strongly reduced in adipocytes after incubation in a hypoxic microenvironment (Regazzetti et al., 2009).

Insulin signaling pathway has been shown to be impaired in adipocytes incubated in hypoxic conditions, occurring an inhibition of the phosphorylation of the insulin receptor, PKB/Akt and AS160 and the subsequent inhibition of PI3K pathway. This direct effect of low oxygen concentration is crucial for the development of insulin resistance within adipose tissue (Regazzetti et al., 2009).

Not only chronic hypoxia, but also intermittent hypoxia (IH) has been positively correlated with the development of insulin resistance and glucose intolerance. IH occurs in obese patients with obstructive sleep apnea (OSA) and is produced by the recurrent collapse of the upper airway during sleep, resulting in a cyclical pattern of oxygen desaturation that lasts 15-60 s, followed by reoxygenation (Dewan et al., 2015). OSA can lead to many comorbidities, such as hypertension and coronary heart disease (Polotsky et al., 2003). Ip et al., showed in humans that sleep disorder indicators of OSA patients tightly correlated with insulin resistance parameters (fasting

serum insulin levels and the insulin resistance index) in both obese and non-obese patients (Ip et al., 2002). Other clinical studies in humans have also demonstrated that IH impairs insulin sensitivity (Louis and Punjabi, 2009). In mice, exposure to IH decreases whole-body insulin sensitivity and muscle-specific glucose utilization in C57Bl/6J mice (Iiyori et al., 2007; Poulain et al., 2015).

Hypoxia is also involved in the generation of endothelial dysfunction. IH leads to oxidative stress characterized by the increased levels of ROS (Lévy et al., 2008). Furthermore, hypoxia reduces nitric oxide (NO) bioavailability and induces the formation of peroxynitrite ($ONOO^-$), which results from the reaction between nitric oxide and the superoxide ion ($O_2^{\cdot-}$). Peroxynitrite has been involved in the endothelial damage inhibiting the activity of endothelial nitric oxide synthase (eNOS) (Zou et al., 2002) and catalase, a known antioxidant enzyme (Bauer G 2015). Oxidative stress also induced the activation of an inflammatory cascade producing the expression of adhesion molecules (Ohga et al., 2003) and the activation of leukocytes (Schulz et al., 2000). Moreover, adipose tissue contributes to endothelial dysfunction by releasing adipokines involved in vascular and endothelial physiology including TNF-α, interleukin-6, complement factors, angiotensinogen, resistin and adipocyte differentiation factor (Lévy et al., 2008).

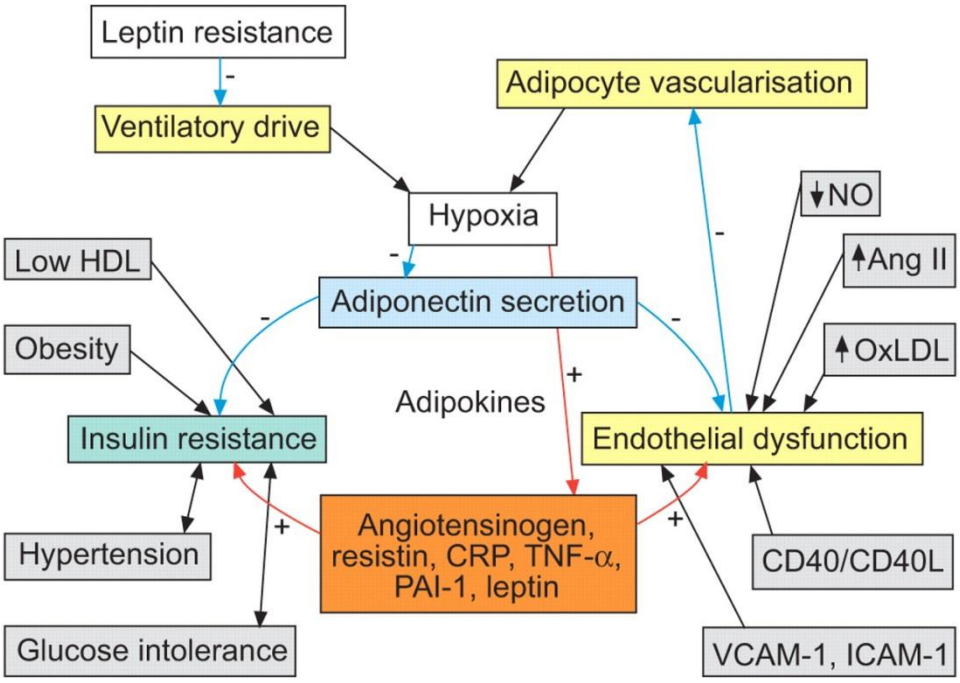

Figure I7. Effect of hypoxia on adipokines secretion and their interactions with insulin metabolism and endothelial function. Red arrows indicate deleterious effect whereas blue arrows indicate protective effects. HDL: high-density lipoprotein; OxLDL: oxidized low-density lipoprotein; CD40L: CD40 ligand; VCAM-1: vascular cell adhesion molecule-1; ICAM-1: intercellular adhesion molecule-1; +: activation/promotion; -: inhibition/protection; ↓: decrease; ↑: increase. Figure from: Lévy et al., 2008.

4. Caveolae: caveolins and cavins

Caveolae are defined as 50-100 nm flask-shape plasma membrane invaginations particularly abundant in adipocytes, fibroblasts, endothelial and epithelial cells as well as in smooth and striated muscle cells. Caveolae membranes are enriched in cholesterol, sphingomyelin and glycosphingolipids, forming specialized detergent-insoluble type of membrane domains or lipid rafts. Loss of caveolae, as a result of mutations or expression changes in caveolins or cavins genes, results in a broad range of diseases, such as muscular dystrophy, lipodystrophy, cardiovascular disease and cancer (Martínez-Outschoorn et al., 2015).

Caveolins are the major membrane proteins of caveolae. So far, it has been reported the existence of three caveolin isoforms: Cav-1, Cav-2 and Cav-3. Cav-1 and Cav-2 are abundant in caveolae rich non-muscle cells, whereas Cav-3 is found in skeletal muscle and in some smooth-muscle cells. All three caveolins show the N and C termini in the cytoplasm and a long hairpin intramembrane domain. Cav-1 also contains a highly conserved region called scaffolding domain (CSD) and a tyrosine phosphorylation site on residue 14 associated with cell signaling transmission (Branza-Nichita et al., 2012; Martinez-Outschoorn et al., 2015). The C-terminal domain, which is close to the intramembrane domain, is modified by palmitoyl groups that insert into the lipid bilayer.

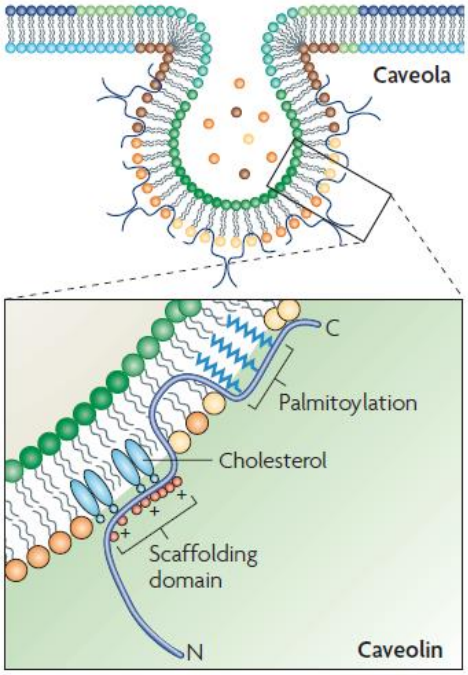

Figure I8. Caveolae and caveolins. Caveolin is inserted into the caveolar membrane, with the N and C termini facing the cytoplasm and a 'hairpin' intramembrane domain embedded within the membrane bilayer. The scaffolding domain is indicated with red circles. The C-terminal domain, which is close to the intramembrane domain, is modified by palmitoyl groups that insert into the lipid bilayer. Figure from: Parton and Simons, 2007.

Caveolins are not the only structural component of caveolae. Over the past few years, a new family of cytoplasmic proteins with previously identified functions, and now known as cavins, has been also found as essential for caveolae structure. The cavin family includes cavin-1 (PTRF; Polymerase I and Transcript Release Factor), cavin-2 (SDPR; serum deprivation response protein), cavin-3 (SRBC; Sdr-related gene product that binds to c-kinase, also known as PRKCDBP; Protein Kinase C Delta Binding Protein) and cavin-4 (MURC; Muscle Related Coiled-Coil Protein). Cavins are cytoplasmic proteins with amino‑terminal coiled-coil domains that form large heteromeric complexes recruited to caveolae in cells expressing caveolins.

4.1. Biogenesis of caveolae

Caveolins and cavins are essential and play an important role in caveolae formation. The importance of Cav-1 in the biogenesis of caveolae has been well established. Studies in Cav-1 knockout mice have shown that, in these animals, caveolae structures

were absent in non-muscle tissues (Drab et al., 2001; Razani et al., 2001, 2002). Moreover, the transient expression of Cav-1 in a lymphocyte cell line, which has no detectable levels of this protein, promotes *de novo* formation of caveolae (Fra et al., 1995). Walser et al showed, in an elegant manner, that Cav-1 expression drives the formation of caveolae structure by its expression in a bacterium which lacks any intracellular membrane system (Walser et al., 2012). It has been reported that generation of caveolae structures involves the binding of Cav-1 to cholesterol molecules in the plasma membrane (Murata et al., 1995), where it could form oligomers (Monier et al., 1996) inducing the typical curvature of caveolae.

Recently, the importance of cavins for the formation of caveolae has been demonstrated. As occurs with Cav-1, cavin-1 and cavin-2 ablation in mice causes loss of caveolae in their tissues (Hansen et al., 2009, 2013; Liu et al., 2008). Moreover, absence of cavin-1 induces endocytosis and subsequent degradation of Cav-1, leading to dramatically reducing the levels of this protein (Liu and Pilch, 2008). On the other hand, cooperation between Cav-1 and cavin-1 is required for the formation of caveolae, as demonstrated by the generation of caveolae structure when cavin-1 expression is induced in cells that lack endogenous cavins, but express endogenous Cav-1 (Hill et al., 2008). A recent study showed that cavin-2 is necessary for the stable expression of cavin-1 and Cav-1 and is involved in the generation of caveolar membrane curvature (Hansen et al., 2009). Less is known about the role of cavin-3 in caveolae, but it is thought to be implicated in the traffic of the caveolar vesicle (McMahon et al., 2009).

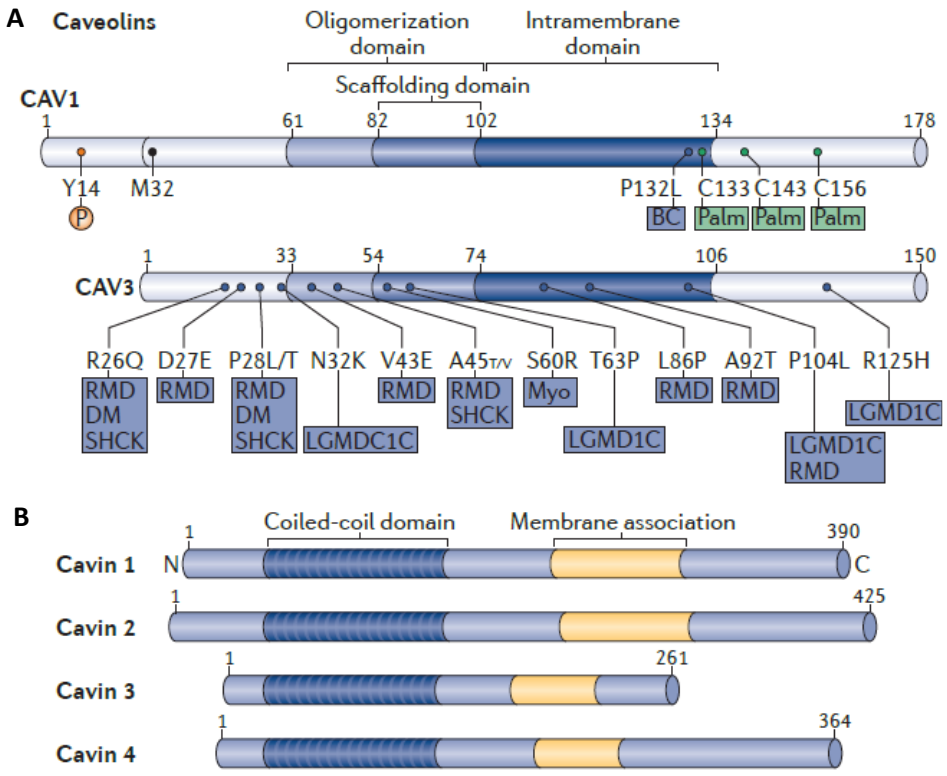

Figure I9. Caveolins and cavins gene structure. A) Schematic representation of Cav-1 and Cav-3 gene. Numbers above the lines correspond to the amino acid in mammalian caveolins. Palmitoylation (Palm) sites in CAV1 are indicated in green, a Tyr phosphorylation site in red (potential phosphorylation sites in CAV3 are not shown). Disease-associated amino acid substitutions in CAV1 and CAV3 are shown in blue. B) Schematic illustration showing the predicted domains of the four mammalian cavins. The conserved predicted coiled-coil domains implicated in protein–protein interactions are indicated in blue and the basic regions implicated in membrane association are shown in yellow. BC, breast cancer; DM, distal myopathy, FHCK, familial hyperCKemia; LGMD1C, limb girdle muscular dystrophy 1C; Myo, myopathy; RMD, Rippling muscle disease; SHCK, spontaneous hyperCKemia. Figure from: Parton and del Pozo, 2013.

4.2. Caveolae functions

Caveolae have been described to be involved in several cell processes including endocytosis, regulation of membrane lipid composition, and as a signaling platform. These specialized regions of the plasma membrane contain a number of signaling components (receptors, transducers, channels, pumps and exchangers) responsible for initiating many of the major cell signaling pathways. More recently, cell protection against mechanical stress within the plasma membrane has been also attributed to caveolae.

4.2.1. Endocytosis

The understanding of the dynamic of caveolae is still object of investigation. However, experiments using microscopy and gene editing technologies have shown that only around 5% of the total population of caveolae undergoes endocytosis. This low contribution to total endocytosis is consistent with other reports indicating that these invaginations have specific cargoes, including GPI-anchored proteins, the insulin receptor, Shiga and cholera toxins, cholesterol, albumin and simian virus 40 (SV40). The regulation of endocytosis mediated by caveolae is dependent on several adaptor proteins including EH-domain containing 2 (EHD2), pacsin 2, and dynamin-2, which have been implicated in the caveolar scission and budding from plasma membrane (Senju and Suetsugu, 2016). The presence of cavin-3 has been also reported to facilitate the release of caveolae from the membrane (McMahon et al., 2009).

4.2.2. Lipid homeostasis

Considerable *in vivo* and *in vitro* evidence supports a role for caveolae in adipocyte lipid metabolism. Mice and human models lacking caveolae, through Cav-1 or cavin-1 ablation, develop lipodystrophy and exhibit loss of subcutaneous fat and glucose intolerance (Ardissone et al., 2013; Rochford, 2014; Schrauwen et al., 2015). It has been reported that caveolae could protect cells, including adipocytes, from lipotoxicity. In this line, overexpression of Cav-1 and Cav-3 in HEK293 cells induced resistance to the lipotoxic effect of prolonged incubation with high levels of fatty acids (Simard et al., 2010). Moreover, Cav-1 deletion in adipocytes increases the rate of lipolysis in these cells (Meshulam et al., 2011). On the other hand, Cav-1 deficiency also leads to altered lipid composition and distribution in the plasma membrane affecting Ras signaling pathway (Ariotti et al., 2014). These data suggest that the role of Cav-1, and therefore of caveolae, in the lipid membrane composition is important for the correct functioning of both, lipid metabolism and efficient signal transduction pathways.

4.2.3. Signal transduction

Caveolae serves as a communication platform promoting the interaction between protein mediators in cell signaling processes (Billaud et al., 2014). Indeed, caveolins have been involved in the regulation of multiple signaling pathways in a negative or positive manner (Boscher and Nabi, 2012). Important evidence in this sense is the identification of multitude of receptors integrated within the caveolae structure. Moreover, the scaffolding domain of Cav-1 has been related to the recruitment of various signaling proteins, exerting differential regulatory roles. In this way, it has been reported that the activities of epidermal growth factor (EGF) receptor, nitric oxide synthase, G proteins, protein kinase C and Src family proteins are negatively regulated by this interaction, whereas insulin receptor (IR), Eph receptors or estrogen receptor are activated (Cheng and Nichols, 2016; Martínez-Outschoorn et al., 2015; Parton and del Pozo, 2013; Parton and Simons, 2007)

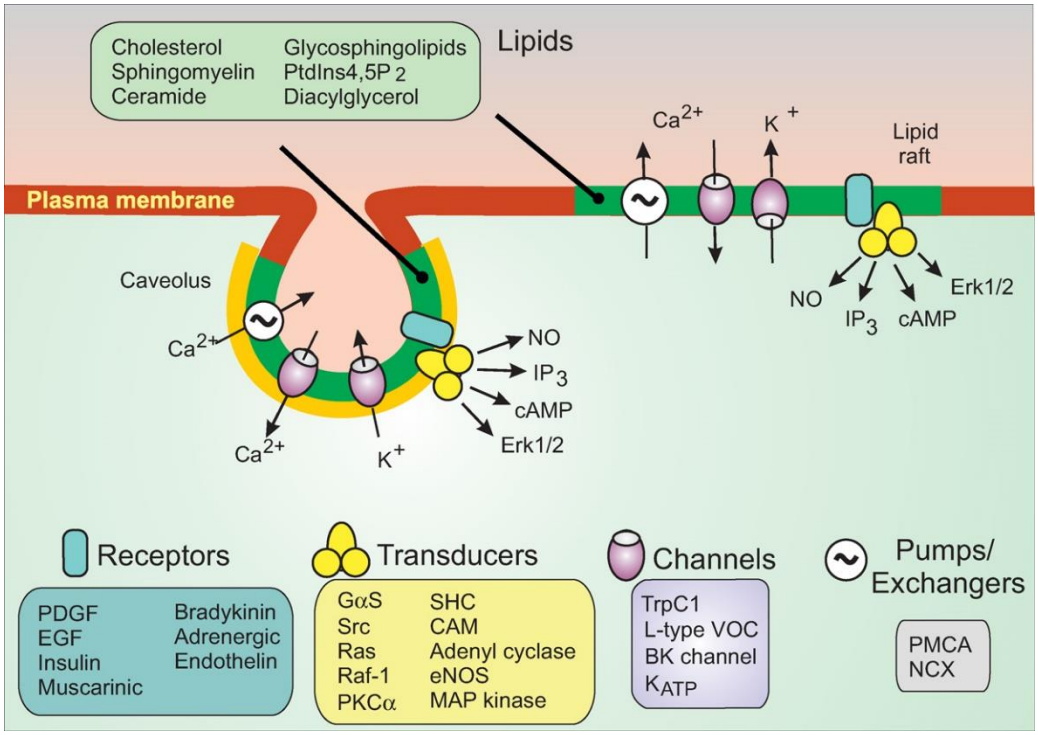

Figure I10. Organization and signaling function of lipid rafts and caveolae. Caveolae are specialized regions of the plasma membrane (green zones), rich in cholesterol and sphingomyelin. Caveolae are constituted having a cytoplasmic coat of caveolin molecules (yellow). They contain a number of signaling components (receptors, transducers, channels, pumps and exchangers) responsible for the initiation of many of the major cell signalling pathways. Figure from: http://www.cellsignallingbiology.org/csb/006/csb006fig6_caveolae_organization.htm.

4.2.4. Mechanoprotection

Since caveolae are highly abundant in mechanically stressed cells, such as muscle cells, fibroblasts, endothelial cells and adipocytes, the role of this structure in mechanoprotection mechanisms has been recently addressed by several laboratories. Experiments using electron microscopy have demonstrated that caveolae are associated with actin cytoskeleton, particularly the stress fibers which are very sensitive to mechanical stress (Echarri and Del Pozo, 2015). Furthermore, Cav-1 and cavin-4 activate RhoA signaling, the main pathway involved in mechanosensing response, resulting in the actomyosin contractility (Echarri and Del Pozo, 2015). On the other hand, mechanical stress produces flattening of caveolae by the dissociation of cavins from the plasma membrane (Sinha et al., 2011). Shear stress, which is constantly suffered by endothelial cells, induces a relocation of caveolae to the trailing edge of the cells (Cheng and Nichols, 2016; Isshiki et al., 2002). Furthermore, Cav-1 knockout mice result in an impaired response to blood flow changes in vessels (Yu et al., 2006). Recently, Nolwenn Briand and colleagues demonstrated for the first time the role of caveolae in the mechanosensing of lipid store fluctuation and the importance of the relation between caveolins and cavins in this function (Briand et al., 2014).

4.3. Caveolae and insulin signaling

Early evidence indicates the importance of caveolae in the regulation of insulin signaling (Yamamoto et al., 1998). A direct interaction between Cav-1 and IR through the scaffolding domain in Cav-1 structure has been demonstrated (Kabayama et al., 2007; Nystrom et al., 1999). Furthermore, ultrastructural experiments also indicate that IR is highly enriched in caveolae in adipocytes plasma membrane (Gustavsson et al., 1999; Sekimoto et al., 2012). This co-localization is also observed in myocytes, hepatocytes, endothelial cells and pancreatic β-cells. *In vitro* studies showed that the stimulation of adipocytes with insulin results in the translocation of glucose transporter GLUT4 within caveolae (Gustavsson et al., 1996). Moreover, insulin stimulation induces IR autophosphorylation and internalization in a process mediated by the rapid tyrosine phosphorylation of Cav-1 (Fagerholm et al., 2009). Further investigation in adipocytes highlighted the importance of caveolae and Cav-1 in insulin-

induced glucose uptake. Repression of Cav-1 protein expression leads to a decrease in GLUT4 translocation to the plasma membrane, triggering the reduction of the insulin-stimulated glucose transport and inhibiting IR phosphorylation (González-Muñoz et al., 2009). The role of the other components of caveolae in the insulin signaling pathway has been also addressed. In cardiomyocytes, fluorescence energy transfer (FRET) experiments have shown that Cav-3 directly interacts with IR. Likewise, haploinsufficiency for Cav-3 in this kind of cells increases the susceptibility to high-fat-induced insulin resistance (Talukder et al., 2016). On the other hand, there is no direct evidence about the role of cavins in the transmission of insulin signaling. However, cavin-1 knockout mice show significantly reduced glucose tolerance and hyperinsulinemia, indicating a potential implication of this protein in the insulin function (Liu et al., 2008). In contrast, cavin-3 ablation in mice has no significant effect in body weight and fat mass when compared to wild type animals, fed with either normal chow or high-fat diets (Liu et al., 2008). Moreover, glucose tolerance is not affected in cavin-3 null mice after both diets (Liu et al., 2014). All these results suggest that cavin-3 is not required for the metabolic function of caveolae *in vivo*.

4.4. Insulin resistance and caveolae

An extensive line of evidence has demonstrated the importance of caveolae in the development of insulin resistance. One of the first reports was the characterization of Cav-1 knockout mice. These mice present postprandial hyperinsulinemia after being fed a high-fat diet (Cohen et al., 2003). Moreover, Cav-1 null mice fed a normal chow diet are significantly unresponsive to insulin due to drastically reduced IR protein levels, without changes in IR mRNA expression, suggesting the stabilization role of Cav-1 over IR in plasma membrane *in vivo* (Cohen et al., 2003). Consistent with this result, skeletal muscle of Cav-3 null mice is insulin resistant, as exemplified by decreased glucose uptake, reduced glucose tolerance test and increased serum lipids. At a molecular level, Cav-3 ablation inhibits insulin-stimulated phosphorylation of IR and downstream molecules, such as IRS-1 (Oshikawa et al., 2004). Furthermore, identification of mutations located in the Cav-1 binding motif of IR supports the clinical importance of the caveolins–IR interaction in the pathogenesis of insulin resistance in humans (Schwencke et al., 2006). Gain of function experiments have demonstrated

that caveolin potently enhances IR signaling when overexpressed in the liver of diabetic obese mice (Otsu et al., 2010).

Low grade chronic inflammation is one of the underlying mechanisms involved in obesity-induced insulin resistance. Treatment of adipocytes with TNF-α, a proinflammatory cytokine, reduces to one fifth the relative ratio of caveolae-associated IR than in normal adipocytes (Sekimoto et al., 2012).

As previously mentioned, obesity results in hypoxia development within adipose tissue, and in this regard results recently obtained by Regazzetti et al suggested a role of caveolae in the hypoxia-induced impairment of insulin signaling in adipocytes. In that work, hypoxia reduced caveolae density in the plasma membrane of adipocytes and downregulated cavin-1 and cavin-2 in 3T3-L1 adipocytes and in epididymal adipose tissue of mice. This effect led to the inhibition of insulin signaling in a HIF-1-dependent mechanism, leading to the establishment of insulin resistance (Regazzetti et al., 2015).

HYPOTHESIS AND AIMS

HYPOTHESIS AND AIMS

1. Hypothesis

Obesity is an important health problem worldwide and courses with hyperplasia and hypertrophy of adipocytes. This situation produces hypoxia within adipose tissue, which has been related to dysregulation of adipocytes function, including development of insulin resistance. It is well known that insulin receptor is located on caveolae, a specialized plasma membrane invagination constituted mainly by two families of proteins: caveolins and cavins. Thus, caveolae promotes the interaction of signaling molecules and therefore, facilitates the appropriate response to stimulus.

Taken all these observations together, our hypothesis is that hypoxia plays an important role in the development of insulin resistance. This effect could be mediated by the disruption of caveolae as a consequence of dysregulation in the expression and activation of caveolins and cavins and the subsequent inhibition of insulin signaling.

2. General aim

The general goal of this project is to explore the effect of hypoxia on caveolae function and insulin signaling, using different experimental models.

3. Specific objectives

1. To study the effect of chronic hypoxia on the differentiation of 3T3-L1 adipocytes.
2. To study the impact of continuous hypoxia (24-48 h) in the expression of caveolae related proteins and insulin response in 3T3-L1 adipocytes.
3. To determine the effect of intermittent hypoxia on caveolae integrity in mouse adipose tissue.
4. To analyze the effect of continuous hypoxia on caveolae structure in human aortic endothelial cells.

MATERIAL AND METHODS

MATERIAL AND METHODS

1. Cell culture

1.1. Culture of 3T3-L1 fibroblasts (ATCC® CL-173™, Rockville)

3T3-L1 cells are able to differentiate from a fibroblast-like phenotype to adipocytes under appropriate conditions and have been widely used for the study of adipogenesis and adipocyte physiopathologies such as inflammation, insulin resistance, type 2 diabetes, etc.

3T3-L1 fibroblasts were maintained in the growing media Dulbecco's Modified Eagle Medium (DMEM; Invitrogen, Carlsbad, CL, USA) with High Glucose (4,5 g/L), 110 mg/L pyruvate and supplemented with 10% of calf bovine serum (Invitrogen, Carlsbad, CL, USA) and 100 U/mL penicillin-streptomycin (Invitrogen, Carlsbad, CL, USA). Two days after confluence, adipocyte differentiation was induced by incubating the cells in DMEM (Invitrogen, Carlsbad, CL, USA) supplemented with 10% Fetal Bovine Serum (FBS) (Invitrogen, Carlsbad, CL, USA), insulin (1 mg/mL) (Sigma-Aldrich, St. Louis, MO, USA), water-soluble dexamethasone (1 mM) (Sigma-Aldrich, St. Louis, MO, USA) and 3-isobutyl-1-methylxanthine (IBMX) (0.5 mM) (Sigma-Aldrich, St. Louis, MO, USA) for 48 hours. The medium was then replaced with DMEM containing 10% FBS and insulin (1 mg/mL) (Sigma-Aldrich, St. Louis, MO, USA) for an additional 48 hours and then maintained with DMEM, 10% FBS without insulin until day 8 of differentiation when cells are considered as mature adipocytes. The cells were cultured in a humidified incubator at 37°C and 5% CO_2.

1.2. Human Aortic Endothelial Cells (HAoEC)

HAoEC (PromoCell®, Heidelberg, Germany) were maintained in Endothelial Cell Growth Medium MV2 (PromoCell®, Heidelberg, Germany) supplemented with 5% Fetal Calf Serum (FCS), 5 ng/mL epidermal growth factor (recombinant human), 10 ng/mL basic fibroblast growth factor (recombinant human), 20 ng/mL insulin-like growth factor (Long R3 IGF-1), 0.5 ng/mL vascular endothelial growth factor 165 (recombinant human), 1 µg/mL ascorbic acid, 0.2 µg/mL (hydrocortisone and 100 U/mL penicillin-streptomycin. All reagents from PromoCell® (Heidelberg, Germany). The cells were cultured in a humidified incubator at 37°C, 5% CO_2.

2. Experimental design

2.1. 3T3-L1 experiments

The studies in 3T3-L1 adipocytes were conducted 8 days after the initiation of the differentiation process. In this point, the cells were incubated in a hypoxia incubator at 1% oxygen (O_2), 5% CO_2 and 94% nitrogen (N_2) for 24 or 48 hours. Cells were then processed as indicated in Fig M1 for further applications.

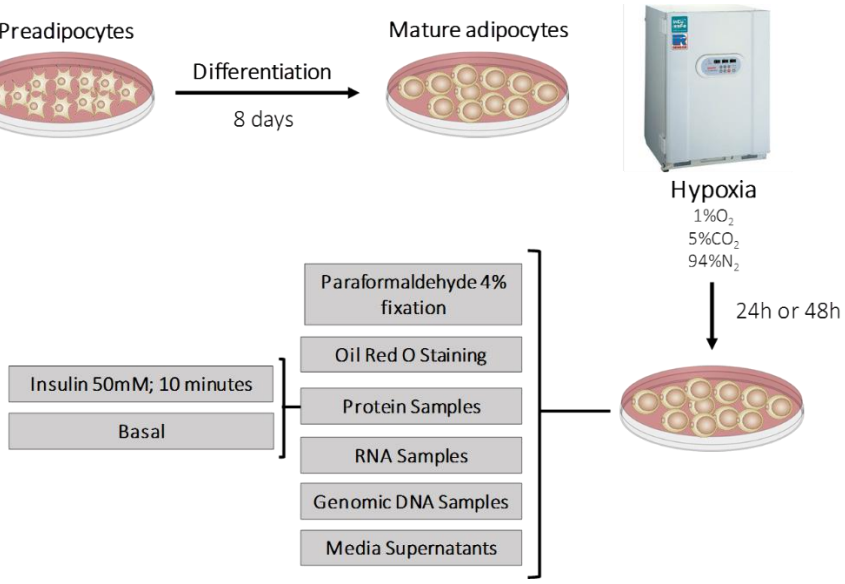

Figure M1. Experimental design for 3T3-L1 cells.

2.2. Intermittent hypoxia experimental model

C57BL/6 mice were divided into 2 groups, exposed to either IH or normoxia (N) (Fig. M2). Animals were exposed to IH stimulus during daytime (8 h/day, cyclic 21-5% Fraction of Inspired Oxygen (FiO_2), 60s cycle (60 events/h) for 14 days or 4 weeks. FiO2 was measured with a gas analyzer (ML206, AD Instruments) throughout the experiment. Control animals (normoxic mice, N) were exposed to air in similar cages to reproduce conditions of IH stimulus. Ambient temperature was maintained at 20–22∘C. Animals were fed on a standard-chow diet. The study was conducted in accordance with the European Convention for the Protection of Vertebrate Animals

Used for Experimental and Other Scientific Purposes (Council of Europe, European Treaties ETS 123, Strasbourg, 18 March 1986) and with the Guide for Care and Use of Laboratory Animals (NIH Publication no. 85-23, revised 1996).

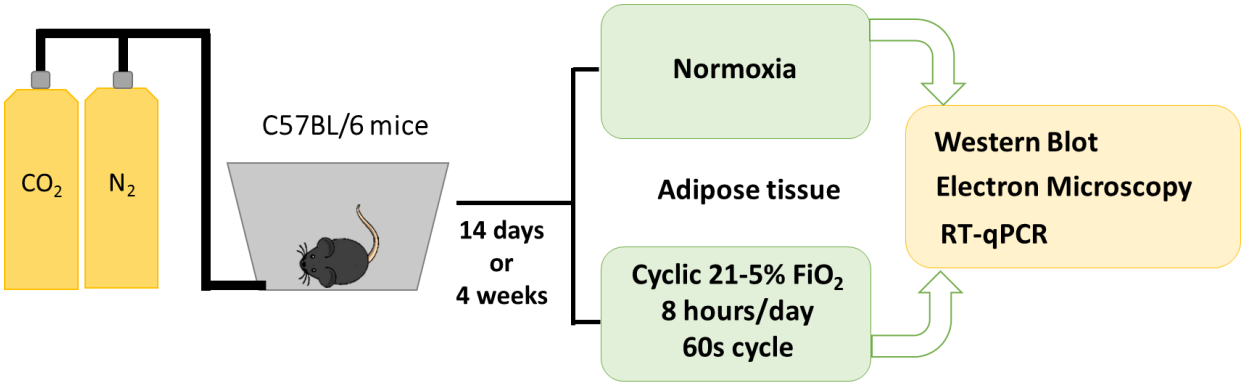

Figure M2. Experimental design to study intermittent hypoxia in adipose tissue

2.3. HAoEC experiments

HAoEC were cultured until confluence and seeded on 6-well plates during 24 hours. The plates were then cultured in hypoxic biosafety cabin during 16 hours. Cells were then processed as indicated in Fig M3 for further applications.

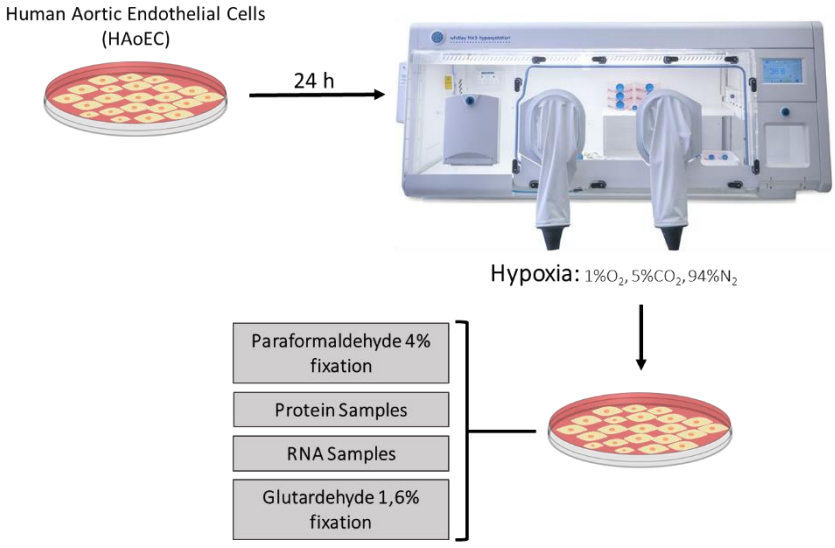

Figure M3. Experimental design for HAoEC

3. Oil red O (ORO) staining

ORO (Sigma-Aldrich, St. Louis, MO, USA), is a fat-soluble diazole dye which stains neutral lipids and cholesterol esters but not biological membranes. In this work ORO staining was used to estimate the degree of adipocyte differentiation. 3T3-L1 pre-adipocytes (day 0) and mature adipocytes at days 8 and 10, incubated in normoxia or hypoxia, were washed twice with phosphate-buffered saline (PBS) and fixed with formaldehyde 3,7% during 15 minutes. After washing three times with isopropanol 60%, cells were stained with ORO stock solution (0.3%w/v in isopropanol), diluted to 40% with water for 30 minutes at room temperature. Cells were then washed four times with PBS and photographed in a light microscope (Olympus Ck2, 40 X magnifications). Finally, incorporated ORO dye was extracted with isopropanol and quantified using a spectrophotometer (Multiskan Spectrum, Thermo Electron Corporation, MA, USA) at 540 nm.

4. 2-[C^{14}]-Deoxyglucose uptake assay

3T3-L1 cells were differentiated as described previously during 8 days (point 1.1). 2-[C^{14}]-Deoxyglucose uptake in 3T3-L1 adipocytes cultured in normoxia or hypoxia with or without 50 µM of a HIF-1 inhibitor LW6 (Millipore, MA, USA; 1:200), was analyzed at both basal state and after insulin stimulation. Cells were incubated in DMEM serum and glucose free for 2 hours in a humidified incubator at 37°C, 5% CO_2, before insulin stimulation Subsequently, cells were stimulated or not with insulin (50 nM) for 10 minutes. 2-C^{14}-deoxyglucose uptake was then initiated by the addition of DMEM, free of serum and glucose, containing 2-deoxyglucose (50 mM) and 2-C^{14}-deoxyglucose (0.075 mCi/mL, (American radiolabeled, Saint Louis, MO, USA). Incubation was continued for 10 minutes and the reaction was terminated by washing cells three times with pre-cold PBS containing 0.05 M glucose. Cells were then incubated with 1mL of lysis buffer (0.1 M NaOH, 0.1% SDS) at 37°C for two hours and the cell lysate was transferred to a tube containing 2 mL of scintillation liquid for radioactivity counting in a scintillation counter (HIDEX 300 SL). 2-Deoxyglucose uptake is reported as [C^{14}] radioactivity, normalized to protein content from the remaining cell lysate, as determined by bicinchoninic acid (BCA) analysis (Thermo Fisher Scientific, Waltham,

MA, USA) (point 7.2.1). Measurements were performed in triplicate under conditions where hexose uptake was linear.

5. Determination of caveolae density in plasma membrane.

Caveolae density in plasma membrane was determined by electron microscopy (EM). Cells were seeded on 6-well plates over a EM coverslip. The day of the experiment the cells were washed with 0.1 M phosphate buffer (pH 7.4) and fixed in 1.6% glutaraldehyde for three days. All the procedure was made at 4°C. After fixation, the cells were rinsed in 0.1 M cacodylate buffer, and postfixed for 1 hour in 1% osmium tetroxide and 1% potassium ferrocyanide in 0.1 M cacodylate buffer to enhance the staining of membranes.

Cells were washed in cold distilled H_2O, quickly dehydrated in cold ethanol, and lastly embedded in epoxy resin. Contrasted ultrathin sections (70 nm) were analyzed under a JEOL 1400 transmission electron microscope (EM) mounted with a Morada Olympus charge-coupled device camera.

6. Extracellular measurement of lactate levels

Lactic acid is the final product of anaerobic glycolysis and is considered to be a good marker of the state of oxygenation in tissues. Lactate level was measured in supernatants of 3T3-L1 cells using ABX Pentra Lactic Acid reagent (Horiba medical, Montpellier, France).

It is an enzymatic colorimetric assay kit which contains two reagents mixed at the moment of use. Briefly, reagent 2 contains lactate oxidase which catalyzes the oxidation of lactate present in the sample, triggering the release of hydrogen peroxide. This product reacts with 4-aminoantipyrine (AAP) and N-ethyl-N-sulfopropyl-m-anisidine (ESPAS) contained in the reagent 1, producing a coloured complex in the presence of peroxidase (Fig. M4). The intensity of the colouring is proportional to the amount of lactate present in the sample and was measured by the ABX Pentra C200 analyzer. Samples were 3 fold-diluted by triplicate. Both, the reagent vial and the samples tube, were placed in the available racks in the ABX Pentra C200 analyzer in order to start the assay.

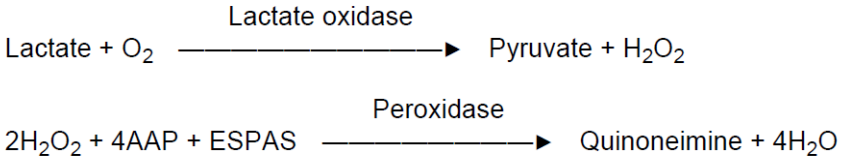

Figure M4. Lactate oxidase reaction to determine lactate levels on 3T3-L1 cells supernatants (ABX Pentra Lactic Acid reagent data sheet).

7. Determination of specific proteins by immunogenic methods

7.1. Extraction of total proteins

Proteins from 3T3-L1 adipocytes were extracted by cell lysis with a specific protein extraction buffer (87% glycerol, 2M Tris-HCl, 5M NaCl, 10% Triton) supplemented with protease inhibitor cocktail (Sigma-Aldrich, St. Louis, MO, USA) 1M NaF, 0.2M sodium orthovanadate (Sigma-Aldrich, St. Louis, MO, USA) and phenylmethanesulfonyl fluoride (PMSF) (Pierce, Rockford, IL, USA) after washing the cells with ice-cold PBS. Protein lysates were obtained by centrifugation at 13,000 rpm, 4°C for 10 minutes.

7.2. Determination of protein concentration

7.2.1. BCA (bicinchoninic acid) protein Assay

Quantification of total protein in the samples of 3T3-L1 cells was determined by the BCA Protein Assay Kit® (Thermo Fisher Scientific, Waltham, MA, USA). This colorimetric method is based on the reduction of Cu^{+2} to Cu^{+1} by protein in an alkaline medium (the biuret reaction). Next, two molecules of BCA chelate one cuprous ion producing a purple-coloured compound which is proportional to the amount of protein in the sample. The assay was carried out in 96-well plates. Protein samples were diluted 10 fold in each well of the plate and a standard curve with known amounts of Bovine Serum Albumin (BSA) was prepared to calculate the protein concentration in the samples. The BCA solution had been prepared mixing 50 parts of BCA Reagent A with 1 part of BCA Reagent B (50:1, Reagent A:B). 20 µL of this solution was added to each well of both, samples and standard dilutions. The plate was then incubated at 37°C for 30 minutes and the absorbance was determined at 540 nm using a spectrophotometer.

7.2.2. Bradford Protein Assay

Quantification of total protein in the samples of HAoEC cells and adipose tissues extracted from mice was determined using the Bradford Protein Assay Kit® (Bio-Rad Laboratories, Hercules, CA, USA). This method involves the binding of Coomassie Brilliant Blue G-250 dye to proteins. Under acidic conditions, the dye is predominantly in the doubly protonated red cationic form (Amax = 470 nm). However, when the dye binds to protein, it is converted to a stable unprotonated blue form (Amax = 595 nm). This blue protein-dye form is proportional to the amount of protein in the sample. Samples were prepared pipetting 20 µL of each into disposable cuvettes. As in the previous procedure a standard curve with known amounts of BSA was prepared. 1 mL of 1X reagent dye was added to each cuvette and incubated at room temperature them for 5 minutes. The absorbance was determined at 595 nm using a spectrophotometer or microplate reader.

7.3. Western Blot

Protein lysates were mixed with loading buffer 4X and denatured by heating at 95°C for 5 minutes. Denatured proteins were resolved in a SDS-PAGE minigels on a Mini-PROTEAN Tetra Cell electrophoresis system (Bio-Rad Laboratories, Hercules, CA, USA) at 130 mV for 90 minutes. Gels were then electroblotted using a Mini Trans Blot® Cell (Bio-Rad Laboratories, Hercules, CA, USA) onto nitrocellulose membranes (Hybond-C Extra, Amersham-Pharmacia, UK). The membranes were blocked with 5% milk or 5% Bovine Serum Albumin in Tris-buffered saline with 0.1% Tween 20 (0.1% TBST) and incubated with specific primary antibodies against HIF-1, Cav-1, Cav-1-Phospho-Tyr^{14}, PTRF/Cavin-1, SDPR/Cavin-2, beta subunit of insulin receptor (IRβ), IRβ-Phospho-Tyr^{1146}, GLUT4, GLUT1, and β-Actin. Detailed information about antibodies and incubation condition is summarized on table M1. Next, the membranes were washed three times with TBST to remove not bound antibodies before incubating them with the correspondent horseradish peroxidase (HRP)-conjugated secondary antibody at the appropriate dilution. Finally, after three washing steps, specific immunoreactive bands were detected by a chemiluminescent ECL assay kit (Lumi-Light ^{plus}, Roche Diagnostic, Mannheim, Germany). β-actin (Sigma-Aldrich, St Louis, MO, USA) was used as an invariant internal control for normalization of protein expression.

Table M1. Antibodies and incubation conditions used for western blot.

Antibody			Incubation condition		Secondary Antibody	
	MW (kDa)	Manufacturer	Dilution	Blocking and incubation solution	Specie	Dilution
phospho-Cav-1 (Tyr14)	24	Santa Cruz Biotechnology Sc-101653	1:5,000	5% BSA TBS-Tween 0,1%	Anti-Rabbit	1:10,000
Phospho-Insulin Receptor β (Tyr1146)	98	Cell Signaling Technology #3021	1:1,000	5% BSA TBS-Tween 0,1%	Anti-Rabbit	1:2,000
IRβ	98	Santa Cruz Biotechnology Sc-711	1:5,000	5% Milk TBS-Tween 0,1%	Anti-Rabbit	1:10,000
GLUT4	50	Sigma-Aldrich G4048	1:3,000	5% Milk TBS-Tween 0,1%	Anti -Rabbit	1:5,000
GLUT1	52	Santa Cruz Biotechnology Sc-7903	1:1,000	5% Milk TBS-Tween 0,1%	Anti -Rabbit	1:2,000
Cav-1	24	Santa Cruz Biotechnology Sc-894	1:10,000	5% Milk TBS-Tween 0,1%	Anti-Rabbit	1:20,000
HIF-1	120	Novus Biological NB100-105	1:250	5% Milk TBS-Tween 0,1%	Anti-Mouse	1:1,000
β-Actin	42	Sigma-Aldrich A1978	1:10,000	5% Milk TBS-Tween 0,1%	Anti-Mouse	1:20,000
Goat Anti-Rabbit IgG (H + L)-HRP	-	Bio-Rad Laboratories 1706515	-	5% Milk TBS-Tween 0,1%	-	-
Sheep Anti-Mouse IgG-HRP	-	GE Healthcare Life Science NXA931	-	5% Milk TBS-Tween 0,1%	-	-

7.4. Immunofluorescence (IF)

7.4.1. HAoEC cells

Cellular location of Cav-1 and PTRF/Cavin-1 in HAoEC after incubation in hypoxia was determined by immunofluorescence (IF). Cells were seeded in 6-well plates with coverslips for IF. The day of the experiment, cells were washed 3 times with Dulbecco's phosphate-buffered saline (DPBS) (Gibco™ Invitrogen Corporation, Grand Island, NY, USA) and fixed with 4% paraformaldehyde (Thermo Fisher Scientific, Waltham, MA, USA) for 15 minutes at room temperature. After 3 washes with DPBS to remove the fixative solution, cells were permeabilized and blocked with 0.1% saponin and 0.2% gelatin in PBS buffer during 10 minutes. Next, each coverslip was incubated with specific primary antibody against Cav-1 (Santa Cruz Biotechnology, 1:200), PTRF (Millipore, MA, USA; 1:200) diluted in a buffer containing 0.01% saponin, 0.2% gelatin and 0.02% sodium azide in PBS (SG/PBS Buffer). The incubation was carried out in a moist chamber overnight at 4°C. Coverslips were then washed 3 times with SG/PBS buffer and incubated with suitable fluorescent secondary antibody, anti-Rabbit (1:500), in a moist chamber for 1 hour at room temperature. Coverslips were washed 4 times with DPBS and placed in the microscope slide over a drop of mowiol® (Sigma-Aldrich, St Louis, MO, USA) mounting medium and visualized in a confocal laser fluorescence microscopy (Zeiss LSM 710, Oberkochen, Alemania).

7.4.2. 3T3-L1 adipocytes

For Cav-1 and GLUT4 location in 3T3-L1 adipocytes by IF, cells were seeded over coverslips. The day of the experiments, cells were washed three times with DPBS and then fixed with 4% paraformaldehyde (Thermo Fisher Scientific, Waltham, MA, USA) for 15 minutes and permeabilized for 20 minutes with 0.1% Triton X-100. Cells were then incubated with specific primary antibody against Cav-1 (Santa Cruz, 1:200) and GLUT4 (Sigma-Aldrich, St. Louis, MO, USA; 1:200) in 1X DPBS with 1% gelatin. Incubation was performed at room temperature for 1 hour. After three washes with a solution of 1X DPBS and 1% gelatin, cells were incubated with Alexa Fluor 633 Goat anti-Rabbit IgG (H+L) secondary antibody (Thermo Fisher Scientific, Waltham, MA, USA) for 1 hour at room temperature. Coverslips were washed 4 times with DPBS and

placed in the microscope slide over a drop of mounting media with Dapi (Sigma-Aldrich, St Louis, MO, USA) and visualized in a LSM 800 confocal laser-scanning microscope (Zeiss, Jena, Germany).

8. Extraction and analysis of RNA

8.1. Total RNA extraction

8.1.1. 3T3-L1 adipocytes

RNA extraction was carried out with TRIzol® Reagent (Invitrogen, Carlsbad, CL, USA) according to manufacturer's instructions. Cells were lysed with 1 mL of TRIzol using a cell scraper and then incubated for 5 minutes at room temperature. 200 µL of chloroform was added to each sample and mixed vigorously by inversion. After 5 minutes of incubation at room temperature, the samples were centrifuged at 12,000 g, 4°C for 15 minutes. The resulting colourless upper aqueous phase containing the RNA was removed carefully and placed in a new 1.5 mL tube previously filled with 1 mL of isopropanol. The mixture was incubated overnight at -20°C to increase RNA precipitation. Samples were next centrifuged at 12,000 g, 4°C for 15 minutes. The resulting pellet was washed with 1 mL of cold 75% ethanol by vortexing and subsequently centrifuged at 7,500 g for 5 minutes. Total RNA pellet was air-dried and resuspended in 15 µL of RNase free water. RNA concentration of the samples was measured using the NanoDrop spectrophotometer (Thermo Fisher Scientific, Waltham, MA, USA) and stored at -80°C for further applications.

8.1.2. HAoEC and adipose tissue samples

RNA extraction of HAoEC cells and adipose tissue samples submitted to intermittent hypoxia was carried out using the RNeasy mini kit (Qiagen N.V, Hilden, Germany). Samples were harvested with 1 mL of QIAzol lysis reagent (Qiagen N.V, Hilden, Germany) and placed in 1.5 ml tubes. 1 mL of 70% ethanol was added to the lysate and transferred to an RNeasy mini spin column. Columns were centrifuged at 8,000 x g for 15 seconds and the flow-through was discarded. DNase treatment was carried out on-column according to manufacturer's instruction (Qiagen N.V, Hilden, Germany). To wash the column, 350 µL Buffer RW1 was added followed by centrifugation for 15 seconds at 8,000 x g. 80 µL DNase I mix containing 10 µL DNase I and 70 µL Buffer RDD,

was added to each column and incubated at the benchtop for 15 minutes. After that time, 350 µL Buffer RW1 was added to each column and then centrifuged at 8,000 x g for 15 seconds. Two washes with 500 µL Buffer RPE were performed, the first one at 8,000 x g for 15 seconds and the second one at 8,000 x g for 2 minutes. The columns were totally dried by placing them in a new 2 mL collection tube and centrifuged at 16,000 x g for 1 minute. Finally, RNA was eluted by adding 30 µL of RNase-free water to each column. The columns were then placed in new 1.5 mL collection tubes and centrifuged at 8,000 x g for 1 minute. The RNA concentration of the samples was measured using the NanoDrop® spectrophotometer (Thermo Fisher Scientific, Waltham, MA, USA) and stored at -80°C for further applications.

8.2. Treatment with DNase

RNA samples were treated with Ambion® DNase-free Kit (Thermo Fisher Scientific, Waltham, MA, USA) before the reverse transcription to avoid genomic DNA contamination. For this purpose, 2 µg of total RNA were diluted to 8 µL with RNase free water. Next, 2 µL of a mixture containing 1 volume of 10X DNase I Buffer and 1 volume of rDNase I was added to each RNA sample. The samples were then incubated at 37°C for 30 minutes in a thermocycler (GeneAmp®PCR System 9600, Roche Diagnostic System). Then, 2 µL of resuspended DNase Inactivation Reagent were added to each sample and centrifuged at 10,000 g for 1 minute. The supernatants were transferred to a new 0.5 mL PCR tube to continue with the reverse transcription reaction.

8.3. Reverse transcription

8.3.1. 3T3-L1 adipocytes

Synthesis of cDNA from RNA samples was carried out using M-MLV Reverse Transcriptase kit (Invitrogen, Carlsbad, CA, USA) following manufacturer's instruction. Briefly, 3 µL of a mix composed by 20 µg/mL Random Primers (Invitrogen, Carlsbad, CA, USA) and 10 Mm dNTP mix (dATP, dGTP, dCTP and dTTP) were added to each tube. Samples were heated at 65°C for 5 minutes in a thermocycler (GeneAmp®PCR System 9600, Roche Diagnostic System) and then chilled on ice quickly. After a brief spin in a picofuge, 7 µL of a mix composed by 4 µL First-Strand Buffer (5X), 2 µL DTT (0.1 M) and

1µL RNase OUT™ Recombinant Ribonuclease Inhibitor (40 units/µL) were added to each tube, followed by incubation at 37°C for 2 minutes. Finally, 1 µL (200 units) of M-MLV RT was added to each sample which were then incubated in turn at 25°C for 10 minutes; 37°C for 50 minutes and at the end at 70°C for 15 minutes to inactivate the enzyme. The cDNA was stored at -20°C until further applications.

8.3.2. HAoEC and adipose tissue samples

Total RNA (500 ng) from HAoEC cells and adipose tissue samples, subjected to intermittent hypoxia, was reverse transcribed using random hexamers and oligo(dT) primers and PrimeScriptTM RT reagent Kit (Takara/Clontech, Mountain View, CA). The following mix reaction was prepared on ice (Table M2).

Table M2. Master mix for reverse transcription of RNA samples using PrimeScriptTM RT reagent Kit°°

Reagent	Volume (µL) Reaction	Final Concentration/Amount
5 × PrimeScriptTM Buffer	2	1X
PrimeScriptTM RT Enzyme Mix I	0.5	
Oligo(dT) Primers (50 µM)	0.5	25 pmol
Random Hexamers (100 µM)	0.5	50 pmol
Total RNA	x	500 ng
RNase-Free Water	x	x

Final Volume: 10 µL

Reaction mixtures were incubated at 37℃ for 15 minutes followed by an inactivation step of the enzyme at 85℃ for 5 seconds. The reaction was performed in a thermocycler. The samples were stored at -20°C until further application.

8.4. Real time Polymerase Chain Reaction (RT-PCR)

Gene expression was assessed by reverse transcription quantitative polymerase chain reaction (RT-qPCR).

8.4.1. Real time PCR: Taqman probes reaction protocol

The expression analysis of 3T3-L1 genes was performed using predesigned TaqMan® probes described in table M3. The genes and probes used in the assays are summarized in table M2. cDNA was amplified in an ABI Prism 7300 HT Sequence Detection System (Applied Biosystems, Foster city, CA, USA), using the TaqMan® Universal PCR Master Mix (Applied Biosystems, Foster city, CA, USA) according to standard conditions: 50°C for 2 minutes and 95°C for 10 minutes, followed by 40 cycles of 15 seconds at 95°C and 1 minutes at 60°C. Cyclophilin (Ppia) was used as invariant internal control for RT-PCR and subsequent normalization. Relative quantification of gene expression was calculated by the $2^{-\Delta\Delta Ct}$ method (Bustin, 2000).

Table M3. Gene probes used in Taqman® reaction protocol.

Gene	Tqman® probe
Insr	Mm_01211875_m1
Akt2	Mm02026778_g1
Slc2a4	Mm00436615_m1
Slc2a1	Mm 00441480_m1
Cav-1	Mm_00483057_m1
Cav-2	Mm 01129337_g1
Sdpr	Mm 00507087_m1
Adipoq	Mm 00456425_m1
Pparg	Mm 00440940_m1
Cbpa	Mm 00514283_s1
Pi3kr3	Mm 00725026_m1
Ppia	Mm 02342430

8.4.2. Real time PCR: SYBR Green I reaction protocol

To determine gene expression levels in HAoEC and adipose tissue, 2X IQ™ SYBR® Green Supermix (Bio-Rad Laboratories, Hercules, CA, USA) was used. The reaction mix contained 10 µL of the master mix (Bio-Rad Laboratories, Hercules, CA, USA) and 100 nM of forward and reverse primers (table M4) was prepared in a final volume of 20 µL. The qPCR was carried out in a CFX96 Touch™ Real-Time PCR Detection System (Bio-Rad Laboratories, Hercules, CA, USA) according to standardized conditions. Briefly, an initial denaturation step at 95°C for 10 minutes was followed by 40 cycles of amplification, alternating between 95°C for 15 seconds, the corresponding annealing temperature for each gene for 30 seconds and 72°C for 30 seconds. After the amplification step, the melting curve analysis was carried out as follows: from 70°C to 90°C for 30 seconds at every increase of 0.5°C. Relative quantification of gene expression was calculated by the $2^{-\Delta\Delta Ct}$ method (Bustin, 2000)

Table M4. Primer sequences of analyzed mouse genes using SYBR Green I® reaction protocol.

	Forward (5'→3')	Reverse (5'←3')
	Sequence	**Sequence**
mCav-1	AACATCTACAAGCCCAACAACAAGG	GGTTCTGCAATCACATCTTCAAAGTC
mCav-2	TGACGCCTACAGCCACCACA	TGACGCCTACAGCCACCACA
mPTRF	AGCAACACCGTGAGCAAGTT	GCCTCGTTGACCTCCAGTTTCT
mSDPR	CCGTGCACACACTCCTGGAT	CACCGAGCCCTCCAGGTT
m36B4	TCCAGGCTTTGGGCATCAC	CTTTATCAGCTGCACATCAC

8.5. RNA microarray

The sense cDNA was prepared from 300 ng of total RNA using the Ambion® WT Expression Kit (Thermo Fisher Scientific, Waltham, MA, USA). The sense strand cDNA was then fragmented and biotinylated with the Affymetrix GeneChip® WT Terminal Labeling Kit. Labeled sense cDNA was hybridized to the Affymetrix Mouse Gene 1.0 ST microarray according to the manufacturer protocols and using GeneChip® Hybridization, Wash and Stain Kit. Genechips were scanned with the Affymetrix

GeneChip® Scanner 3000. Both background correction and normalization were done using RMA (Robust Multichip Average) algorithm (Irizarry et al., 2003). After quality assessment, a filtering process was performed to eliminate low expression probe sets. Applying the criterion of an expression value greater than 16 in 3 samples for each experimental condition (normoxia and hypoxia), 24819 probe sets were selected for statistical analysis. R and Bioconductor were used for preprocessing and statistical analysis (Gentleman, 2005). LIMMA (Linear Models for Microarray Data) was used to find out the probe sets that showed significant differential expression between experimental conditions (Smyth, 2004). Adjusted p value was calculated with Benjamini-Hochberg procedure. Genes were selected as significant using criteria of B> 5. The Log Odds or B value is the odds or probability that the gene is differentially expressed, meaning that a gene with B=0 has a 50% chance to be differentially expressed. Functional enrichment analysis of Gene Ontology (GO) categories was carried out using standard hypergeometric test.

9. Extraction and analysis of DNA

9.1. Chromatin Immunoprecipitation (ChIP) assay

The ChIP-IT Express Enzymatic Kit (Active Motif, Carlsbad, California) was used to determine the binding of HIF-1 to Hypoxia Response Elements (HRE) in 3T3-L1 adipocytes after hypoxia treatment. Fig M5 summarizes the process, which was carried out according to the manufacturer's instructions. Briefly, cells were fixed with 4% formaldehyde to fix protein/DNA interactions and then sheared by enzymatic digestion. Sheared chromatin was incubated with a specific antibody against HIF-1, and antibody-bound protein/DNA complexes were precipitated using magnetic Protein G-coupled beads. The precipitated chromatin was then eluted and the cross links between proteins and DNA reversed. The recovered DNA was analyzed by qPCR and specific primers to identify DNA HREs.

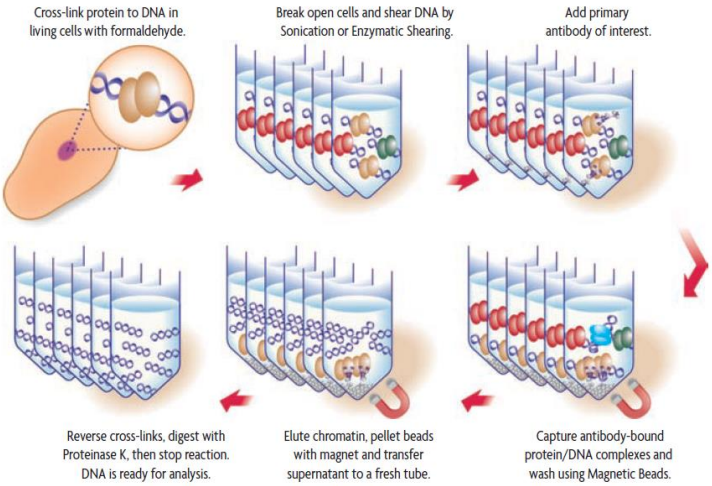

Figure M5. Flow chart of ChIP process using the ChIP-IT Express® Enzymatic Kit.

9.1.1. Preparation of sheared chromatin

9.1.1.1. Cell fixation

3T3-L1 cells were growth in 15 cm plates, differentiated for 8 days and incubated for 48 hours in hypoxia as previously described. Before harvesting the cells the following solutions were freshly prepared:

Volumes for 1 plate of 15 cm.

Formaldehyde 1% (Fixation Solution):

19.46 mL DPBS 1X (Invitrogen, Carlsbad, CL, USA)

540 µL 36.5% formaldehyde (Sigma-Aldrich, St. Louis, MO, USA)

Glycine Stop-Fix Solution

8 mL sterile H_2O

1 mL glycine (Sigma-Aldrich, St. Louis, MO, USA)

1 mL 10X PBS (Active Motif, Carlsbad, California)

Cell Scraping Solution

4.5 mL sterile H_2O

0.5 mL 10X PBS (Active Motif, Carlsbad, California)

25 µL PMSF (was added just before use) (Sigma-Aldrich, St. Louis, MO, USA)

The medium was removed and cells were washed with cold DPBS 1X (Invitrogen, Carlsbad, CL, USA). 20 mL of fixation solution was added to each plate and incubated for 10 minutes at room temperature. The fixative solution was poured off and cells were washed with ice-cold DPBS before the addition of 10 mL Glycine stop-fix solution to each plate. After 5 minutes of incubation, the glycine stop-fix solution was removed and cells were washed again with ice-cold DPBS 1X. Cells of each plate were harvested with 5 mL ice-cold Cell Scraping Solution and collected in 15 mL conical tubes. Next, the tubes were centrifuged at 720 x g for 10 minutes at 4°C to pellet the cells. The supernatants were subsequently removed and discarded and the pellets were stored at -80°C after the addition of 1 µL 100 mM PMSF and 1 µL PIC until the chromatin shearing step was performed.

9.1.1.2. Chromatin shearing

For chromatin shearing, pellets were thawed on ice and resuspended in 1 mL ice-cold lysis buffer supplied by the kit (Active Motif) and supplemented with 5 µL PIC and 5 µL PMSF. The tubes were vortexed and incubated on ice for 30 minutes. During this incubation, a working stock of Enzymatic Shearing Cocktail (200 U/mL) was prepared by diluting the supplied Enzymatic Shearing Cocktail 1:100 with 50% glycerol in dH_2O. Cells of each tube were transferred to an ice-cold Dounce homogenizer and homogenized on ice with 10 strokes to aid in nuclei release. Cells were then transferred to a 1.5 mL microcentrifuge tube and centrifuged for 10 minutes at 2,400 x g at 4°C to pellet the nuclei. Supernatant was removed from each tube and the pellet was resuspended in 350 µL Digestion Buffer supplied by the kit and supplemented with 1.75 µL PIC and 1.75 µL PMSF. After 5 minutes of incubation at 37°C, 17 µL of the working stock of Enzymatic Shearing Cocktail (200 U/mL) was added to each tube. The incubation time for efficient chromatin shearing for this experiment was optimized to 15 minutes at 37°C. The reaction was then stopped by adding 7 µL ice-cold 0.5 M EDTA to each tube and placing them on ice for 10 minutes. Next, the sheared chromatin samples were centrifuged for 10 minutes at 18,000 x g at 4°C. Supernatant was carefully transferred to a new 1.5-mL microcentrifuge tube and distributed as follows:

- 10 µL to carry out the INPUT. Stored at -20°C.

- 25 µL to carry out the CLEANUP step to validate shearing efficiency. Stored at -20°C.
- 140 µL for the immunoprecipitation step. Stored -80°C.

9.1.2. DNA clean-up

The 25 µL aliquots of sheared chromatin were thawed and the volume was adjusted to 200 µL with dH_2O. When all samples were ready, 10 µL 5M NaCl was added to each tube and heated at 65°C overnight to reverse the protein/DNA cross links. The next day, 1 µL RNase A was added to each sample, which were then incubated at 37°C for 15 minutes. After a brief spin in a picofuge, 10 µL Proteinase K (Active Motif, Carlsbad, California) was added to each sample followed by incubation at 42 °C for 1.5 hours.

9.1.2.1. DNA extraction

After proteinase K incubation, DNA from each sample was phenol/chloroform extracted and precipitated following manufacturer's instruction. Briefly, 200 µL of Ultrapure™ Phenol:Chloroform:Isoamyl Alcohol (25:24:1) pH 8.0 (Thermo Fisher Scientific, Waltham, MA, USA) was added to each sample and centrifuged at 13,000 x g for 10 minutes at 4°C. The supernatants (aqueous phase) were then transferred to a fresh microcentrifuge tube and 20 µL 3M sodium acetate pH 5.2 and 500 µL absolute ethanol were added and mixed by vortex. The mix was stored at -20°C overnight in order to precipitate the DNA. The next day, samples were centrifuged at 16,000 x g for 10 minutes at 4°C. The supernatants were removed and discarded and the pellets were washed with 500 µL 70% of ice-cold ethanol. The samples were again centrifuged at 16,000 x g speed for 5 minutes, the supernatants were removed and the pellets were allowed to air dry before resuspending them in 30 µL dH_2O. DNA concentration of each sample was determined in a NanoDrop® Spectrophotometer ND-1000. In order to verify fragmentation efficiency, 500 ng Clean Up-DNA was loaded and resolved in a 1% agarose gel at 100 mV for 50 minutes. The band pattern was visualized using a Bio-Rad ChemiDoc XRS System.

9.1.3. Chromatin immunoprecipitation

For immunoprecipitation, 5 µg of chromatin from each sample was used. The antibody against HIF-1α (H1alpha67, Novus Biologicals) used for this experiment has been ChIP-validated previously and 3 µg was used for each sample. The procedure followed was according to manufacturer's instruction.

Fixed and sheared chromatin samples stored at -80°C were thawed on ice and the immunoprecipitation reactions were prepared as shown in table M4.

Table M5. Composition of immunoprecipitation reaction mix.

Reactive	< 60 µl Chromatin	>60 µl Chromatin
dH_2O (q.s.)*	100 µL	200 µL
ChIP Buffer 10X	10 µL	20 µL
Proteinase Inhibitor Cocktail	1 µL	1 µL
Chromatin (5 µg)	20-60 µL	61-100 µL
Protein G-Magnetic Beads	25 µL	25 µL
6- Antibody (3 µg)	1-3 µg (2.5 µL)	1-3 µg (2.5 µL)
Final Volume	**100 µl**	**200 µl**

*q.s.: "quantum sufficit"/quantity required

The volume of each reagent was according to chromatin concentration determined in the Clean-Up step. If the volume of chromatin necessary for 5 µg is less than 60 µL, the final volume of the reaction is 100 µL. If the volume of chromatin is more than 60 µL, the final volume of the reaction is 200 µL.

Once the immunoprecipitation reaction mixes were prepared, the tubes were placed on a tube rotator and incubated overnight at 4 °C. After incubation, the tubes were briefly centrifuged and placed on a magnetic stand to pellet the beads. The supernatants were discarded and the beads were washed once with 800 µL ChIP Buffer 1 and then twice with 800 µL ChIP Buffer 2. Next, the beads were resuspended with 50 µL Elution Buffer AM2 and incubated 15 minutes at room temperature in a tube rotator before 50 µL of the Reverse Cross-linking Buffer were added to the eluted chromatin. The beads were then precipitated using the magnetic bar and the supernatants which contained the chromatin, were transferred to a fresh tube. At this

time, the inputs of all samples were prepared as follows: 500 ng of input DNA aliquots obtained in the chromatin shearing step were mixed with the required volume of ChIP Buffer 2 to reach 98 µl and added together with 2 µl of NaCl.

The ChIP and Input DNA samples were incubated then at 95°C for 15 minutes in a thermocycler (Bio-Rad Laboratories, Hercules, CA, USA) and 2 µL Proteinase K was added to each tube. The samples were incubated then at 37°C for 1 hour and the reaction was stopped by adding 2 µL Proteinase K Stop Solution. The DNA samples obtained were stored at -20°C until the qPCR analysis.

9.1.4. PCR analysis

A potential HRE (5'-[AG]CGTG-3') for the binding of HIF-1α to the Cav-1 promoter was previously identified by a bioinformatic analysis with TRANSFAC® of the NCBI sequence NC_000072.6. The HRE is located at -442 upstream transcription starting site (TSS) and was amplified and quantified by RT-qPCR in the immunoprecipitated samples with the following pair of primers: Fw-CCCAGCCATCTCGCTTCTAT and Rv-CCCAGCCATCTCGCTTCTAT. A mix containing SYBR Green Master Mix 2X (Bio-Rad Laboratories, Hercules, CA, USA), 10 µM Primers Mix (Sigma-Aldrich, St. Louis, MO, USA) and the immunoprecipitated or the input DNA was prepared in a final volume of 20 µL. The RT-qPCR was carried out in a 7300 Fast Real-Time PCR System (Applied Biosystems, Foster city, CA, USA) under optimal conditions. An initial denaturation step at 95 °C for 10 minutes was followed by 45 cycles of amplification, alternating between 95 °C for 15 seconds and 65°C (annealing temperature) for 1 minute. After the amplification step, the melting curve analysis was carried out as follows: from 70 °C to 90 °C, 15 seconds at every increase of 0.5 °C. Relative quantification of gene expression was calculated by the $2^{-\Delta\Delta Ct}$ method (Bustin, 2000).

10. Statistical analysis

All data are represented as the mean ± standard deviation. Once normality and homogeneity of variance analysis were assessed, a parametric or nonparametric analysis was selected. Statistically significant differences among three or more groups were analysed by one-way analysis of variance (ANOVA) or two-way ANOVA, followed by Tukey post-hoc analysis. Comparisons between two groups were carried out by t-

test (as parametric test) or by Mann-Witney U test (as nonparametric test). The significance level was set to $p < 0.05$ and classified by asterisks as follows: $p < 0.05$ (*); $p < 0.01$ (**); $p < 0.001$ (***). The statistical analysis was calculated through GraphPad Prism software for Windows (version 5.04).

RESULTS

RESULTS

1. Effect of hypoxia on 3T3-L1 adipocytes.

1.1. Continuous hypoxia inhibits adipogenesis in 3T3-L1 adipocytes

In order to study how hypoxia could affect the differentiation process of 3T3-L1 pre-adipocytes, we established a continuous hypoxia model. 3T3-L1 cells were differentiated in hypoxia (1% O_2) during 10 days, starting at the first day after the hormonal cocktail was added (day 0). At the end of this period mRNA and protein samples were extracted for analysis. Hypoxic response of the cells was confirmed by measuring HIF-1 α expression by western blot. As expected, HIF-1α protein expression was significantly induced in 3T3-L1 cells ($P<0.05$) after 10 days of incubation under hypoxia (Fig R1).

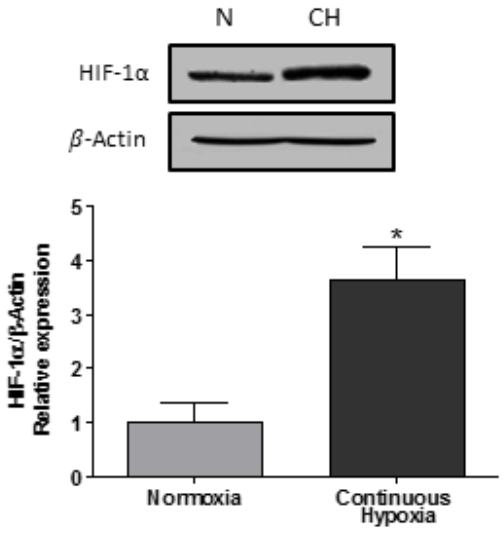

Figure R1. ***HIF-1α protein expression is induced during 3T3-L1 differentiation after 10 days of incubation under hypoxia.*** 3T3-L1 preadipocytes were treated with the differentiation hormonal cocktail and incubated in hypoxia (1% O_2) throughout the differentiation process. After 10 days, HIF-1α protein expression level was determined by western blot. Values were normalized to β-actin and mean of fold change vs normoxia condition ± SEM was represented (n=3). * $P<0.05$. N: Normoxia; CH: Continuous Hypoxia.

The main phenotypic feature of mature adipocytes is the accumulation of fat in the cytoplasm. Therefore, in order to estimate the effect of hypoxia on the adipogenesis process, we determined the triglyceride content of the cells using ORO staining. Incubation of 3T3-L1 cells in hypoxia (1% O_2) throughout the differentiation process

strongly reduced triglyceride accumulation (P<0.001) when compared to cells maintained in normoxia (Fig R2).

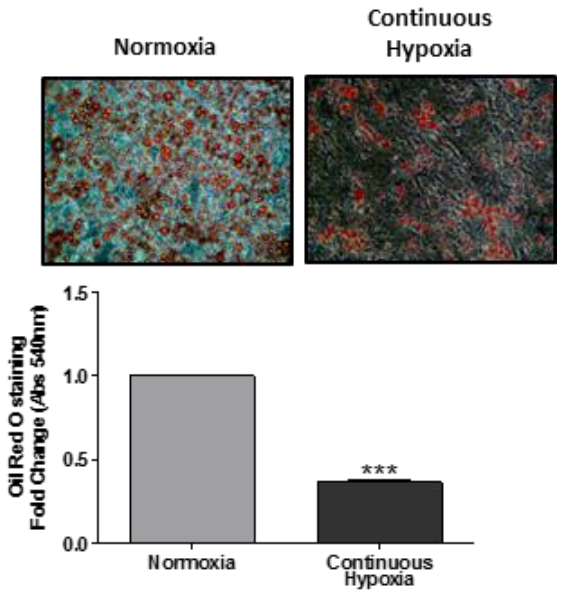

Figure R2. ***Anti-adipogenic effect of hypoxia during 3T3-L1 cells differentiation.*** ORO staining of 3T3-L1 cells differentiated in hypoxia (1% O_2) for 10 days. Stained cells were photographed and ORO staining was quantified measuring the absorbance at 540 nm. Means of fold change ± SEM are represented for each group (n=6). ***P<0.001.

To investigate the status of insulin signaling in 3T3-L1 cells after the differentiation process, expression of insulin signaling-related genes was determined by RT-PCR. *Insr* (IR; P<0.05), *Akt2* (Akt2/PKB; P<0.01) and *Slc2a4* (GLUT4; P<0.001), mRNAs were downregulated in 3T3-L1 cells differentiated in hypoxia for 10 days compared to cells cultured under normoxia (Fig R3A). Moreover, protein expression of insulin receptor determined by western blot was also significantly reduced (P<0.05) after continuous incubation in hypoxia (Fig R3B).

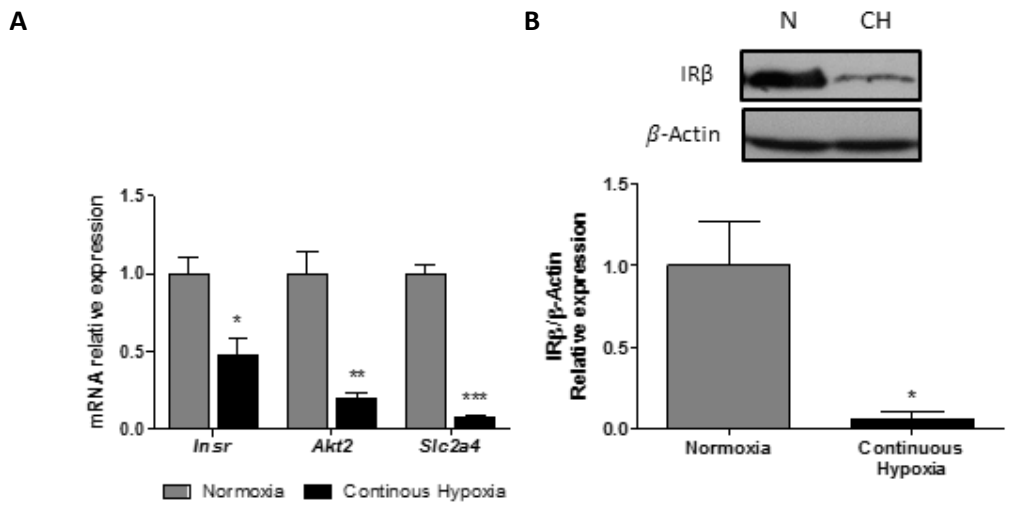

Figure R3. ***Insulin signaling is downregulated in 3T3-L1 cells differentiated under hypoxia.*** 3T3-L1 preadipocytes were treated with the differentiation hormonal cocktail and incubated in normoxia or hypoxia (1% O_2) for 10 days. (A) mRNA expression of Insulin receptor (*Insr*), Akt2/PKB (*Akt2*) and GLUT4 (*Slc2a4*) were determined by RT-PCR. Cyclophilin (*Ppia*) gene was used as endogenous control for normalization and the expression level was represented as fold change vs normoxia condition ± SEM (n=3). (B) IRβ protein expression was determined by western blot. Values were normalized to β-actin and means of fold change vs normoxia condition ± SEM were represented (n=3). * P<0.05. N: Normoxia; CH: Continuous Hypoxia.

Since there exists ample evidence indicating the importance of caveolae in the insulin signaling transmission, we have determined the expression of Cav-1 in 3T3-L1 cells after differentiation in continuous hypoxia. In agreement with the data previously shown regarding insulin signaling (Fig R3), Cav-1 expression, at both mRNA and protein level, was significantly reduced (P<0.05) after 10 days of differentiation in hypoxia compared to normoxia group (Fig R4).

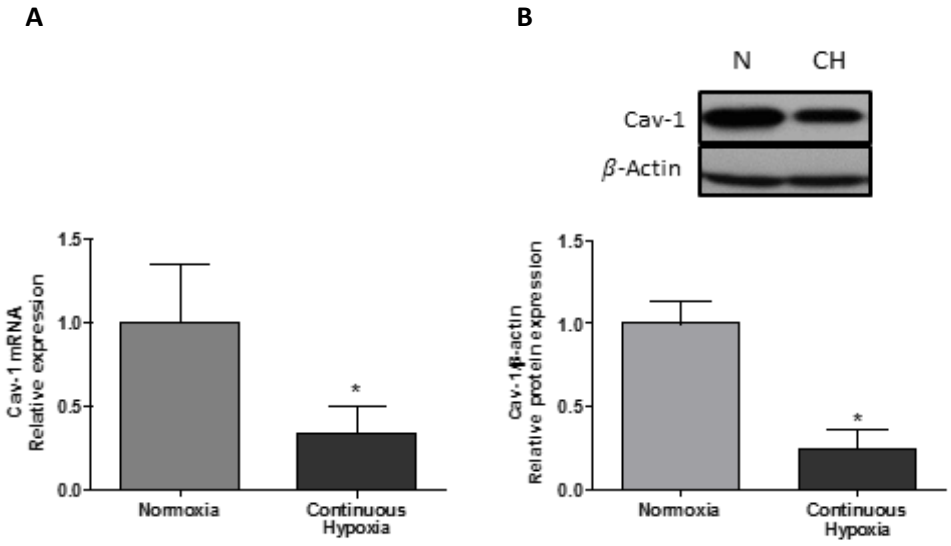

Figure R4. ***Caveolin-1 expression is reduced in 3T3-L1 cells differentiated under hypoxia.*** 3T3-L1 preadipocytes were treated with the differentiation hormonal cocktail and incubated in hypoxia (1% O2) for 10 days. (A) mRNA expression of *Cav-1* was determined by RT-PCR. Cyclophilin (*Ppia*) gene was used as endogenous control for normalization and the expression level was represented as fold change vs normoxia condition ± SEM (n=3). (B) Cav-1 protein expression was determined by western blot. Values were normalized to β-actin and means of fold change vs normoxia condition ± SEM were represented (n=3). * P<0.05. N: Normoxia; CH: Continuous Hypoxia.

These results demonstrate that continuous hypoxia during differentiation in 3T3-L1 adipocytes strongly inhibit adipogenesis. Therefore, the cells after 10 days of differentiation still retained mostly a fibroblast-like phenotype (Fig R2), with reduced expression levels of adipocyte characteristic proteins (Fig R3,4).

Hence, since our aim was to investigate hypoxia-induced dysregulation in mature adipocyte functions, in the following set of experiments, 3T3-L1 pre-adipocytes were first differentiated for 8 days and then submitted to hypoxia.

1.2. Hypoxia during 48 hours induces insulin resistance in 3T3-L1 adipocytes

To determine the effect of hypoxia in already differentiated 3T3-L1 adipocytes, cells at day 8 after starting the differentiation process were incubated in hypoxia (1% O_2) for 48 hours until day 10. ORO staining to measure intracellular triglyceride accumulation in normoxia group at days 0, 8 and 10 showed a time-dependent increase (Fig R5) (P<0.05, P<0.01). However, incubation of adipocytes at day 8 of differentiation under

hypoxia for 48 hours, reduced triglyceride accumulation at day 10 (P<0.01) when compared to cells maintained in normoxia (Fig R5).

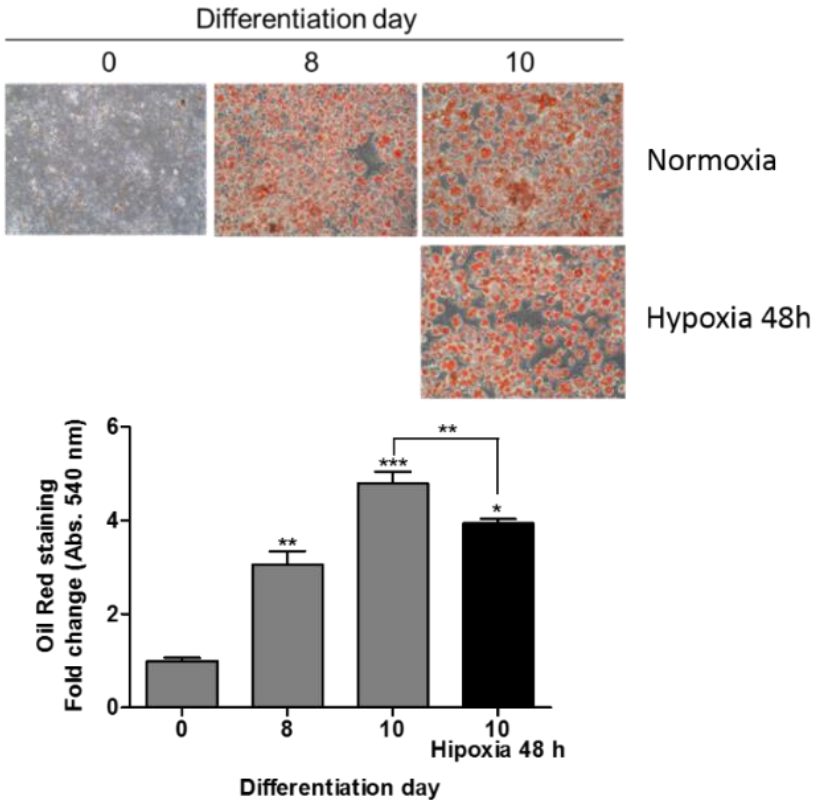

Figure R5. ***Hypoxia for 48 hours significantly reduces triglyceride accumulation in 3T3-L1 adipocytes.*** ORO staining of 3T3-L1 cells at day 0, 8 and 10 of differentiation in normoxia and at day 10 after 48 hours of hypoxia (1% O_2). Stained cells were photographed and ORO staining was quantified measuring the absorbance at 540 nm. Means of fold change ± SEM are represented for each group (n=6). *P<0.05, **P<0.01, ***P<0.001.

Since hypoxia has been considered one of the factors responsible for the development of insulin resistance in obese adipose tissue, we have also analyzed the insulin signaling status in 3T3-L1 adipocytes after 48 hours of hypoxia. A significant reduction in mRNA expression of *Insr* (IR; P<0.01), *Akt2* (AKT2; P<0.01) and *Slc2a4* (GLUT4; P<0.001), as well as in the protein level of GLUT4 (P<0.01), were produced by hypoxia (Fig R6A, R6C). Furthermore, IR phosphorylation induced by insulin stimulation was reduced after 48 hours of hypoxia (Fig R6B). On the other hand, hypoxia induced the expression of GLUT1 (P<0.001), which is a facilitated glucose transporter responsible

for insulin-independent basal glucose uptake and a well-known HIF-1α target gene Fig R6C).

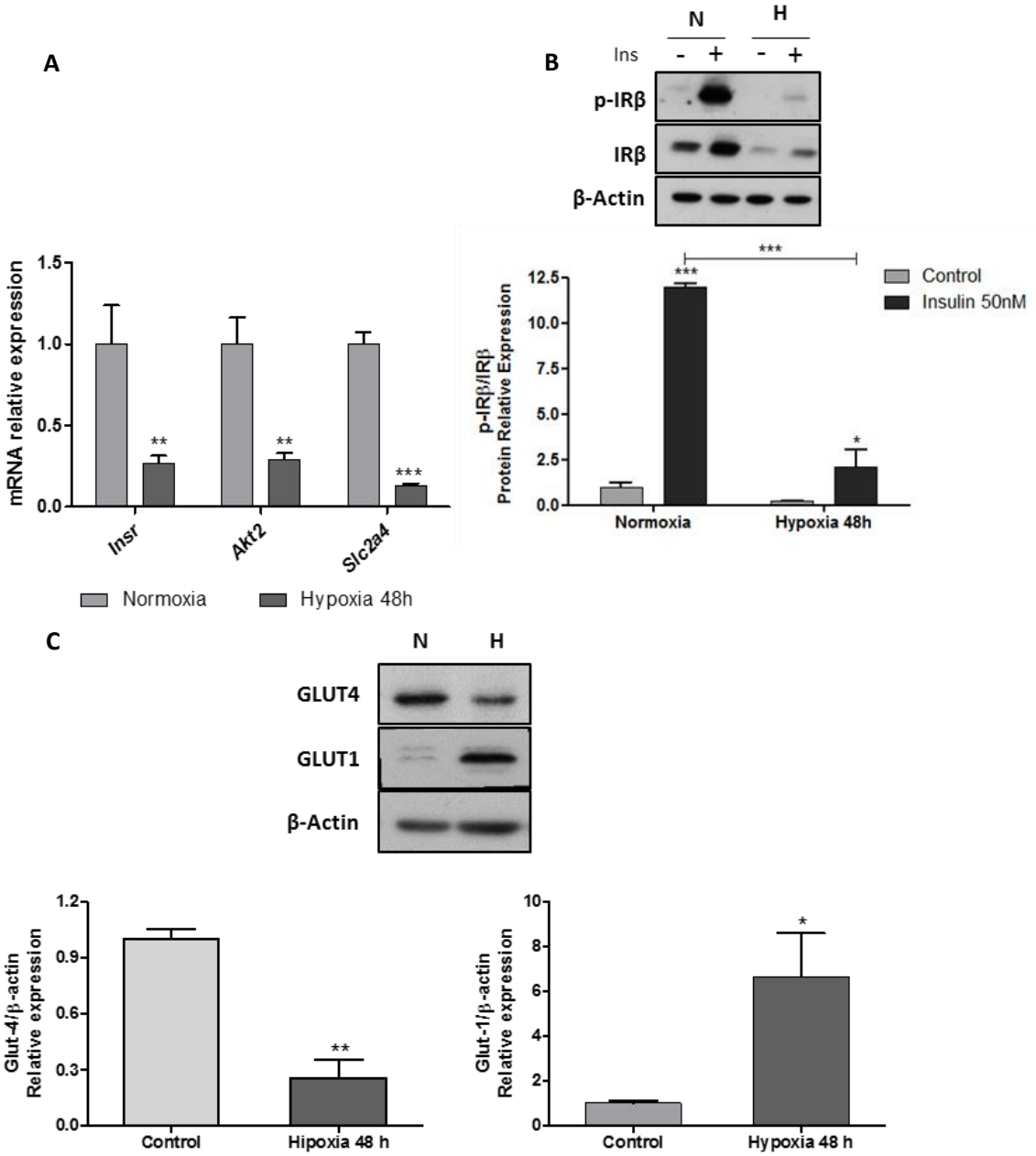

Figure R6. ***Hypoxia for 48 hours downregulates the expression of genes involved in insulin signaling and modulates glucose transporters levels.*** 3T3-L1 adipocytes differentiated during 8 days were incubated in normoxia or hypoxia (1% O2) for 48 hours. (A) Insulin receptor (*Insr*), Akt2/PKB (*Akt2*) and GLUT4 (*Slc2a4*) mRNA expression were determined by RT-PCR. Cyclophilin (*Ppia*) gene was used as endogenous control for normalization and the expression level was represented as fold change vs normoxia condition ± SEM. (B) Cells were stimulated or not with 50nM of insulin and then lysed to detect the phosphorylation of the β subunit of insulin receptor by western blot. Values were normalized to total insulin receptor levels. (C) Cells were lysed and Glut4 and Glut1 protein expression was determined by western blot. Values were normalized to β-actin. Means of fold change vs normoxia condition ± SEM were represented (n=4). * P<0.05, **P<0.01, ***P<0.001. N: Normoxia; H: Hypoxia 48h.

Considering the alterations in the expression of glucose transporters observed in 3T3-L1 adipocytes incubated in hypoxia, 2-deoxyglucose uptake assay was used to determine if the glucose uptake pattern under hypoxia conditions was modified. 3T3-L1 cells were differentiated for 8 days and submitted to hypoxia (1% O_2) for 48 hours. After 48 hours of low concentration of oxygen, basal glucose uptake was significantly increased and adipocytes lost insulin-induced glucose uptake ($P<0.01$). Adipocytes were also pretreated with 50µM LW6, a specific HIF-1 inhibitor, before being incubated under hypoxia. HIF-1 inhibition increased ($P<0.001$) the 2-deoxyglucose uptake induced by insulin in both, normoxia and hypoxia incubated cells (Fig R7A). Moreover, lactate release to supernatant was higher ($P<0.001$) in adipocytes submitted to hypoxia for 48 hours than in cells incubated in normoxia (Fig R7B).

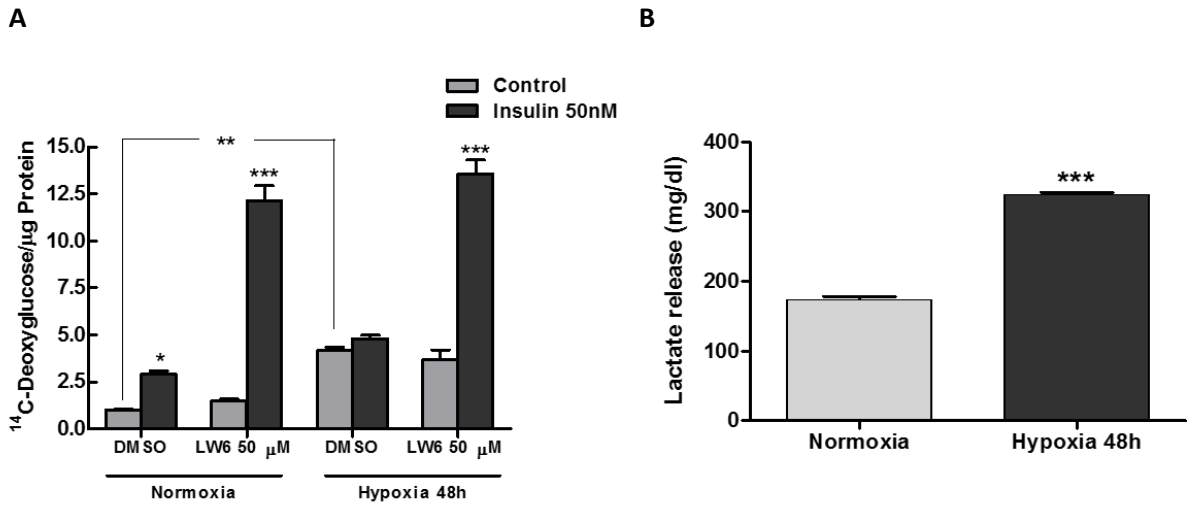

Figure R7. ***Hypoxia for 48 hours increases basal glucose uptake and lactate production accompanied by inhibition of insulin sensitivity in 3T3-L1 adipocytes.*** (A) 3T3-L1 adipocytes differentiated during 8 days were treated with or without 50µM LW6 (HIF-1 inhibitor) for 30 minutes and incubated in normoxia or hypoxia (1% O_2) during 48 hours. Cells were stimulated with 50 nM insulin for 10 minutes. 2-Deoxy-[^{14}C]-glucose uptake was measured as described in materials and methods. Values were normalized with protein concentration and represent means ± SEM (n=6). * $P<0.05$, ** $P<0.01$, *** $P<0.001$. (B). Lactate levels were determined in supernatant of 3T3-L1 adipocytes differentiated during 8 days after incubation in normoxia or hypoxia (1% O_2) during 48 hours, as indicated in material and methods. Values were represented as means ± SEM (n=6).

In order to elucidate if hypoxia could affect the cellular location of GLUT4 in 3T3-L1 adipocytes and therefore constitute a mechanism for the development of insulin

resistance, an immunofluorescence study with an antibody against GLUT4 was carried out. As shown in Fig R8, insulin stimulation (50 nM) induced the traffic of GLUT4 vesicles from the cytoplasm to the plasma membrane, which will allow the increase in the uptake of glucose by the cells. However, when adipocytes were incubated in a hypoxic environment, the mobilization of GLUT4 to the plasma membrane after insulin stimulation was not observed.

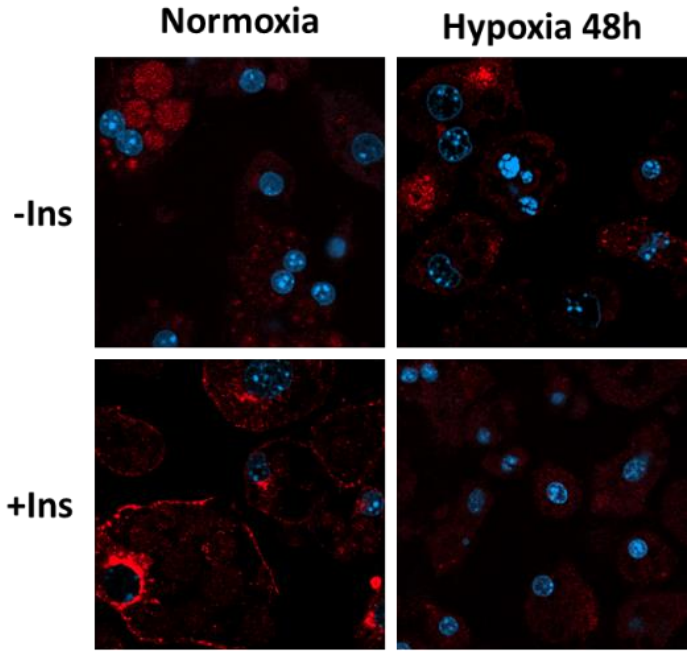

Figure R8. ***Glut4 translocation to the plasma membrane induced by insulin is abolished after 48 hours of hypoxia.*** 3T3-L1 adipocytes differentiated during 8 days were cultured in hypoxia (1% O2) for 48 hours and stimulated or not with 50 nM insulin for 10 minutes before being fixed with 4% paraformaldehyde. After permeabilization with 0.1% triton X100, the cells were incubated with primary antibody against Glut4 and subsequently with a fluorescent secondary antibody and Dapi to stain the nuclei. Images were captured using a confocal microscopy.

1.3. Hypoxia during 48 hours affects the expression and function of caveolins and cavins in 3T3-L1 adipocytes

As indicated previously, caveolae play an important role in the transmission of many cell signals including insulin. We therefore investigated the expression levels of Cav-1,

Cav-2, and SDPR/Cavin-2 which are responsible of the biogenesis and function of caveolae.

Incubation of 3T3-L1-differentiated cells under hypoxia for 48 hours was able to reduce the mRNA expression of Cav-1, Cav-2 and SDPR/Cavin-2 ($P<0.05$, $P<0.01$, $P<0.01$; Fig R9A). Cav-1 is phosphorylated and activated by insulin and incubation of adipocytes in hypoxia for 48 hours completely abolished the insulin-induced phosphorylation of Cav-1 ($P<0.001$; Fig R9B).

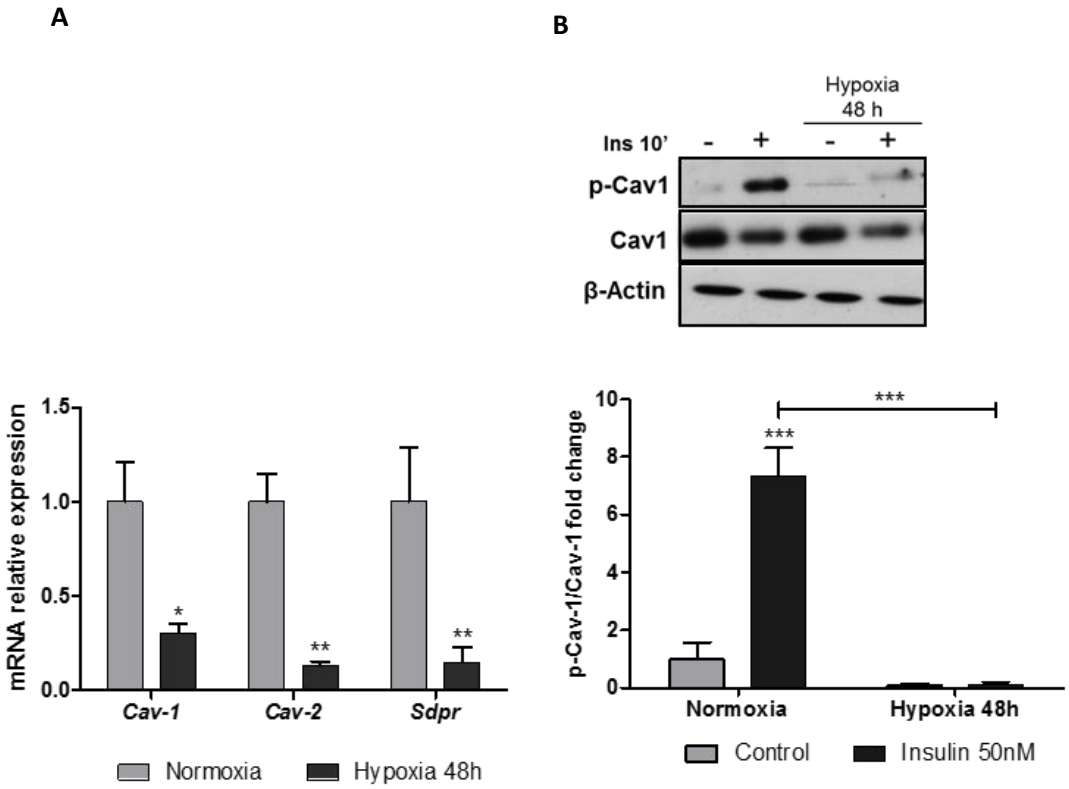

Figure R9. ***Hypoxia reduces Cav-1 and Cav-2 gene expression and Cav-1 phosphorylation induced by insulin.*** 3T3-L1 preadipocytes were treated with the differentiation hormonal cocktail until day 8 and incubated in normoxia or hypoxia (1% O2) for 48 hours. (A) *Cav-1*, *Cav-2, Sdpr* mRNA expression were determined by RT-PCR. Cyclophilin (*Ppia*) gene was used as endogenous control for normalization and the expression level was represented as fold change vs normoxia condition ± SEM (n=4-6). (B) Cells were stimulated or not with 50 nM insulin for 10 minutes, lysed and phospho-Cav-1 protein expression was determined by western blot. Values were normalized with total Cav-1 and means of fold change vs normoxia condition ± SEM were represented (n=4). * $P<0.05$, **$P<0.01$, ***$P<0.001$.

Since caveolae are also structures related to cell trafficking processes and Cav-1 could be mobilized into the cell, we hypothesized that hypoxia could induce a loss of

caveolae in the plasma membrane disrupting insulin signaling. Fig R10 shows by immunofluorescence that Cav-1 in mature 3T3-L1 adipocytes cultured in normoxia condition is mainly located in the plasma membrane. However, after 48 hours of hypoxia, the presence of Cav-1 in plasma membrane became diffused and there was an increase of the fluorescence signal in the cytoplasm. Stimulation with insulin did not produce any apparent change in the Cav-1 cellular location either in normoxic or hypoxic cells (Fig R10).

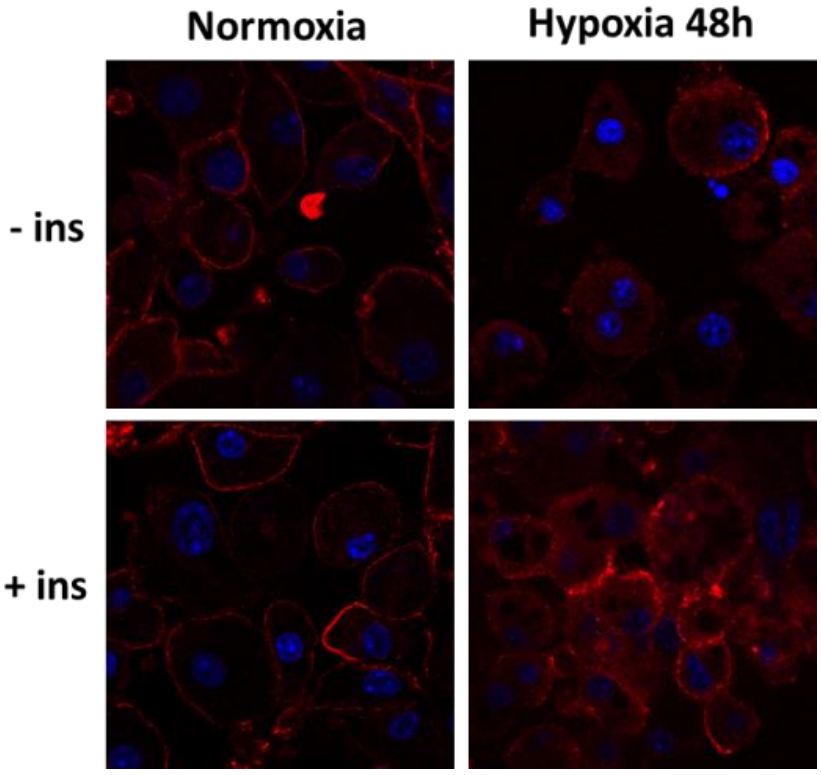

Figure R10. ***Membrane localization of Cav-1 is compromised in 3T3-L1 adipocytes incubated in hypoxia for 48 hours.*** 3T3-L1 adipocytes differentiated during 8 days were cultured in hypoxia for 48 hours and stimulated or not with 50 nM insulin for 10 minutes before being fixed with 4% paraformaldehyde. After permeabilization with 0.1% triton X100, cells were incubated with a specific primary antibody against Cav-1 and subsequently with a fluorescent secondary antibody and Dapi to stain the nuclei. Images were captured using a confocal microscopy.

1.4. Caveolins and cavins, but not insulin signaling related genes, are regulated by HIF-1.

The main mediator of hypoxia effects is the family of hypoxia inducible transcription factor (HIF), of which 3 isoforms have been identified so far (HIF-1, HIF-2 and HIF-3). HIF-1 has been related to the deleterious effect of hypoxia in the physiology of the cells. Thereby, the regulatory role of HIF-1 in the expression of caveolin genes was studied treating cells with 20 µM echinomycin, which strongly inhibits the binding of HIF-1 to hypoxia response elements (HRE) in the DNA.

To validate the treatment, we measured the mRNA expression of *Slc2a1* (GLUT1), which is a known target gene for HIF-1. As expected, 24 and 48 hours of hypoxia strongly increased the mRNA expression of *Slc2a1* and the treatment with 20 µM echinomycin reverted this effect to normoxia levels (P<0.001) in both situations (Fig R11).

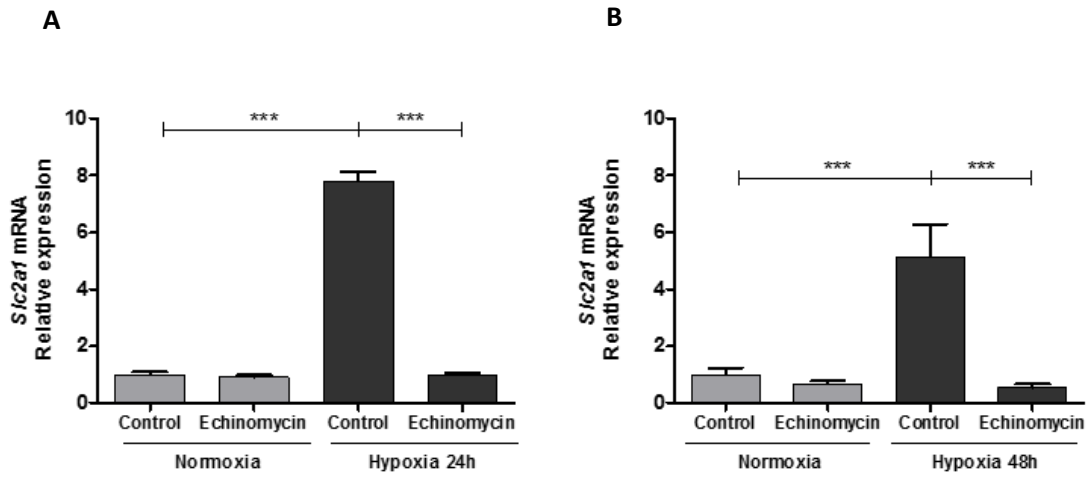

Figure R11. ***Slc2a1 (GLUT1) gene is regulated by HIF-1 in 3T3-L1 adipocytes incubated in hypoxic condition.*** 3T3-L1 adipocytes differentiated during 8 days were incubated with or without 20 µM echinomycin in normoxia or hypoxia condition (1% O2) for (A) 24 or (B) 48 hours. GLUT1 (*Slc2a1*) mRNA expression was determined by RT-PCR. Cyclophilin (*Ppia*) gene was used as endogenous control for normalization and the expression level was represented as fold change vs normoxia condition ± SEM (n=6). ***P<0.001.

As shown in Fig R12A, we observed a significant increase in *Insr* (IR) expression after 24 hours of hypoxia. Nevertheless, treatment with 20 µM echinomycin downregulated the expression of this gene in both, normoxia and hypoxia conditions (P<0.001). On the

other hand, hypoxia significantly reduced the mRNA expression of *Akt2* (Akt/PKB; P<0.001; Fig R12B). In this case, echinomycin downregulated *Akt2* mRNA expression in normoxia but it did not show any effect on the hypoxia-reduced expression (Fig R12B). Hypoxia also reduced significantly *Slc2a4* mRNA (GLUT4; P<0.05), whereas echinomycin did not show any effect on this protein levels in normoxia, but was able to restore the reduced mRNA expression of this gene observed under hypoxia (P<0.001; Fig R12C).

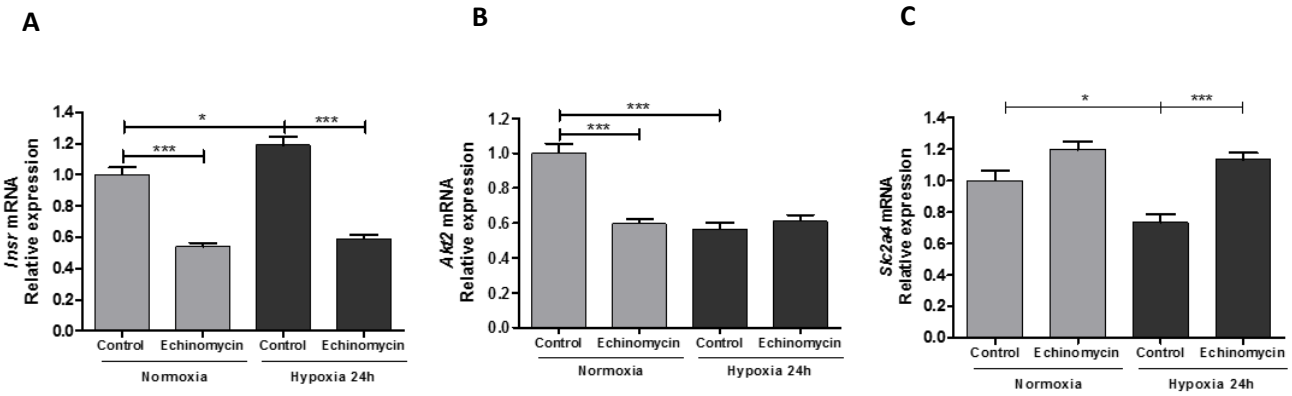

Figure R12. ***Insulin signaling intermediates expression is not regulated by HIF-1.*** 3T3-L1 adipocytes differentiated during 8 days were incubated with or without 20 µM echinomycin in normoxia or hypoxia condition (1% O2) for 24 hours. *(A)* Insulin receptor (*Insr*), (B) Akt/PKB (*Akt2*) and (C) GLUT4 (*Slc2a4*) mRNA expression was determined by RT-PCR. Cyclophilin (*Ppia*) gene was used as endogenous control for normalization and the expression level was represented as fold change vs normoxia condition ± SEM (n=6). * P<0.05, **P<0.01, ***P<0.001.

We then evaluated the role of HIF-1 in the regulation of Cav-1, Cav-2 and SDPR/Cavin-2 using the same experimental design. The mRNA expression of the three genes was reduced by hypoxia and the inhibition of HIF-1 with echinomycin restored the expression levels observed in normoxia (P<0.001; Fig R13).

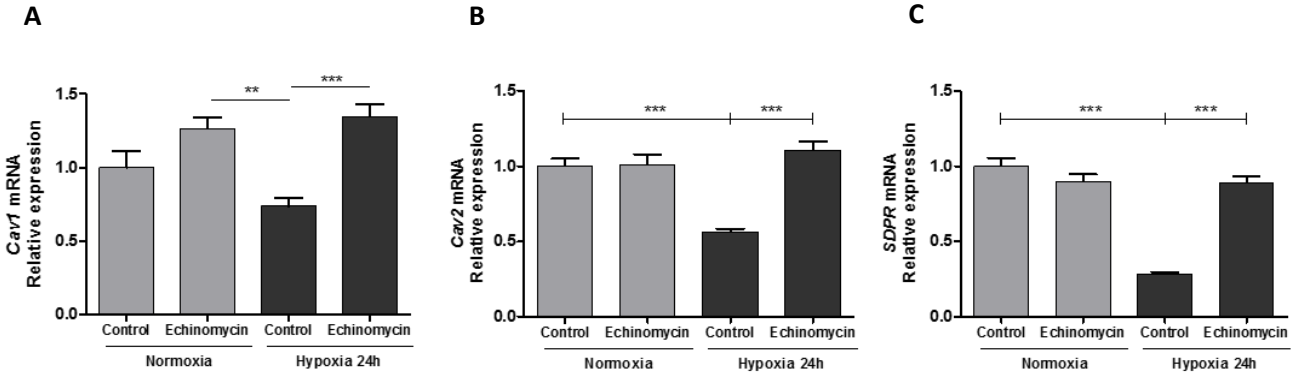

Figure R13. ***Caveolae structural proteins mRNA expression is regulated by HIF-1*.** 3T3-L1 adipocytes differentiated during 8 days were incubated with or without 20 µM echinomycin in normoxia or hypoxia condition (1% O2) for 24 hours. *(A) Cav-1*, (B) *Cav-2* and (C) *SDPR/Cavin2* mRNA expression were determined by RT-PCR. Cyclophilin (*Ppia*) gene was used as endogenous control for normalization and the expression level was represented as fold change vs normoxia condition ± SEM (n=6). **P<0.01, ***P<0.001.

Considering previous results, which suggested that HIF-1 could regulate the expression of the main structural proteins of caveolae, a bioinformatics analysis using the TRANSFAC® professional database of the 5'-upstream sequence of Cav-1 was carried out. The promoter analysis showed the presence of a consensus hypoxia response element (HRE), located at -442 upstream TSS. A chromatin immunoprecipitation (ChIP) assay was performed to evaluate the binding of HIF-1 to this HRE detected in the Cav-1 promoter sequence in 3T3-L1 adipocytes. Cells were cultured, differentiated for 8 days and submitted to hypoxia during 48 hours, and finally total chromatin was extracted after fixation. Chromatin bound to HIF-1 was immunoprecipitated and binding to the Cav-1 HRE element analyzed was quantified by RT-PCR. The percentage of immunoprecipitated chromatin normalized to the corresponding input chromatin is represented in Fig R14. This figure shows a significant increase in the binding of HIF-1 to the analyzed HRE element in the Cav-1 promoter after 48 hours of hypoxia, which was completely prevented by the treatment with 20 µM echinomycin (P<0.001).

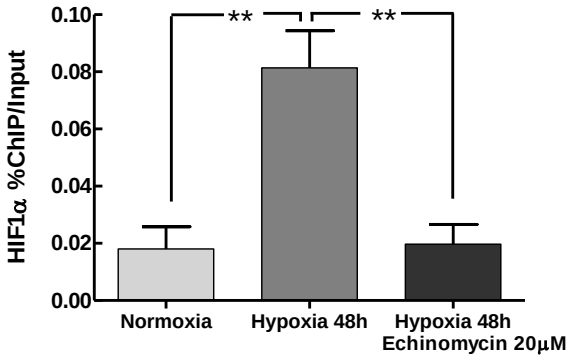

Figure R14. ***HIF-1 regulates Cav-1 mRNA expression through the binding to a hypoxia response element (HRE) present in the Cav-1 gene promoter sequence.*** 3T3-L1 adipocytes differentiated during 8 days were incubated for 48 hours in normoxia or hypoxic condition with or without echinomycin, before they were fixed with 4% paraformaldehyde and immunoprecipitated with antibodies specific for HIF-1. The presence of a hypoxia response element in the Cav-1 gene promoter sequence was analyzed by RT-

PCR in the immunoprecipitated DNA. Values were represented as the percentage of HIF-1 binding vs input ± SEM (n=4). **P<0.01.

1.5. Hypoxia induces a substantially different gene expression pattern compared to normoxia

We performed a gene expression array in order to gain insight into possible mechanisms by which hypoxia could contribute to induce insulin resistance in 3T3-L1 mature adipocytes. To discriminate those hypoxia-regulated genes that could be relevant, B values greater than 5 and fold change (FC) values greater than 1 and less than -1 were considered to select genes for further analysis. Gene Ontology (GO) enrichment analysis was then carried out to classify genes differentially expressed according to their function.

GO Term	*P* Value	Gene symbol
Caveola	0.00022	*Cav2, Lipe, Hmox1, Igf1r, Atp1a2, Sorbs1, Slc2a1, Dlc1, Atp1b3, Scarb1, Sdpr, Irs1, Bmpr2*
Cellular response to insulin stimulus	0.00027	*Ccnd2, Kat2b, Nr1h3, Rps6kb1, Srebf1, Prkdc, Sorbs1, Stat1, Pik3r3, Pde3b, Dlc1, Bcar1, Ucp2, Apobec1, Pik3r1, Ghr, Irs1*
Carbohydrate transport	0.00280	*Slc2a4, Slc35b4, Rps6kb1, Slc35a5, Adipoq, Sorbs1, Aqp7, Slc2a1, Klf15, Ednra, Scarb1, Irs1, Sort1, G630090E17Rik*
Response to starvation	0.00414	*Angptl4, Srebf1, Pfkfb1, Hspa5, Acads, Gabarapl1, Adm, Gnpat, Acat1, Jun, Acadm, Bmpr2*
1-phosphatidylinositol-3-kinase regulator activity	0.00555	*Pik3r3, Pik3r1*
Cellular carbohydrate metabolic process	0.00659	*Eno2, Pgam1, Igf1, Ogdh, Pmm1, St3gal6, Adipoq, Gpd1, Man2a1, Pcx, Sorbs1, Pfkfb1, Dhtkd1, Idh1, Atf3, Pfkfb3, Dolpp1, Pck1, Aimp1, Coq3, H6pd, Rbks, Pgm1, Dgat2, Phka2, Pygb, Ppip5k1, B3galt2, Cog7, Hk1, Pomt1, Pik3r1, Atf4, Gm1840, Mgat2, Irs1, Itpk1, Acadm, Ppp1r3c*

Table R1. ***Cellular processes affected in 3T3-L1 adipocytes after 48 hours of hypoxia determined by GO enrichment analysis of the gene expression microarray results.*** Functional enrichment analysis of Gene Ontology (GO) categories was carried out using standard hypergeometric test. P value indicates the statistical significance of enrichment (n=4).

Selected genes and cellular processes are summarized in table R1. Differentially expressed genes are involved in caveolae structure and function (13 genes), cellular response to insulin stimulus (17 genes), carbohydrate transport (14 genes), response to starvation (12 genes), 1-phosphatidylinositol-3-kinase regulator activity (2 genes) and cellular carbohydrate metabolic processes (39 genes).

From this group of 79 differentially expressed genes, 20 genes were upregulated by hypoxia in 3T3-L1 mature adipocytes. Enolase 2 (*Eno2*), growth hormone releasing hormone (*Ghr*), adrenomedullin (*Adm*) and GLUT1 (*Slc2a1*) were the most significantly upregulated genes, as shown in table R2. Interestingly, expression of insulin growth factor 1 (*Igf1*) and its receptor (*Igf1r*) were also increased by hypoxia with a significant adjusted *P* value.

Genes	logFC	adj.P.Val	B
Eno2	3.424	6.05E-13	29.084
Ghr	3.422	5.41E-10	18.757
Adm	3.215	6.06E-11	22.483
Slc2a1	2.277	3.35E-11	24.114
Pgam1	2.083	6.98E-11	22.133
Hk1	1.547	2.22E-07	10.190
Jun	1.514	8.10E-09	14.839
Igf1r	1.464	2.65E-09	16.397
Igf1	1.464	2.65E-09	16.397
Pmm1	1.448	2.85E-07	9.840
Itpk1	1.287	5.83E-09	15.293
Hspa5	1.230	3.23E-07	9.681
Atf4	1.176	1.39E-08	14.055
Atf3	1.172	1.24E-06	7.900
Hmox1	1.139	1.36E-07	10.867
Gm1840	1.124	4.36E-07	9.283
Aimp1	1.049	2.25E-08	13.365
Bcar1	1.043	6.57E-08	11.883
Pgm1	1.025	2.40E-07	10.085
Gabarapl1	1.014	4.42E-07	9.267

Table R2. U*pregulated genes related to caveolae structure and function and carbohydrate metabolism in 3T3-L1 adipocytes after 48 hours of hypoxia.* Adjusted p value was calculated with Benjamini-Hochberg procedure. The Log Odds or B value is the odds or probability that the gene is differentially expressed. Genes were selected as significant using criteria of B> 5 (n=4).

Hypoxia also induced a strong downregulating effect on gene expression. In the biological processes selected after the GO enrichment analysis, the expression of 59 out of the 79 selected differentially expressed genes was significantly decreased after 48 hours of hypoxia (table R3). Among the genes more negatively affected by hypoxia stand out genes related with glucose metabolism (*B3galt2, Pck1, Pfkfb1*) and lipid biosynthesis (*Gpd1*). Remarkably, genes directly related to insulin signaling (*Irs1*) and caveolae structure (*Sdpr*) were also downregulated with a high value of fold change.

Genes	logFC	adj.P.Val	B	Genes	logFC	adj.P.Val	B	Genes	logFC	adj.P.Val	B
B3galt2	-4.362	1.22E-08	14.223	***Ppp1r3c***	-1.772	5.73E-10	18.658	***Ogdh***	-1.206	5.23E-09	15.482
Pck1	-4.174	1.37E-09	17.272	***Kat2b***	-1.769	9.04E-10	17.972	***Coq3***	-1.190	4.72E-07	9.180
Pfkfb1	-3.566	1.28E-10	21.010	***Ednra***	-1.639	9.75E-09	14.544	***Srebf1***	-1.166	6.53E-07	8.746
Gpd1	-3.506	3.35E-11	24.002	***Pfkfb3***	-1.638	1.30E-07	10.928	***Ccnd2***	-1.138	7.08E-09	15.047
Atp1a2	-2.974	4.98E-10	18.916	***G630090E17Rik***	-1.626	2.39E-08	13.284	***Rps6kb1***	-1.128	1.92E-08	13.601
Sdpr	-2.972	7.07E-11	22.091	***Acads***	-1.593	4.20E-09	15.799	***Phka2***	-1.115	9.73E-08	11.331
Pik3r3	-2.631	8.17E-11	21.709	***Pik3r1***	-1.572	6.82E-09	15.092	***H6pd***	-1.092	1.14E-06	8.014
Irs1	-2.522	6.40E-09	15.170	***Pomt1***	-1.534	1.07E-09	17.641	***Dlc1***	-1.092	5.71E-08	12.074
Stat1	-2.430	9.15E-10	17.953	***Pygb***	-1.495	2.79E-10	19.662	***Bmpr2***	-1.076	7.90E-07	8.496
Sort1	-2.420	9.26E-10	17.929	***Lipe***	-1.467	1.37E-09	17.276	***Atp1b3***	-1.074	7.82E-09	14.900
Aqp7	-2.286	1.18E-07	11.060	***St3gal6***	-1.458	1.19E-06	7.960	***Mgat2***	-1.049	9.30E-07	8.284
Adipoq	-2.185	3.35E-11	23.675	***Cav2***	-1.398	2.21E-09	16.645	***Ucp2***	-1.038	2.40E-07	10.088
Klf15	-2.028	8.84E-10	18.006	***Ppip5k1***	-1.372	1.12E-07	11.146	***Scarb1***	-1.036	6.61E-09	15.131
Pcx	-2.013	9.84E-11	21.397	***Angptl4***	-1.352	4.00E-08	12.570	***Dhtkd1***	-1.031	3.35E-07	9.631
Pde3b	-1.986	8.17E-11	21.774	***Sorbs1***	-1.323	2.64E-07	9.955	***Slc35b4***	-1.027	1.74E-06	7.446
Dgat2	-1.939	6.06E-11	22.453	***Prkdc***	-1.316	4.44E-09	15.728	***Man2a1***	-1.020	3.38E-08	12.807
Gnpat	-1.863	7.92E-11	21.923	***Nr1h3***	-1.247	6.59E-06	5.744	***Dolpp1***	-1.018	1.15E-08	14.312
Idh1	-1.839	9.13E-11	21.555	***Slc35a5***	-1.230	4.30E-07	9.301	***Rbks***	-1.014	7.23E-06	5.629
Slc2a4	-1.811	2.06E-10	20.190	***Apobec1***	-1.230	3.40E-08	12.798	***Cog7***	-1.008	8.78E-07	8.356
Acadm	-1.780	1.28E-10	20.995	***Acat1***	-1.226	8.20E-09	14.812				

Table R3. ***Downregulated genes related to caveolae structure and function and carbohydrate metabolism in 3T3-L1 adipocytes after 48 hours of hypoxia.*** Adjusted p value was calculated with Benjamini-Hochberg procedure. The Log Odds or B value is the odds or probability that the gene is differentially expressed. Genes were selected as significant using criteria of B> 5 (n=4).

The results of the expression array were validated by RT-PCR in 3T3-L1 adipocytes after 24 and 48 hours of hypoxia incubation. The determination of gene expression after 24 hours serves as an indication of the time course of hypoxia-regulation of the analyzed genes. Selected genes for validation considered not only the insulin related genes, but also genes involved in other processes importantly affected such as adipocyte differentiation.

As shown in Fig R18, mRNA expression of adiponectin (*Adipoq*), phosphoinositide-3-kinase regulatory subunit 3 (*Pik3r3*) and CCAAT/enhancer binding protein (*Cbpa*) were significantly downregulated at 24 ($P<0.001$) and 48 hours of hypoxia ($P<0.01$). Nevertheless, peroxisome proliferator activated receptor gamma (*Pparg*) expression level remained unaltered after 24 hours of hypoxia and its expression only decreased after 48 hours of hypoxia ($P<0.01$).

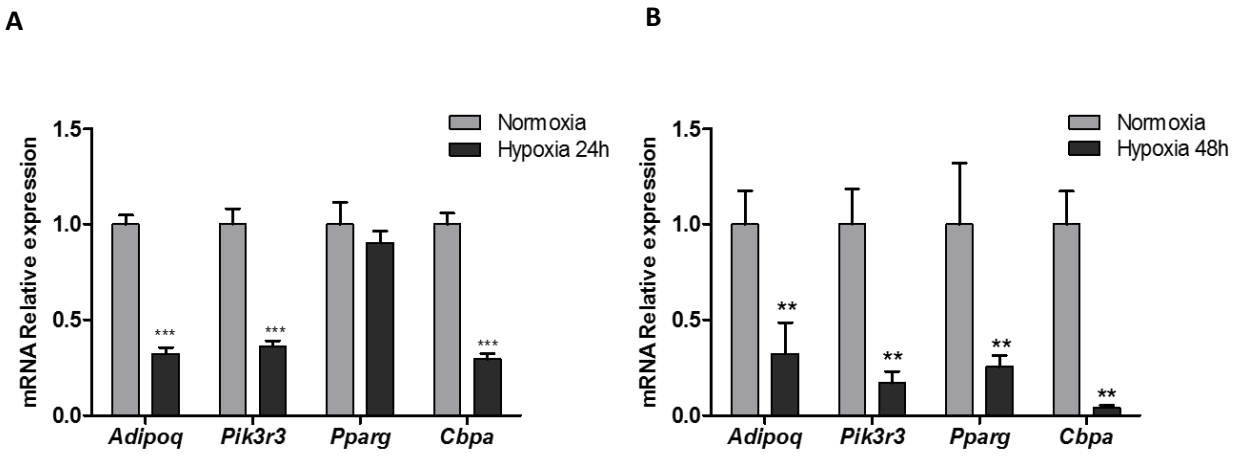

Figure R18. ***Hypoxia downregulates the mRNA expression of genes related to adipocyte differentiation and insulin sensitivity.*** 3T3-L1 preadipocytes were treated with the differentiation hormonal cocktail for 8 days and incubated in normoxia or hypoxia condition (1% O2) for (A) 24 or (B) 48 hours. Adiponectin (*Adipoq*), Phosphatidylinositol 3-kinase regulatory subunit gamma (*Pik3r3*), PPAR-γ (*Pparg*) and CEBPα (*Cbpa*) mRNA expression were determined by RT-PCR. Cyclophilin (*Ppia*) gene was used as endogenous control for normalization and the expression level was represented as fold change vs normoxia condition ± SEM (n=6). * P<0.05, **P<0.01, ***P<0.001.

2. Effect of intermittent hypoxia in mouse white adipose tissue.

Obesity is often associated with the development of obstructive sleep apnea (OSA). OSA is characterized by chronic intermittent hypoxia (IH) due to repetitive upper airway collapses during sleep. IH is thought to be related to OSA-associated metabolic alterations, such as insulin resistance and type 2 diabetes. For this reason, we evaluated the effect of intermittent hypoxia in the caveolae structure using an animal model. Epididymal fat tissue and carotids from C57BL/6 mice exposed to either IH (FiO2 21-5%, 1 min cycle, 8 h/day) or normoxia conditions for 14 days were used for the analysis. Pictures obtained by electronic microscopy showed that mice submitted to IH for 14 days experienced reduced caveolae density in plasma membrane in the carotids (P<0.05), adipose tissue (P<0.05) and in the periaortic adipose tissue (P<0.01; Fig R19).

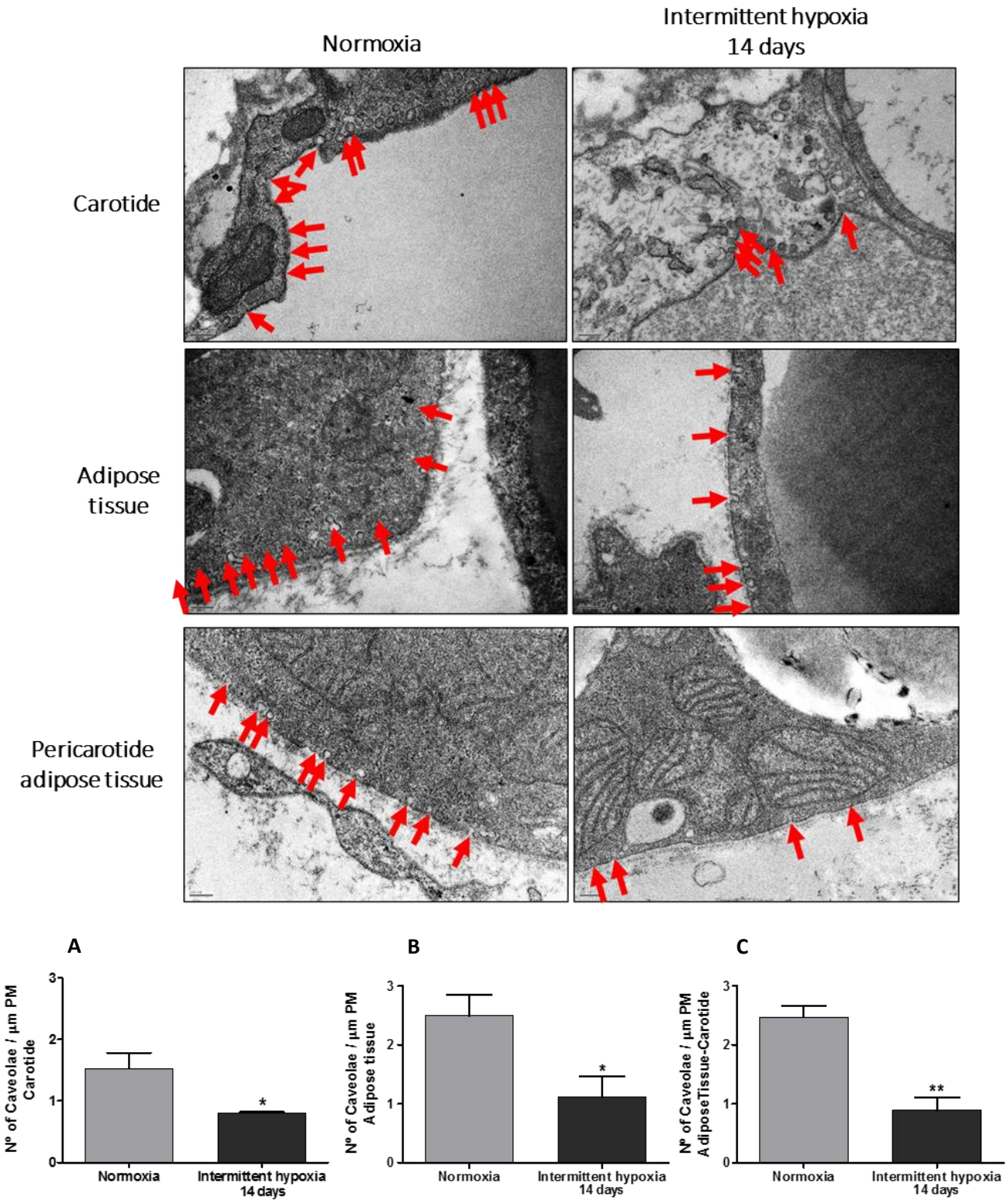

Figure R19. ***Intermittent hypoxia during 14 days reduces caveolae density in (A) carotid, (B) adipose tissue and (C) Periaortic adipose tissue of mice.*** Caveolae density was determined by transmission electronic microscopy. The density of caveolae in plasma membrane of around 20 pictures of each condition and tissue were quantified using imageJ software. (Normoxia, n=4; Intermittent hypoxia, n=3). * P<0.05, **P<0.01.

Thereafter, total RNA was extracted from the adipose tissue of the mice submitted to intermittent hypoxia and mRNA expression of caveolins and cavins were measured by RT-PCR. The expression of *Sdpr*, which encodes the protein SDPR/Cavin-2, was significantly reduced (P<0.05) after 14 days of intermittent hypoxia (Fig R20). The expression of *Cav-1*, *Cav-2* and *Ptrf/Cavin-1* was also reduced but did not reach significant differences probably due to an insufficient number of animals used for the experiment (n=3).

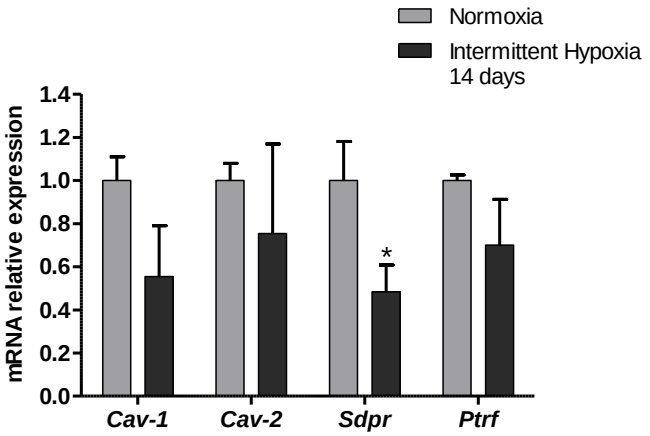

Figure R20. ***Intermittent hypoxia for 14 days reduces mRNA expression of SDPR/Cavin-2 in white adipose tissue.*** C57BL/6 mice were submitted to intermittent hypoxia (8 h/day, cyclic 21-5% FiO2, 60s cycle) for 14 days. White adipose tissues were then removed and total RNA was extracted. Cav-1 (*Cav-1*), Cav-2 (*Cav-2*), SDPR/Cavin-2 (*Sdpr*) and PTRF/Cavin-1 (*Ptrf*) mRNA expression were determined by RT-PCR. Acidic ribosomal phosphoprotein P0 (*36B4*) gene was used as endogenous control for normalization and the expression level was represented as fold change vs mice maintained in normoxia condition (Normoxia, n=4; Intermittent hypoxia, n=3). * P<0.05.

The intermittent hypoxia condition used for the previous experiment mimics a mild sleep apnea without considering other factors such as obesity or insulin resistance. For this reason, mRNA was also extracted from the white adipose tissues of mice submitted to IH for 4 weeks, which represents a severe sleep apnea leading to significant and measurable alterations. Mice subjected to this extreme condition showed an important downregulation of cavin genes, *Sdpr* and *Ptrf* (P<0.01), and *Cav-2* (P<0.05; Fig R21). These results point to cavins as mediators in the dysregulation of caveolae as a consequence of chronic intermittent hypoxia.

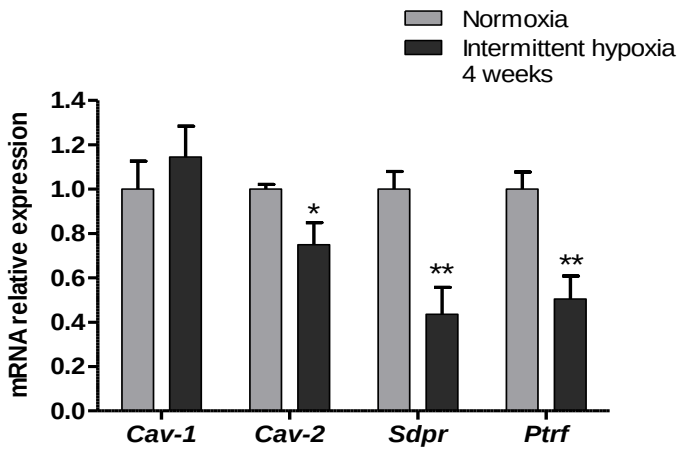

Figure R21. ***Expression of cavins and Cav-2 genes are downregulated in adipose tissue of mice submitted to intermittent hypoxia*****.** C57BL/6 mice were submitted to intermittent hypoxia (8 h/day, cyclic 21-5% FiO2, 60s cycle) for 4 weeks. White adipose tissues were then removed and total RNA was extracted. Cav-1 (*Cav-1*), Cav-2 (*Cav-2*), SDPR/Cavin-2 (*Sdpr*) and PTRF/Cavin-1 (*Ptrf*) mRNA expression were determined by RT-PCR. Acidic ribosomal phosphoprotein P0 (*36B4*) gene was used as endogenous control for normalization and the expression level was represented as fold change vs mice maintained in normoxia condition (Normoxia, n=4; Intermittent hypoxia, n=4). * P<0.05, ** P<0.01.

3. Effect of hypoxia in the caveolae structure of human aortic endothelial cells.

It is well known that insulin is able to induce vasodilatation by activating endothelial nitric oxide synthase (eNOS) in endothelial cells (EC) mainly through the PI3K/PKB pathway (Fisslthaler et al., 2003).

In order to evaluate the insulin response of primary HAoEC (Human Aortic Endothelial Cells), these cells were stimulated with 100 nM insulin for 10 minutes. After this time, cells were harvested and the phosphorylation of insulin receptor was determined by western blot. As shown in Fig R22, IRβ phosphorylation was significantly increased due to insulin stimulation (P<0.01).

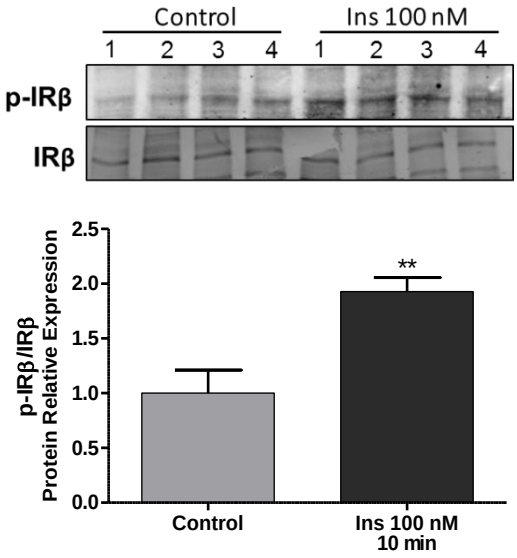

Figure R22. ***Insulin induces insulin receptor phosphorylation in primary human aortic endothelial cells*.** Human aortic endothelial cells (HAoEC) were grown until confluence and stimulated with 100 nM insulin for 10 minutes. Cells were then lysed and phospho-IRβ protein expression was determined by western blot. Values were normalized with total IRβ and means of fold change vs normoxia condition ± SEM were represented (n=4). **P<0.01.

Previous results have shown that caveolae density in adipocyte plasma membrane is reduced by hypoxia (Regazzetti et al., 2015). Taking into account that EC, like adipocytes, are also enriched in caveolae and the lack of evidence showing the hypoxia effects on caveolae in this cell type, we submitted primary HAoEC to hypoxia (1% O_2) for 16 hours to investigate its effect on caveolae. The density of caveolae in the plasma membrane of HAoEC incubated in normoxia and hypoxia was determined by transmission electronic microscopy (TEM). Fig R23 shows that hypoxia strongly reduced the number of caveolae per micrometer of plasma membrane compared with the same cells incubated in normoxia (P<0.001).

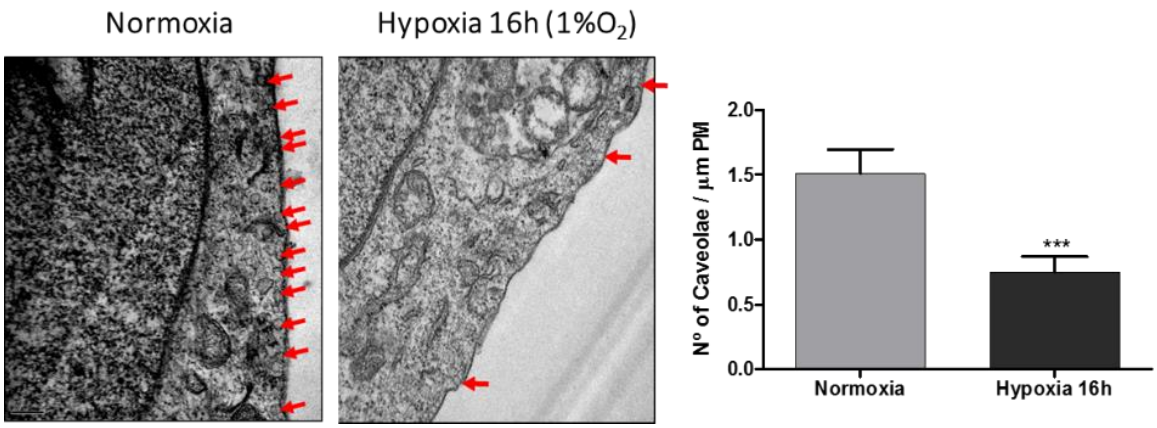

Figure R23. ***Hypoxia induces the loss of caveolae in HAoEC plasma membrane*****.** Cells were incubated in normoxia or in hypoxia (1% O2) for 16 hours. Caveolae structures were identified by transmission electronic microscopy. The density of caveolae in plasma membrane of around 20 pictures of each condition and tissue were quantified using imageJ software. Quantification is expressed as number of caveolae per micrometer of plasma membrane (PM) (n=4). ***P<0.001.

Due to this result, we performed an IF study to determine the location of Cav-1 and PTRF/Cavin-1 in the HAoEC cells exposed to hypoxia. Interestingly, the incubation of HAoEC in hypoxia seemed to produce an accumulation of Cav-1 in the nucleus which was not observed in cells incubated in normoxia condition (Fig R24). However PTRF/Cavin-1 is expressed in the nucleus in both, normoxia and hypoxia conditions. This result was expected since this protein was first described as a factor in ribosomal RNA transcription (Fig R24).

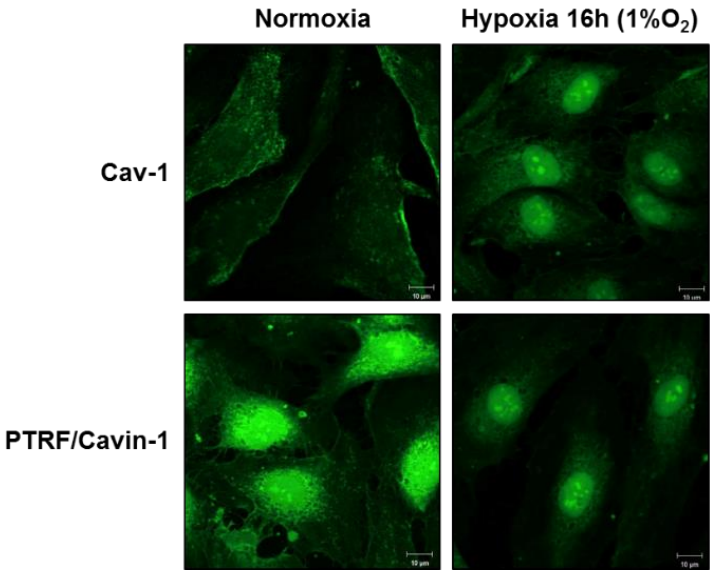

Figure R24. ***Cav-1 and PTRF/Cavin-1 are accumulated in the nucleus after 16 hours of hypoxia (1% O2).*** Immunofluorescence of endogenous caveolin-1 (upper panel) and PTRF/Cavin-1 (lower panel). Bar scale is 10 mm.

DISCUSION

DISCUSION

1. Effect of hypoxia in the 3T3-L1 differentiation process

One of the features of obesity is the hypertrophy and hyperplasia of adipocytes which leads to reduced levels of oxygen within adipose tissue. It is well known that hypoxia induces a dysregulation of adipocyte physiology, including increased expression and secretion of proinflammatory adipokines and altered glucose and lipid metabolism.

To investigate the contribution of hypoxia to the development of insulin resistance in adipocytes, we used the 3T3-L1 cell line model. These cells are one of the most well characterized and robust models to study the molecular events of adipocyte differentiation. Confluent 3T3-L1 preadipocytes are normally differentiated into adipocytes in a synchronized way. At confluence, the cell-cell contact induces the expression of very early adipocyte differentiation markers, including lipoprotein lipase (LPL) and type VI collagen (A2COL6) (Ntambi and Kim, 2000). The addition of a defined adipogenic cocktail composed by the glucocorticoid dexamethasone (Dex), the growth factor insulin, the phosphodiesterase inhibitor isobutilmethylxanthine (IBMX) and fetal bovine serum (FBS), is needed to trigger a transcriptional cascade responsible for the formation of mature adipocytes. Within 1 hour after the addition of the cocktail, there is an increase in the expression of c-fos, c-jun, junB, c-myc and CCAAT/enhancer binding proteins (C/EBP) β and δ, and cells undergo a postconfluent mitosis and subsequent growth arrest (Bernlohr et al., 1985). After removal of IBMX and Dex from the culture medium, expression of C/EBPδ dissipates over the subsequent 48 h, whereas the decline of C/EBPβ is observed around day 8. The activity of C/EBPβ and δ induces the expression of peroxisome proliferator-activated receptor γ (PPARγ) (Clarke et al., 1997; Wu et al., 1995) and C/EBPα, which have been identified as responsible for terminal differentiation through the transcription of many genes involved in the development and maintenance of the adipocyte phenotype (Gregoire et al., 1998). Finally, among the markers of adipocyte differentiation, and as a result of the action of the transcription factors commented before, there is caveolin-1 (Cav-1), whose mRNA is strongly induced between days 2 and 4 of 3T3-L1 adipocyte differentiation and exhibits a similar pattern of induction during differentiation as the mRNAs encoding IR and GLUT4 (Scherer et al., 1994). Our group has previously demonstrated that

expression of Cav-1, one of the main proteins of caveolae, is enhanced during 3T3-L1 adipogenesis and can be regulated by epigenetic mechanisms (Palacios-Ortega et al., 2014).

In this project we show that hypoxia strongly inhibits the differentiation process of 3T3-L1 adipocytes, demonstrated by the strong reduction of triglyceride accumulation and the subsequent absence of lipid droplets in the cytoplasm (Fig R2). This result is positively correlated with an increase of the HIF-1 expression (Fig R1), suggesting the involvement of this transcription factor in the inhibitory mechanism of adipogenesis in 3T3-L1 cells. In this sense, it has been previously reported that HIF-1 represses PPARγ2 promoter activation through the induction of the DEC1/Stra13 target gene, a member of the Drosophila hairy/Enhancer of split (HES) (Yun et al., 2002). Furthermore, in differentiated human preadipocytes, acute exposure to hypoxia (3% O_2) during 24 hours inhibits LPL activity (Mahat et al., 2016), one of the earliest markers of adipocyte differentiation. Very recently, other group, using an experimental model similar to ours, also observed that incubation of 3T3-L1 preadipocytes in 1% O_2 during the differentiation process reduced the expression of adipogenesis markers and inhibited the formation of lipid droplets, as well as diminished lipogenesis, which dropped by 43% (Weiszenstein et al., 2016). Moreover, this work also supports the role of HIF-1 in the inhibitory effect of hypoxia over adipogenesis.

In our study, incubation of mature 3T3-L1 adipocytes in hypoxia during 48 hours also reduces the triglyceride content of the cells compared to the control group (Fig R5). This result could be easily explained by the well-known lipolytic effect of hypoxia (Trayhurn, 2014). One of the mechanisms proposed for the hypoxia-induced lower levels of fatty acid in adipocytes *in vivo* is the inhibition of LPL activity, which promotes the hydrolysis of dietary triglycerides and the subsequent uptake of fatty acids within adipocytes (Dijk et al., 2016; Mahat et al., 2016). It has been demonstrated that the hypoxia-induced gene angiopoietin-like protein 4 (*ANGPTL4*) promotes LPL degradation and inactivation (Dijk et al., 2016; González-Muniesa et al., 2011; Makoveichuk et al., 2013). However, in our *in vitro* cell culture model this mechanism should not be very relevant, since the culture medium do not constitute an important triglyceride source. Besides the impaired lipid uptake in adipocytes induced by

hypoxia, recent evidence in human visceral adipose tissue suggests that a lower pressure of oxygen downregulates the expression level of genes involved in *de novo* lipogenesis (García-Fuentes et al., 2015). These data confirm that the reduced levels of triglycerides observed in 3T3-L1 adipocytes after 48 hours of hypoxia are at least partially due to both the increase of lipolysis and the inhibition of *de novo* lipogenesis.

2. Effect of hypoxia on the structure and function of caveolae in 3T3-L1 cells

Several studies have been performed in order to elucidate the role of Cav-1 in cell function, but they are mostly focused on cancer. Studies in different types of cancer expressing a hypoxic profile have shown that Cav-1 is upregulated and associated with larger tumor size, higher tumor grade and stage, resistance to conventional therapies, and poor prognosis (Bourseau-Guilmain et al., 2016; Campbell et al., 2003; Karam et al., 2007; Shen et al., 2008; Wang et al., 2012). In contrast, there exists also evidence in this field suggesting that Cav-1 could be downregulated during hypoxic condition in gastric (Kannan et al., 2014), colon or ovarian carcinoma cells (Bender et al., 2000; Wiechen et al., 2001), among others. On the other hand, it is well recognized that adipocyte is the cell type where caveolae are more abundant. The regulation of this specialized invagination in adipose tissue under hypoxia is not well understood, and limited studies regarding this point have been published. In this context, Regazzetti and colleagues observed in 3T3-L1 adipocytes that hypoxia, through a HIF-1 dependent mechanism, downregulates the expression of cavins 1 and 2, which are necessary for the biogenesis of caveolae. Therefore, these cells showed a reduced number of caveolae in its plasma membrane compared with the control cells (Regazzetti et al., 2015).

In this work, we have observed that Cav-1 mRNA and protein levels are downregulated in both hypoxic models assayed: 3T3-L1 adipocytes differentiated in hypoxia (Fig R4), and mature adipocytes incubated in hypoxia for 48 hours (Fig R9). We have also found that Cav-2 and SDPR/Cavin-2 genes are downregulated in 3T3-L1 adipocytes cultured under hypoxia for 48 hours (Fig R9). This inhibitory role of hypoxia over the caveolae components suggests that its structure could be compromised. This idea is supported by the disruption observed in the typical Cav-1 localization in adipocyte plasma membrane after 48 hours of hypoxia, determined by immunofluorescence (Fig R8).

Furthermore, the results obtained using echinomycin, a drug able to block HIF-1 binding to its HRE in the DNA, suggest that the expression of the main caveolae components are directly regulated by HIF-1. 3T3-L1 adipocytes treated with echinomycin during the incubation in hypoxia for 24 hours exhibit a rise in the expression levels of Cav-1, Cav-2 and SDPR/Cavin-2, compared to the same cells incubated in hypoxia without echinomycin (Fig R13). The idea of a HIF-1-dependent mechanism had been postulated previously by Regazzetti et al for cavin-1 and cavin-2. In this study, we show that expression of caveolins 1 and 2 might also be regulated by this mechanism under hypoxia. In addition to the data obtained with echinomycin, we also demonstrate by ChIP analysis the binding of HIF-1 to an HRE previously identified in the mouse Cav-1 promoter sequence by a bioinformatic analysis. This was confirmed in cells pretreated with echinomycin, which abolishes HIF-1 binding to DNA (Fig R14). This result represents the first experimental evidence of Cav-1 as a target gene for HIF-1 in adipocytes. Results obtained by Wang et al, support our observation but in human renal carcinoma cells (Wang et al., 2012). They identified a possible HRE in the Cav-1 human promoter sequence and, using two approaches, electrophoretic mobility shift assay (EMSA) and ChIP, demonstrated the binding of HIF-1 and HIF-2 to this element. Also, a genome-wide identification of HIF binding sites by a probabilistic model integrating transcription-profiling data and *in silico* binding site prediction, predicted Cav-1 as one of the 216 HIF-target genes (Ortiz-Barahona et al., 2010).

The sustained hypoxia studied in this work mimics, in a certain way, the low oxygen levels experimented by adipose tissue due to its expansion in obesity. However, this tissue could also be affected by other pattern of hypoxia such as intermittent hypoxia (IH). This cyclical pattern of reduced oxygen levels followed by reoxygenation is characteristic in patients suffering of obstructive sleep apnea (OSA), a highly prevalent comorbidity in obesity. To study the effect of this kind of hypoxia, the group of Arnaud et al (Poulain et al., 2015) kindly provided us samples of adipose tissue obtained from mice submitted to IH, which mimics the one experimented by OSA patients during the night. The results obtained in this work suggest that a mild IH (for 14 days) in mice produces a loss of caveolae in the plasma membrane of adipose tissue and in the carotids (Fig R19). This was accompanied by a significant downregulation of

SDPR/cavin-2, but not of the other cavins and caveolins genes (Fig R20). Other investigations have shown that the deletion of SDPR/cavin-2 is able to induce loss of endothelial caveolae in lung and adipose tissue (Hansen et al., 2013). Nevertheless, our results are still preliminary, due to the limited sample size used in the experiment and the lack of data about protein expression levels and cell localization of the caveolae components. Conversely to most of the patients suffering OSA, who also experiment a mild intermittent hypoxia, the mouse model that we have used, lacks other associated deleterious factors, including obesity or genetic vulnerability. This could be the reason for the absence of measurable alterations in the expression profile of caveolae protein components observed in these mice (Fig R20). We therefore evaluated the expression of caveolins and cavins using samples of adipose tissue from mice submitted to a longer IH (4 weeks) resulting in a more severe condition. In these mice, the expression of Cav-2, PTRF/cavin-1 and SDPR/cavin-2 is clearly downregulated. However, the expression of Cav-1 remains stable (Fig R21). These results are also preliminary and it is necessary to look in-depth into the implications of this expression pattern, consequence of IH, for caveolae structure and function.

3. Effect of hypoxia on the structure and function of caveolae in endothelial cells

Hypoxia is not restricted to adipose tissue and affects other tissues in different ways. In this sense, obesity could produce sleep disorders such as the obesity hypoventilation syndrome, which limits O_2 availability in the blood flow producing general hypoxia. Other situations include chronic obstructive pulmonary disease (COPD), interstitial lung diseases, chronic exposure to high altitude and some rare neonatal diseases that are associated with the appearance of hypoxia (Ghofrani et al., 2006). All these conditions induce, through different mechanisms, the development of endothelial cell dysfunction, which may lead to vascular problems such as pulmonary and systemic hypertension (Chan and Vanhoutte, 2013; Lévy et al., 2008). Taking all this information into account, together with the fact that endothelial cells are one of the cell types with a higher density of caveolae in their membranes, and the well-established regulatory role of caveolins and caveolae in endothelial nitric oxide synthase (eNOS) localization and NO production, we have analyzed the effect of hypoxia on caveolae density in the plasma membrane of human aortic endothelial

cells. We observed a significant decrease of caveolae density in the plasma membrane after 16 hours of hypoxia (Fig R23). Interestingly, immunofluorescence staining shows that hypoxia induces the migration of both Cav-1 and PTRF/Cavin-1 from the plasma membrane to the nucleus (Fig R24). Despite that, these results are still preliminary and further studies are necessary to analyze in-depth this effect. For example, mobilization of crucial proteins involved in the structure of caveolae could result in the loss of integrity of these invaginations and explain the results observed with electron microscopy. Disruption of endothelial caveolae has been previously reported as a mechanism for the aberrant endothelium-dependent relaxation and contractility, and, therefore, for the proper maintenance of the myogenic tone (Je et al., 2004). These impairments course with eNOS uncoupling and the consequent imbalance in NO production and calcium signaling (Xu et al., 2007).

On the other hand, Cav-1 mobilization to the nucleus was rather surprising, since Cav-1 is a well-known plasma membrane protein. Chretien A et al reported the increased expression of cytoplasmic and nuclear Cav-1 during establishment of H_2O_2-induced premature senescence in fibroblasts (Chrétien et al., 2008). Nevertheless, PTRF/Cavin-1 was initially discovered in the nucleus participating in the mechanism of transcription termination by RNA polymerase I (Pol I) (Jansa et al., 1998). Recent results suggest that PTRF could collaborate with Cav-1 in cellular senescence in fibroblasts through its targeting to caveolae (Bai et al., 2011). Nonetheless, PTRF translocation to the nucleus in response to metabolic challenges, including the compromise in nutrient availability and insulin stimulation, has been recently described in adipocytes (Liu and Pilch, 2016). In this case Cav-1 remains in the plasma membrane, since cells still respond to insulin or nutrient changes; however, we have seen that in hypoxia insulin signaling is compromised. Hypoxia seems to induce a senescent phenotype in human mesenchymal stem cells, confirmed by the expression of the senescence-associated beta-galactosidase (SA-β-gal) only expressed in senescent cells (Kim et al., 2016). Moreover, hypoxia reduces cellular energy supply and represents a metabolic stress (Mekhail et al., 2006) that, at least acutely, could be mediated by both PTRF/cavin-1 and Cav-1 in the nucleus. The possible effect of Cav-1 on the role of PTRF/cavin-1 in

rRNA transcription in the nucleus in endothelial cells under hypoxia is something that needs to be addressed more deeply and further experiments are necessary.

4. Effect of hypoxia on caveolin-1 phosphorylation

As mentioned in the introduction, Cav-1 displays two main functional domains: the tyrosine 14 (Y14) phosphorylation site and the oligomerization domain that also contains the scaffolding domain. This phosphorylation could be catalyzed mainly by Src kinase, but other kinases including *Fyn*, *Yes* and *c-Abl* have also been implicated, through a chronic or punctual effect in response to growth factor treatment or integrin activation (Boscher and Nabi, 2012). It is well established that insulin induces the phosphorylation of Cav-1 on this Y14 residue. In this work, we observe that hypoxia completely abolishes the insulin-induced phosphorylation of the Y14 residue of Cav-1 in mature 3T3-L1 adipocytes (Fig R9B). Previous reports of our group showed a positive correlation between reduced insulin sensitivity and the decrease of Cav-1 phosphorylation in this cell type (Palacios-Ortega et al., 2014, 2015). Moreover, it is well known that Cav-1 is directly phosphorylated by the tyrosine kinase activity of the IR after insulin stimulation, promoting its activation and the subsequent signal transduction leading to the translocation of GLUT4 to the adipocyte plasma membrane (Yamamoto et al., 1998). In agreement with all these observations, we have found that hypoxia significantly reduces insulin-stimulated glucose uptake (Fig R7A) and also GLUT4 expression (Fig R6C).

5. Hypoxia as an important factor for insulin resistance development

Other aim of this work was to study the effect of hypoxia on insulin signaling and the importance of the caveolae in this process. Our results show that differentiation of 3T3-L1 adipocyte under hypoxia suppresses the expected increase of gene expression of IR (*Insr*), Akt2 (*Akt2*) and GLUT4 (*Slc2a4*), and also of the protein level of IR (Fig R3). Since one of the main functions of insulin is the synthesis of triacylglycerols (Czech et al., 2013), constituting the most important adipogenic stimulus added to the differentiation cocktail, it is expected that the decay in expression of IR, both at mRNA and protein level, throughout the differentiation process, would contribute to the reduced fat storage observed in the hypoxic 3T3-L1 adipocytes (Fig R2).

In mature 3T3-L1 adipocytes, hypoxia incubation for 48 hours induces a significant downregulation of all mediators of the insulin pathway analyzed: IR, Akt and GLUT4 (Fig R6A). We also observe the absence of IR phosphorylation after insulin stimulation when the adipocytes are incubated at low O_2 levels compared to those incubated in normoxia (Fig R6B). These results correlate well with the downregulation of the caveolae-related proteins analyzed. A strong line of investigation has established the importance of caveolae in the insulin signaling transmission. Yamamoto et al have shown that the CSD of Cav-1 interacts directly with caveolin-binding motifs that exist in the IR (Yamamoto et al., 1998). Moreover, cholesterol depletion using β-cyclodextrin treatment in primary adipocytes isolated from rats, induced the loss of caveolae invaginations, attenuating IR signaling and glucose transport (Gustavsson et al., 1999; Parpal et al., 2001). Insulin signaling was rescued by spontaneous recovery or by exogenous replenishment of cholesterol, suggesting that IR is dependent on the caveolae environment for a successful signal transmission (Gustavsson et al., 1999). On the other hand, the effect of hypoxia on caveolae integrity and its consequences for the insulin pathway have been addressed previously. Regazzetti et al. observed an important downregulation of insulin signaling mediators after acute hypoxia on 3T3-L1 adipocytes (Regazzetti et al., 2009). A few years later, the same group proposed that the caveolae disappearance is produced by the reduced levels of cavin-1 and 2, as a new mechanism for the development of insulin resistance in both human and 3T3-L1 adipocytes (Regazzetti et al., 2015). Taking all these data into account, together with the reduction in caveolae density we have observed in adipose tissue submitted to intermittent hypoxia (Fig R19), and in HAoEC cells submitted to continuous hypoxia (Fig R23), our results suggest that the hypoxia-induced disruption of caveolae in the plasma membrane of 3T3-L1 adipocytes could be behind the general downregulation of the insulin signaling pathway.

One of the main final effects of insulin signaling in adipocytes is the translocation of the glucose transporter GLUT4 from the internal glucose storage vesicles (GSV) to the plasma membrane. As previously described, we observe an enhanced basal glucose uptake independent of insulin stimulation after 48 hours of hypoxia (Fig R7A). The alterations of the glucose uptake pattern observed in the 3T3-L1 adipocytes are

consistent with the changes in the expression profile obtained for the glucose transporters GLUT1 and GLUT4 (Fig R6C). On one hand, the important increase in basal glucose uptake is probably due to the upregulation of GLUT1, a facilitative glucose transporter independent of insulin, that has a 184 bp hypoxia-responsive element (HRE) in the promoter (Hayashi et al., 2004). On the other hand, the loss of insulin-stimulated glucose uptake (Fig R7A) is probably a consequence of the downregulation of GLUT4. In this context, previous studies in adipocytes have shown that, following 48-h or longer exposure to hypoxia, there is a marked fall in GLUT4 gene expression and a loss of GLUT4 protein (Wood et al., 2009). In the same line, results obtained from the immunofluorescence staining suggest that hypoxia impairs the insulin-stimulated GLUT4 translocation to the plasma membrane of 3T3-L1 adipocytes, as shown by the diffuse signal observed in this group of cells when compared to controls in normoxia (Fig R8). In this sense, we have not been able to find previous reports supporting the effect of hypoxia on GLUT4 translocation. However, in normoxia, it has been described that knockdown of HIF-1α expression in myocytes results in abrogation of insulin-stimulated glucose uptake associated with impaired mobilization of GLUT4 to the plasma membrane (Sakagami et al., 2014). Taking into account that HIF-1 is the main mediator of the molecular response to hypoxia, and that we have shown that Cav-1 gene can be a direct target for this transcription factor, we addressed the hypothesis that HIF-1 could also be responsible for the effects observed in insulin signaling under hypoxia.

To face this question, we treated 3T3-L1 adipocytes with LW6, a small molecule that inhibits the accumulation of HIF-1α via upregulation of VHL protein expression, and therefore promoting the degradation of this transcription factor (Lee et al., 2010). However, LW6 seems to have a direct effect enhancing the sensitivity of insulin-stimulated GLUT4 mediated glucose uptake, since it is patent both in normoxia and in hypoxia conditions (Fig R7A). On the other hand, basal glucose uptake, principally mediated by GLUT1, whose expression is upregulated in hypoxia, is not reduced by LW6 (Fig R7A). It is well known that GLUT1 is the main responsible for basal glucose uptake in adipocytes; however, GLUT3 is also involved in this function and it has been reported to be upregulated by hypoxia in human adipocytes (Wood et al., 2007).

Moreover, knockdown of GLUT3 with siRNA significantly reduced myocyte glucose uptake (Copland et al., 2007). However, the mechanism for the hypoxia-induced upregulation of GLUT3 is unknown and the role of HIF-1 in this mechanism is uncertain, although a putative HRE, that could be critical in GLUT3 promoter activity, has been described (Yu et al., 2012). In this sense, further studies are required in order to elucidate the participation of this glucose transporter in basal uptake of glucose in 3T3-L1 adipocytes and whether GLUT3 might be involved in the upregulation of non-insulin-mediated sugar transport by a HIF-1 independent mechanism.

Since LW6 is defined as an indirect HIF-1 inhibitor and in our case it did not show any effect on hypoxia-induced GLUT1 activity, we designed experiments using echinomycin, which reduces directly HIF-1 transcriptional activity by blocking its binding to DNA, in order to assay the effect of this transcription factor on the expression of several insulin signaling mediators. We first measured the expression of *Slc2a1* gene (GLUT1) in adipocytes incubated under hypoxia and treated with echinomycin. As expected, *Slc2a1* expression was increased in the hypoxic cells after 24 and 48 hours of treatment, and echinomycin abolishes this effect (Fig R11). Furthermore, echinomycin treatment restores the expression of *Slc2a4* (GLUT4) diminished by 24 hours of hypoxia compared to their counterpart hypoxic echinomycin-free adipocytes (Fig R12C). These results support the role of HIF-1 in the altered glucose uptake pattern observed in hypoxia through the expression of both *Slc2a1* and *Slc2a4*.

We also determined the expression of other insulin signaling mediators under hypoxia, with or without previous treatment of the cells with echinomycin. A previous work from Regazzetti and colleagues did not observe changes in the expression levels of *Insr* (IR) after 16 hours of hypoxia in adipocytes (Regazzetti et al., 2009). However, in our experiment we submitted 3T3-L1 adipocytes to 24 hours of hypoxia slightly inducing the expression of *Insr* (IR), but reducing the mRNA expression of *Akt2* significantly (Fig R12B). On the other hand, echinomycin decreases the expression of *Insr* and *Akt2* in normoxia and *Insr* in hypoxia. Therefore, in this case the hypoxia-dependent effect on the insulin signaling intermediates does not seem to be mediated by HIF-1, since echinomycin is not able to revert them. In this regard, although echinomycin is a

potent inhibitor of HIF-1 binding to DNA, it also interferes with the activity of other transcription factors, including Sp1 (Vlaminck et al., 2007), which has been involved in the transcriptional regulation of, for example, IR (Costa et al., 2008; Foti et al., 2003).

The hypoxia-induced increase in *Insr* and decrease in *Akt2* expression is difficult to explain, since both effects seem contradictory in relation to insulin signaling transmission. They may be part of a delayed response to low oxygen concentration, considering also that Akt is involved in a variety of different signaling pathways, such as inflammation or oxidative stress responses.

6. Gene expression profile induced by hypoxia

In order to elucidate new mechanisms involved in the response to hypoxia, we have performed a gene expression array in search for genes with differential expression in 3T3-L1 adipocytes incubated under hypoxia for 48 hours. The Gene Ontology (GO) enrichment analysis leads to 6 categories related to insulin response and carbohydrates metabolism (Table R1). The most significant category of genes corresponds to those related to caveolae. Some of these gene expression changes have been validated by RT-PCR in this work, including the downregulation of *Cav-2* and *Sdpr* and the upregulation of *Slc2a1*.

In the microarray, the gene with the highest level of upregulation is enolase 2 (*Eno2*) (Table R2). There are no reports about the role of *Eno2* in adipocytes, except a recent work in human Simpson-Golabi-Behmel syndrome (SGBS) adipocytes, which also overexpressed this gene in response to hypoxia. The authors identified a HRE in the *Eno2* promoter suggesting that HIF-1 might be responsible for *Eno2* mRNA upregulation in human adipocytes (Leiherer et al., 2014). Since *Eno1*, the isoform of enolase expressed mainly in cancer cells, participates in anaerobic glycolysis contributing to the Warburg effect (Fu et al., 2015), perhaps *Eno2* could contribute to the adaptation of adipocytes to the hypoxic environment in obesity. Other interesting genes strongly upregulated by hypoxia include growth hormone releasing hormone (*Ghrh*) and insulin-like growth factor 1 (*Igf1*) and its receptor, *Igf1r* (Table R2). In regard to this, it is well established that growth hormone (GH) hypersecretion is positively correlated with the development of insulin resistance (Rose and Clemmons,

2002). When GH is secreted in excess, it acts directly to block insulin signaling, inducing resistance to stimulation of downstream molecules, such as insulin receptor substrate-1 (IRS-1) and PI3K, which are important for glucose transport in muscle and fat and for the inhibition of hepatic gluconeogenesis (Clemmons, 2004). Moreover, Clemmons et al. reviewed the relation between IGF-1 secretion and GH and pointed out that GH regulates IGF-1 concentrations inducing cell growth (Clemmons, 2004). GH also plays an important role in cell surviving in periods of food deprivation, stimulating lipolysis and inhibiting insulin-induced suppression of hepatic gluconeogenesis (Sakharova et al., 2008).

An interesting gene that is strongly downregulated by hypoxia is sortilin (*Sort1)* (Table R3). This gene has been investigated as an essential component of the GSVs, being responsible not only for the formation of vesicles, but also for their insulin responsiveness (Huang et al., 2013; Shi and Kandror, 2005). *Sort1* downregulation by hypoxia could be part of the underlying mechanism for the absence of insulin-induced GLUT4 translocation in 3T3-L1 adipocytes observed in our study (Fig R8).

In accordance with these results, 3T3-L1 adipocytes incubated in hypoxia also show downregulation of genes involved in the insulin signaling pathway, including *Irs1*, *Slc2a4* and the subunit regulators of Pi3K: *Pik3r3* and *Pik3r1* (Table R3). Furthermore, the expression of adiponectin (*Adipoq*) is also downregulated in response to hypoxia (Table R3). This adipokine is a known insulin sensitizer hormone, and its lower expression has been pointed out as one of the main effects that contribute to the development of insulin resistance in adipose tissue of obese patients (Trayhurn, 2014). In this sense, it was previously reported that adiponectin expression was upregulated in adipocytes from knockout mice with HIF1-deficient adipose tissue, which was associated with amelioration in obesity and insulin resistance (Jiang et al., 2011).

The gene expression changes observed throughout this work, including upregulation of *Slc2a1* and downregulation of the caveolae-related genes *Sdpr*, *Cav-2* and *Slc2a4*, contribute to validate the results obtained in the differential expression array. In addition to that, we have analyzed by RT-qPCR the expression of four additional genes revealed as differentially expressed in hypoxia in the microarray experiment: the above mentioned *Adipoq* and *Pik3r3*, plus *Pparg* and *Cbpa*, which were selected since

they are directly involved in adipocyte differentiation, a process that, as discussed earlier in this work, is strongly affected by hypoxia. The expression of all these genes, which was reduced in the array experiment, was analyzed after 24 and 48 hours of hypoxia. All these genes resulted significantly downregulated after 48 hours of hypoxia, confirming the array results (Fig R18B). As a matter of fact, 24 hours of lower oxygen levels were enough to downregulate the expression of all these genes except *Pparg*, whose expression remained stable after this time (Fig R18A).

7. Strengths and limitations

This work provides new clues for the molecular mechanisms induced by hypoxia in obesity and its comorbidities. Up to now, the experimental evidence of hypoxia effects on the transcriptional regulation of genes involved in caveolae structure and function, and the repercussion on insulin signaling in adipocytes, is limited. This question has been only addressed by Regazzetti et al. using modern techniques (Regazzetti et al., 2015). Our study complements their findings providing novel insights including the identification of a HRE in Cav-1 promoter, using *in silico* analysis, and demonstrating the ability of HIF-1 to bind to it, assayed by chromatin immunoprecipitation. The methodology selected to study the transcriptional regulation of caveolae genes by HIF-1, determines with high confidence the interaction between the transcription factor and its binding elements in the target DNA. However, this study has some limitations. For example, the use of functional techniques to measure the actual transcriptional-regulatory activity of HIF-1 on Cav-1 promoter strength would allow to confirm this finding.

One of the major concerns is the lack of assays studying gain or loss of function, which would allow to establish a direct connection between the loss of caveolae integrity, the disruption of insulin signaling and the other metabolic effects observed in adipocytes after incubation in hypoxia. These experimental approaches are difficult to perform in the cell line selected for this work, due to the limited transfection efficiency reported (Kilroy et al., 2009).

In addition, most of the work was carried out in cultured cells since it is easier, less expensive and provides a more homogenous response towards the different

experimental conditions, including hypoxia. Nevertheless, it would be advisable to test our hypothesis in animal models, or at least in primary adipocytes isolated from obese animals or from rodents submitted to different models of hypoxia. The major advantage of this approach is the ability to obtain adipocytes extracted from various locations or depots, from animals of different ages or enduring different comorbidities, as well as to take into account the important influence of other tissues, inflammation or dietary factors.

Finally, the insufficient sample size used to obtain the results from the intermittent hypoxia mouse model, and the lack of information about the protein expression profile, make difficult to come to definitive conclusions regarding the effect of intermittent hypoxia in the caveolae status and the subsequent dysregulation of adipose tissue in these mice.

8. Corollary

In summary, this work corroborates the role of caveolae structure for the proper functioning of insulin signaling and, therefore, for competent adipocyte physiology in response to hypoxia, including adipogenesis and glucose metabolism. All models of hypoxia assayed in this work induce the downregulation of genes essential for caveolae formation and function that compromise also their integrity in the plasma membrane. This effect is positively correlated with the loss of insulin responsiveness and with the impairment of lipid metabolism in adipocytes. Moreover, this work shows that HIF-1 is directly involved in the molecular regulation of this response mechanism, since it regulates the expression of *Cav-1* and seems to play also a role in the regulation of *Cav-2* and *Sdpr* expression. Furthermore, hypoxia importantly modifies the overall gene expression pattern in adipocytes.

Broadening the knowledge of the response to hypoxia will contribute to the elucidation of the underlying mechanisms related to the deleterious effects of low oxygen in adipocytes, including the increase of GH and IGF-1 release, promotion of insulin resistance through caveolae disruption, and downregulation of *Sort1*, which could explain the absence of insulin-induced GLUT4 translocation to the plasma membrane in 3T3-L1 adipocytes.

CONCLUSIONS

CONCLUSIONS

1. Chronic hypoxia strongly inhibits the 3T3-L1 adipocyte differentiation process.
2. Continuous hypoxia for 48 hours reduces the triglyceride content in 3T3-L1 mature adipocytes.
3. Continuous hypoxia for 48 hours downregulates insulin signaling and reduces insulin-mediated GLUT4 translocation and glucose uptake, driving to development of insulin resistance.
4. Continuous hypoxia for 48 hours increases GLUT1 expression, basal glucose uptake and lactate production, clearly indicating a shift from aerobic to anaerobic metabolism in adipocytes.
5. Hypoxia, whether chronic, continuous (48 hours) or intermittent, produces alterations in caveolae structure, suggesting that caveolae disruption is implicated in the development of obesity-related insulin resistance
6. The use of echinomycin, which inhibits HIF1 binding to Hypoxia Response Elements (HRE), indicates that the expression of GLUT1 (*Slc2a1*) and GLUT4 (*Slc2a4*) genes is regulated by HIF-1 in hypoxic adipocytes, contributing to explain the altered glucose uptake pattern observed in hypoxia.
7. The use of echinomycin also indicates that the expression of Cav-1, Cav-2 and SDPR/Cavin-2 genes is regulated by HIF-1 in hypoxic adipocytes, contributing to explain the changes in caveolae density observed in hypoxia.
8. Chromatin immunoprecipitation demonstrates that the hypoxia response element present in mouse Cav-1 promoter (-442 TSS) is regulated directly by HIF-1.
9. A microarray analysis of gene expression confirms that pathways related to caveolae structure and function, insulin response, glucose transport and lipid biosynthesis are affected by hypoxia. This analysis also highlights the involvement of other genes such as *Sort1*, *Ghrh* and *Igf* in the effects of hypoxia on adipocytes
10. In summary, hypoxia compromise caveolae integrity and function through the downregulation of structural proteins by a Hif-1-dependent mechanism in

adipocytes, resulting in the impairment of insulin response and lipid metabolism.

REFERENCES

REFERENCES

Ardissone, A., Bragato, C., Caffi, L., Blasevich, F., Maestrini, S., Bianchi, M.L., Morandi, L., Moroni, I., and Mora, M. (2013). Novel PTRF mutation in a child with mild myopathy and very mild congenital lipodystrophy. BMC Med. Genet. *14*, 89.

Ariotti, N., Fern??ndez-Rojo, M.A., Zhou, Y., Hill, M.M., Rodkey, T.L., Inder, K.L., Tanner, L.B., Wenk, M.R., Hancock, J.F., and Parton, R.G. (2014). Caveolae regulate the nanoscale organization of the plasma membrane to remotely control Ras signaling. J. Cell Biol. *204*, 777–792.

Arsham, A.M., Howell, J.J., and Simon, M.C. (2003). A novel hypoxia-inducible factor-independent hypoxic response regulating mammalian target of rapamycin and its targets. J. Biol. Chem. *278*, 29655–29660.

Bai, L., Deng, X., Li, J., Wang, M., Li, Q., An, W., a, D., and Cong, Y.-S. (2011). Regulation of cellular senescence by the essential caveolar component PTRF/Cavin-1. Cell Res. *21*, 1088–1101.

Bailey, C.J. (2005). Treating insulin resistance in type 2 diabetes with metformin and thiazolidinediones. Diabetes. Obes. Metab. *7*, 675–691.

Barja-Fernandez, S., Leis, R., Casanueva, F.F., and Seoane, L.M. (2014). Drug development strategies for the treatment of obesity: How to ensure efficacy, safety, and sustainable weight loss. Drug Des. Devel. Ther. *8*, 2391–2400.

Bender, F.C., Reymond, M.A., Bron, C., and Quest, A.F.G. (2000). Caveolin-1 levels are down-regulated in human colon tumors, and ectopic expression of caveolin-1 in colon carcinoma cell lines reduces cell tumorigenicity. Cancer Res. *60*, 5870–5878.

Bernlohr, D.A., Bolanowski, M.A., Kelly, T.J., and Lane, M.D. (1985). Evidence for an increase in transcription of specific mRNAs during differentiation of 3T3-L1 preadipocytes. J. Biol. Chem. *260*, 5563–5567.

Billaud, M., Lohman, A.W., Johnstone, S.R., Biwer, L.A., Mutchler, S., and Isakson, B.E. (2014). Regulation of cellular communication by signaling microdomains in the blood vessel wall. Pharmacol. Rev. *66*, 513–569.

Boscher, C., and Nabi, I. (2012). Caveolin-1: role in cell signaling. Adv Exp Med Biol 29–50.

Bourseau-Guilmain, E., Menard, J.A., Lindqvist, E., Indira Chandran, V., Christianson, H.C., Cerezo Magaña, M., Lidfeldt, J., Marko-Varga, G., Welinder, C., and Belting, M. (2016). Hypoxia regulates global membrane protein endocytosis through caveolin-1 in cancer cells. Nat. Commun. *7*, 11371.

Brahimi-Horn, M.C., and Pouysségur, J. (2007). Oxygen, a source of life and stress. FEBS Lett. *581*, 3582–3591.

Branza-Nichita, N., Macovei, A., and Lazar, C. (2012). Caveolae-Dependent Endocytosis in Viral Infection. Mol. Regul. Endocytosis 1–32.

Briand, N., Prado, C., Mabilleau, G., Lasnier, F., Le Lièpvre, X., Covington, J.D., Ravussin, E., Le Lay, S., and Dugail, I. (2014). Caveolin-1 expression and cavin stability regulate caveolae dynamics in adipocyte lipid store fluctuation. Diabetes *63*, 4032–4044.

Bruno, J., Brumfield, A., Chaudhary, N., Iaea, D., and McGraw, T.E. (2016). SEC16A is a RAB10 effector required for insulin-stimulated GLUT4 trafficking in adipocytes. J. Cell Biol. *214*, jcb.201509052.

Bustin, S. (2000). Absolute quantification of mRNA using real-time reverse transcription polymerase chain reaction assays. J. Mol. Endocrinol. *25*, 169–193.

Campbell, L., Gumbleton, M., and Griffiths, D.F.R. (2003). Caveolin-1 overexpression predicts poor disease-free survival of patients with clinically confined renal cell carcinoma. Br. J. Cancer *89*, 1909–1913.

Chan, C.K., and Vanhoutte, P.M. (2013). Hypoxia, vascular smooth muscles and endothelium. Acta Pharm. Sin. B *3*, 1–7.

Chen, B., Lam, K.S.L., Wang, Y., Wu, D., Lam, M.C., Shen, J., Wong, L., Hoo, R.L.C., Zhang, J., and Xu, A. (2006). Hypoxia dysregulates the production of adiponectin and plasminogen activator inhibitor-1 independent of reactive oxygen species in adipocytes. Biochem. Biophys. Res. Commun. *341*, 549–556.

Cheng, J.P.X., and Nichols, B.J. (2016). Caveolae: One Function or Many? Trends Cell

Biol. *26*, 177–189.

Choi, C.S., Kim, Y.-B., Lee, F.N., Zabolotny, J.M., Kahn, B.B., and Youn, J.H. (2002). Lactate induces insulin resistance in skeletal muscle by suppressing glycolysis and impairing insulin signaling. Am. J. Physiol. Endocrinol. Metab. *283*, E233–E240.

Chrétien, A., Piront, N., Delaive, E., Demazy, C., Ninane, N., and Toussaint, O. (2008). Increased abundance of cytoplasmic and nuclear caveolin 1 in human diploid fibroblasts in H2O2-induced premature senescence and interplay with p38αMAPK. FEBS Lett. *582*, 1685–1692.

Christian K.Roberts, Andrea L.Hevener, and R.J.B. (2014). Metabolic Syndrome and Insulin Resistance: Underlying Causes and Modification by Exercise Training. Compr Physiol *3*, 1–58.

Clarke, S.L., Robinson, C.E., and Gimble, J.M. (1997). CAAT / Enhancer Binding Proteins Directly Modulate Transcription from the Peroxisome Proliferator- Activated Receptor g 2 Promoter. Biochem. Biophys. Res. Commun. *240*, 99–103.

Clemmons, D.R. (2004). The relative roles of growth hormone and IGF-1 in controlling insulin sensitivity. J. Clin. Invest. *113*, 25–27.

Cohen, A.W., Combs, T.P., Scherer, P.E., and Lisanti, M.P. (2003). Role of caveolin and caveolae in insulin signaling and diabetes. Am. J. Physiol. Endocrinol. Metab. *285*, E1151–E1160.

Copland, J.A., Pardini, A.W., Wood, T.G., Yin, D., Green, A., Bodenburg, Y.H., Urban, R.J., and Stuart, C.A. (2007). IGF-1 controls GLUT3 expression in muscle via the transcriptional factor Sp1. Biochim. Biophys. Acta - Gene Struct. Expr. *1769*, 631–640.

Costa, V., Foti, D., Paonessa, F., Chiefari, E., Palaia, L., Brunetti, G., Gulletta, E., Fusco, a, and Brunetti, a (2008). The insulin receptor: a new anticancer target for peroxisome proliferator-activated receptor-gamma (PPARgamma) and thiazolidinedione-PPARgamma agonists. Endocr. Relat. Cancer *15*, 325–335.

Czech, M.P., Tencerova, M., Pedersen, D.J., and Aouadi, M. (2013). Insulin signalling mechanisms for triacylglycerol storage. Diabetologia *56*, 949–964.

Deng, W., Feng, X., Li, X., Wang, D., and Sun, L. (2016). Hypoxia-inducible factor 1 in autoimmune diseases. Cell. Immunol. *303*, 7–15.

Després, J.P. (2012). Body fat distribution and risk of cardiovascular disease: An update. Circulation *126*, 1301–1313.

Dewan, N.A., Nieto, F.J., and Somers, V.K. (2015). Intermittent hypoxemia and OSA: Implications for comorbidities. Chest *147*, 266–274.

DiGirolamo, M., Newby, F.D., and Lovejoy, J. (1992). Lactate production in adipose tissue: a regulated function with extra-adipose implications. FASEB J. *6*, 2405–2412.

Dijk, W., Beigneux, A.P., Larsson, M., Bensadoun, A., Young, S.G., and Kersten, S. (2016). Angiopoietin-like 4 (ANGPTL4) promotes intracellular degradation of lipoprotein lipase in adipocytes. J. Lipid Res. *7*, 956–963.

Drab, M., Verkade, P., Elger, M., Kasper, M., Lohn, M., Lauterbach, B., Menne, J., Lindschau, C., Mende, F., Luft, F.C., et al. (2001). Loss of caveolae, vascular dysfunction, and pulmonary defects in caveolin-1 gene-disrupted mice. Science (80-.). *293*, 2449–2452.

Echarri, A., and Del Pozo, M.A. (2015). Caveolae - mechanosensitive membrane invaginations linked to actin filaments. J. Cell Sci. *128*, 2747–2758.

Fagerholm, S., Örtegren, U., Karlsson, M., Ruishalme, I., and Strålfors, P. (2009). Rapid insulin-dependent endocytosis of the insulin receptor by caveolae in primary adipocytes. PLoS One *4*.

Fisslthaler, B., Benzing, T., Busse, R., and Fleming, I. (2003). Insulin enhances the expression of the endothelial nitric oxide synthase in native endothelial cells: A dual role for Akt and AP-1. Nitric Oxide - Biol. Chem. *8*, 253–261.

Foti, D., Iuliano, R., Chiefari, E., and Brunetti, A. (2003). A nucleoprotein complex containing Sp1, C/EBP beta, and HMGI-Y controls human insulin receptor gene transcription. Mol. Cell. Biol. *23*, 2720–2732.

Fra, A.M., Williamson, E., Simons, K., and Parton, R.G. (1995). De novo formation of caveolae in lymphocytes by expression of VIP21-caveolin. Proc. Natl. Acad. Sci. U. S. A.

92, 8655–8659.

Fridlyand, L.E., and Philipson, L.H. (2006). Reactive species and early manifestation of insulin resistance in type 2 diabetes. Diabetes. Obes. Metab. *8*, 136–145.

Fu, Q.F., Liu, Y., Fan, Y., Hua, S.N., Qu, H.Y., Dong, S.W., Li, R.L., Zhao, M.Y., Zhen, Y., Yu, X.L., et al. (2015). Alpha-enolase promotes cell glycolysis, growth, migration, and invasion in non-small cell lung cancer through FAK-mediated PI3K/AKT pathway. J Hematol Oncol *8*, 22.

García-Fuentes, E., Santiago-Fernández, C., Gutiérrez-Repiso, C., Mayas, M.D., Oliva-Olivera, W., Coín-Aragüez, L., Alcaide, J., Ocaña-Wilhelmi, L., Vendrell, J., Tinahones, F.J., et al. (2015). Hypoxia is associated with a lower expression of genes involved in lipogenesis in visceral adipose tissue. J. Transl. Med. *13*, 373.

Gentleman, R. (2005). Bioinformatics and computational biology solutions using R and Bioconductor.

Ghofrani, H.A., Voswinckel, R., Reichenberger, F., Weissmann, N., Schermuly, R.T., Seeger, W., and Grimminger, F. (2006). Hypoxia- and non-hypoxia-related pulmonary hypertension - Established and new therapies. Cardiovasc. Res. *72*, 30–40.

Ginsberg, H.N. (2000). Insulin resistance and cardiovascular disease. J. Clin. Invest. *106*, 453–458.

Gl??ck, A.A., Aebersold, D.M., Zimmer, Y., and Medov??, M. (2015). Interplay between receptor tyrosine kinases and hypoxia signaling in cancer. Int. J. Biochem. Cell Biol. *62*, 101–114.

González-Muniesa, P., De Oliveira, C., Pérez De Heredia, F., Thompson, M.P., and Trayhurn, P. (2011). Fatty acids and hypoxia stimulate the expression and secretion of the adipokine ANGPTL4 (angiopoietin-like protein 4/ fasting-induced adipose factor) by human adipocytes. J. Nutrigenet. Nutrigenomics *4*, 146–153.

González-Muñoz, E., López-Iglesias, C., Calvo, M., Palacín, M., Zorzano, A., and Camps, M. (2009). Caveolin-1 loss of function accelerates glucose transporter 4 and insulin receptor degradation in 3T3-L1 adipocytes. Endocrinology *150*, 3493–3502.

Goossens, G.H., and Blaak, E.E. (2015). Adipose Tissue Dysfunction and Impaired Metabolic Health in Human Obesity: A Matter of Oxygen? Front. Endocrinol. (Lausanne). *6*, 1–5.

Govers, E. (2015). Obesity and Insulin Resistance Are the Central Issues in Prevention of and Care for Comorbidities. Healthcare *3*, 408–416.

Gregoire, F.M., Smas, C.M., and Sul, H.S. (1998). Understanding adipocyte differentiation. Physiol. Rev. *78*, 783–809.

Gustavsson, J., Parpal, S., and Strålfors, P. (1996). Insulin-stimulated glucose uptake involves the transition of glucose transporters to a caveolae-rich fraction within the plasma membrane: implications for type II diabetes. Mol. Med. *2*, 367–372.

Gustavsson, J., Parpal, S., Karlsson, M., Ramsing, C., Thorn, H., Borg, M., Lindroth, M., Peterson, K.H., Magnusson, K.E., and Strâlfors, P. (1999). Localization of the insulin receptor in caveolae of adipocyte plasma membrane. FASEB J. *13*, 1961–1971.

Hagen, T., Taylor, C.T., Lam, F., and Moncada, S. (2003). Redistribution of intracellular oxygen in hypoxia by nitric oxide: effect on HIF1alpha. Science *302*, 1975–1978.

Hansen, C.G., Bright, N.A., Howard, G., and Nichols, B.J. (2009). SDPR induces membrane curvature and functions in the formation of caveolae. Nat Cell Biol *11*, 807–814.

Hansen, C.G., Shvets, E., Howard, G., Riento, K., and Nichols, B.J. (2013). Deletion of cavin genes reveals tissue-specific mechanisms for morphogenesis of endothelial caveolae. Nat. Commun. *4*, 1831.

Harris, A.L. (2002). Hypoxia — a Key Regulatory Factor in Tumour Growth. Nat. Rev. Cancer *2*, 38–47.

Hashimoto, T., Yokokawa, T., Endo, Y., Iwanaka, N., Higashida, K., and Taguchi, S. (2013). Modest hypoxia significantly reduces triglyceride content and lipid droplet size in 3T3-L1 adipocytes. Biochem. Biophys. Res. Commun. *440*, 43–49.

Hayashi, M., Sakata, M., Takeda, T., Yamamoto, T., Okamoto, Y., Sawada, K., Kimura, A., Minekawa, R., Tahara, M., Tasaka, K., et al. (2004). Induction of glucose transporter

1 expression through hypoxia-inducible factor 1?? under hypoxic conditions in trophoblast-derived cells. J. Endocrinol. *183*, 145–154.

Henry, R.R. (2003). Insulin resistance: From predisposing factor to therapeutic target in type 2 diabetes. Clin. Ther. *25*.

Hill, M.M., Bastiani, M., Luetterforst, R., Kirkham, M., Kirkham, A., Nixon, S.J., Walser, P., Abankwa, D., Oorschot, V.M.J., Martin, S., et al. (2008). PTRF-Cavin, a Conserved Cytoplasmic Protein Required for Caveola Formation and Function. Cell *132*, 113–124.

Holdsworth, M., El Ati, J., Bour, A., Kameli, Y., Derouiche, A., Millstone, E., and Delpeuch, F. (2013). Developing national obesity policy in middle-income countries: A case study from North Africa. Health Policy Plan. *28*, 858–870.

Hosogai, N., Fukuhara, A., Oshima, K., Miyata, Y., Tanaka, S., Segawa, K., Furukawa, S., Tochino, Y., Komuro, R., Matsuda, M., et al. (2007). Adipose tissue hypoxia in obesity and its impact on adipocytokine dysregulation. Diabetes *56*, 901–911.

Huang, S., and Czech, M.P. (2007). The GLUT4 Glucose Transporter. Cell Metab. *5*, 237–252.

Huang, G., Buckler-Pena, D., Nauta, T., Singh, M., Asmar, A., Shi, J., Kim, J.Y., and Kandror, K. V (2013). Insulin responsiveness of glucose transporter 4 in 3T3-L1 cells depends on the presence of sortilin. Mol. Biol. Cell *24*, 3115–3122.

Hubbard, S.R. (1997). Crystal structure of the activated insulin receptor tyrosine kinase in complex with peptide substrate and ATP analog. EMBO J. *16*, 5572–5581.

Hurt, R.T., Frazier, T.H., McClave, S.A., and Kaplan, L.M. (2011). Obesity epidemic: overview, pathophysiology, and the intensive care unit conundrum. JPEN. J. Parenter. Enteral Nutr. *35*, 4S–13S.

Iiyori, N., Alonso, L.C., Li, J., Sanders, M.H., Garcia-Ocana, A., O'Doherty, R.M., Polotsky, V.Y., and O'Donnell, C.P. (2007). Intermittent hypoxia causes insulin resistance in lean mice independent of autonomic activity. Am. J. Respir. Crit. Care Med. *175*, 851–857.

Ip, M.S.M., Lam, B., Ng, M.M.T., Lam, W.K., Tsang, K.W.T., and Lam, K.S.L. (2002). Obstructive sleep apnea is independently associated with insulin resistance. Am. J.

Respir. Crit. Care Med. *165*, 670–676.

Irizarry, R.A., Bolstad, B.M., Collin, F., Cope, L.M., Hobbs, B., and Speed, T.P. (2003). Summaries of Affymetrix GeneChip probe level data. Nucleic Acids Res. *31*, e15.

Isshiki, M., Ando, J., Yamamoto, K., Fujita, T., Ying, Y., and Anderson, R.G.W. (2002). Sites of Ca(2+) wave initiation move with caveolae to the trailing edge of migrating cells. J. Cell Sci. *115*, 475–484.

Jansa, P., Mason, S.W., Hoffmann-Rohrer, U., and Grummt, I. (1998). Cloning and functional characterization of PTRF, a novel protein which induces dissociation of paused ternary transcription complexes. EMBO J. *17*, 2855–2864.

Je, H.-D., Gallant, C., Leavis, P.C., and Morgan, K.G. (2004). Caveolin-1 regulates contractility in differentiated vascular smooth muscle. Am. J. Physiol. Heart Circ. Physiol. *286*, H91–H98.

Jiang, C., Qu, A., Matsubara, T., Chanturiya, T., Jou, W., Gavrilova, O., Shah, Y.M., and Gonzalez, F.J. (2011). Disruption of hypoxia-inducible factor 1 in adipocytes improves insulin sensitivity and decreases adiposity in high-fat diet-fed mice. Diabetes *60*, 2484–2495.

Jiang, C., Kim, J.-H., Li, F., Qu, A., Gavrilova, O., Shah, Y.M., and Gonzalez, F.J. (2013). Hypoxia-inducible factor 1α regulates a SOCS3-STAT3-adiponectin signal transduction pathway in adipocytes. J. Biol. Chem. *288*, 3844–3857.

Jiménez, C., Hernández, C., Pimentel, B., and Carrera, A.C. (2002). The p85 regulatory subunit controls sequential activation of phosphoinositide 3-kinase by Tyr kinases and Ras. J. Biol. Chem. *277*, 41556–41562.

Kabayama, K., Sato, T., Saito, K., Loberto, N., Prinetti, A., Sonnino, S., Kinjo, M., Igarashi, Y., and Inokuchi, J. (2007). Dissociation of the insulin receptor and caveolin-1 complex by ganglioside GM3 in the state of insulin resistance. Proc. Natl. Acad. Sci. U. S. A. *104*, 13678–13683.

Kadowaki, T., Yamauchi, T., Kubota, N., Hara, K., Ueki, K., and Tobe, K. (2006). Adiponectin and adiponectin receptors in insulin resistance , diabetes , and the

metabolic syndrome. Www . Jci . Org *116*.

Kaelin, W.G., and Ratcliffe, P.J. (2008). Oxygen Sensing by Metazoans: The Central Role of the HIF Hydroxylase Pathway. Mol. Cell *30*, 393–402.

Kannan, A., Krishnan, A., Ali, M., Subramaniam, S., Halagowder, D., and Sivasithamparam, N.D. (2014). Caveolin-1 promotes gastric cancer progression by up-regulating epithelial to mesenchymal transition by crosstalk of signalling mechanisms under hypoxic condition. Eur. J. Cancer *50*, 204–215.

Karam, J.A., Lotan, Y., Roehrborn, C.G., Ashfaq, R., Karakiewicz, P.I., and Shariat, S.F. (2007). Caveolin-1 overexpression is associated with aggressive prostate cancer recurrence. Prostate *67*, 614–622.

Karpe, F., Fielding, B. a, Ilic, V., Macdonald, I. a, Summers, L.K.M., and Frayn, K.N. Response Is Related to Aspects of Insulin Sensitivity. *2*, 2467–2473.

Kilroy, G., Burk, D.H., and Floyd, Z.E. (2009). High efficiency lipid-based siRNA transfection of adipocytes in suspension. PLoS One *4*, 1–8.

Kim, D.S., Ko, Y.J., Lee, M.W., Park, H.J., Park, Y.J., Kim, D.I., Sung, K.W., Koo, H.H., and Yoo, K.H. (2016). Effect of low oxygen tension on the biological characteristics of human bone marrow mesenchymal stem cells. Cell Stress Chaperones 1–11.

Klein, R. (1995). Hyperglycemia and microvascular and macrovascular disease in diabetes. In Diabetes Care, pp. 258–268.

Koritzinsky, M., Rouschop, K.M.A., van den Beucken, T., Magagnin, M.G., Savelkouls, K., Lambin, P., and Wouters, B.G. (2007). Phosphorylation of eIF2?? is required for mRNA translation inhibition and survival during moderate hypoxia. Radiother. Oncol. *83*, 353–361.

Koumenis, C., Naczki, C., Koritzinsky, M., Rastani, S., Diehl, A., Sonenberg, N., Koromilas, A., and Wouters, B.G. (2002). Regulation of protein synthesis by hypoxia via activation of the endoplasmic reticulum kinase PERK and phosphorylation of the translation initiation factor eIF2alpha. Mol. Cell. Biol. *22*, 7405–7416.

Lee, K., Kang, J.E., Park, S.K., Jin, Y., Chung, K.S., Kim, H.M., Lee, K., Kang, M.R., Lee,

M.K., Song, K. Bin, et al. (2010). LW6, a novel HIF-1 inhibitor, promotes proteasomal degradation of HIF-1α via upregulation of VHL in a colon cancer cell line. Biochem. Pharmacol. *80*, 982–989.

Lee, K.Y., Gesta, S., Boucher, J., Wang, X.L., and Kahn, C.R. (2011). The differential role of Hif1β/Arnt and the hypoxic response in adipose function, fibrosis, and inflammation. Cell Metab. *14*, 491–503.

Leiherer, A., Geiger, K., Muendlein, A., and Drexel, H. (2014). Hypoxia induces a HIF-1?? dependent signaling cascade to make a complex metabolic switch in SGBS-adipocytes. Mol. Cell. Endocrinol. *383*, 21–31.

Lévy, P., Pépin, J.L., Arnaud, C., Tamisier, R., Borel, J.C., Dematteis, M., Godin-Ribuot, D., and Ribuot, C. (2008). Intermittent hypoxia and sleep-disordered breathing: Current concepts and perspectives. Eur. Respir. J. *32*, 1082–1095.

Liu, L., and Pilch, P.F. (2008). A critical role of cavin (polymerase I and transcript release factor) in caveolae formation and organization. J. Biol. Chem. *283*, 4314–4322.

Liu, L., and Pilch, P.F. (2016). PTRF/Cavin-1 promotes efficient ribosomal RNA transcription in response to metabolic challenges. Elife *5*, 1–20.

Liu, L., Brown, D., McKee, M., LeBrasseur, N.K., Yang, D., Albrecht, K.H., Ravid, K., and Pilch, P.F. (2008). Deletion of Cavin/PTRF Causes Global Loss of Caveolae, Dyslipidemia, and Glucose Intolerance. Cell Metab. *8*, 310–317.

Liu, L., Hansen, C.G., Honeyman, B.J., Nichols, B.J., and Pilch, P.F. (2014). Cavin-3 knockout mice show that cavin-3 is not essential for caveolae formation, for maintenance of body composition, or for glucose tolerance. PLoS One *9*, 1–8.

Liu, P., Cheng, H., Roberts, T.M., and Zhao, J.J. (2009). Targeting the phosphoinositide 3-kinase pathway in cancer. Nat. Rev. Drug Discov. *8*, 627–644.

Lolmède, K., Durand de Saint Front, V., Galitzky, J., Lafontan, M., and Bouloumié, a (2003). Effects of hypoxia on the expression of proangiogenic factors in differentiated 3T3-F442A adipocytes. Int. J. Obes. Relat. Metab. Disord. *27*, 1187–1195.

Lopes, H.F., Corrêa-Giannella, M.L., Consolim-Colombo, F.M., and Egan, B.M. (2016).

Visceral adiposity syndrome. Diabetol. Metab. Syndr. *8*, 40.

Losso, J.N., and Bawadi, H.A. (2005). Hypoxia inducible factor pathways as targets for functional foods. J. Agric. Food Chem. *53*, 3751–3768.

Louis, M., and Punjabi, N.M. (2009). Effects of acute intermittent hypoxia on glucose metabolism in awake healthy volunteers. 1538–1544.

Low Wang, C.C., Goalstone, M.L., and Draznin, B. (2004). Impact Cardiovascular Biology. Diabetes *53*, 2735–2740.

Lu, H., Gao, Z., Zhao, Z., Weng, J., and Ye, J. (2016). Transient hypoxia reprograms differentiating adipocytes for enhanced insulin sensitivity and triglyceride accumulation. Int. J. Obes. (Lond). *40*, 121–128.

Mahat, B., Chassé, É., Mauger, J.-F., and Imbeault, P. (2016). Effects of acute hypoxia on human adipose tissue lipoprotein lipase activity and lipolysis. J. Transl. Med. *14*, 212.

Makoveichuk, E., Vorrsjö, E., Olivecrona, T., and Olivecrona, G. (2013). Inactivation of lipoprotein lipase in 3T3-L1 adipocytes by angiopoietin-like protein 4 requires that both proteins have reached the cell surface. Biochem. Biophys. Res. Commun. *441*, 941–946.

Martinez-Outschoorn, U.E., Sotgia, F., and Lisanti, M.P. (2015). Caveolae and signalling in cancer. Nat. Rev. Cancer *15*, 225–237.

Mazzatti, D., Lim, F.-L., O'Hara, A., Wood, I.S., and Trayhurn, P. (2012). A microarray analysis of the hypoxia-induced modulation of gene expression in human adipocytes. Arch. Physiol. Biochem. *118*, 112–120.

McMahon, K.-A., Zajicek, H., Li, W.-P., Peyton, M.J., Minna, J.D., Hernandez, V.J., Luby-Phelps, K., and Anderson, R.G.W. (2009). SRBC/cavin-3 is a caveolin adapter protein that regulates caveolae function. EMBO J. *28*, 1001–1015.

Mekhail, K., Rivero-Lopez, L., Khacho, M., and Lee, S. (2006). Restriction of rRNA synthesis by VHL maintains energy equilibrium under hypoxia. Cell Cycle *5*, 2401–2413.

Meshulam, T., Breen, M.R., Liu, L., Parton, R.G., and Pilch, P.F. (2011).

Caveolins/caveolae protect adipocytes from fatty acid-mediated lipotoxicity. J. Lipid Res. *52*, 1526–1532.

Mlinar, B., Marc, J., Jane??, A., and Pfeifer, M. (2007). Molecular mechanisms of insulin resistance and associated diseases. Clin. Chim. Acta *375*, 20–35.

Monier, S., Dietzen, D.J., Hastings, W.R., Lublin, D.M., and Kurzchalia, T. V. (1996). Oligomerization of VIP21-caveolin in vitro is stabilized by long chain fatty acylation or cholesterol. FEBS Lett. *388*, 143–149.

Murata, M., Peranen, J., Schreiner, R., Wieland, F., Kurzchalia, T. V, and Simons, K. (1995). VIP21/caveolin is a cholesterol-binding protein. Proc. Natl. Acad. Sci. U. S. A. *92*, 10339–10343.

Ntambi, M.J., and Kim, Y.-C. (2000). Symposium: Adipocyte Function, Differentiation and Metabolism Regulation of Leptin Production in Humans. J. Nutr *130*, 3127–3131.

Nystrom, F.H., Chen, H., Cong, L.N., Li, Y., and Quon, M.J. (1999). Caveolin-1 interacts with the insulin receptor and can differentially modulate insulin signaling in transfected Cos-7 cells and rat adipose cells. Mol. Endocrinol. *13*, 2013–2024.

O'Rourke, R.W., Meyer, K.A., Gaston, G., White, A.E., Lumeng, C.N., and Marks, D.L. (2013). Hexosamine Biosynthesis Is a Possible Mechanism Underlying Hypoxia's Effects on Lipid Metabolism in Human Adipocytes. PLoS One *8*.

Ohga, E., Tomita, T., Wada, H., Yamamoto, H., Nagase, T., and Ouchi, Y. (2003). Effects of obstructive sleep apnea on circulating ICAM-1, IL-8, and MCP-1. J. Appl. Physiol. *94*, 179–184.

De Oliveira, E.M., Sandri, S., Knebel, F.H., Contesini, C.G.I., Campa, A., and Filippin-Monteiro, F.B. (2013). Hypoxia increases serum amyloid A3 (SAA3) in differentiated 3T3-L1 adipocytes. Inflammation *36*, 1107–1110.

Ortiz-Barahona, A., Villar, D., Pescador, N., Amigo, J., and del Peso, L. (2010). Genome-wide identification of hypoxia-inducible factor binding sites and target genes by a probabilistic model integrating transcription-profiling data and in silico binding site prediction. Nucleic Acids Res. *38*, 2332–2345.

Oshikawa, J., Otsu, K., Toya, Y., Tsunematsu, T., Hankins, R., Kawabe, J., Minamisawa, S., Umemura, S., Hagiwara, Y., and Ishikawa, Y. (2004). Insulin resistance in skeletal muscles of caveolin-3-null mice. Proc. Natl. Acad. Sci. U. S. A. *101*, 12670–12675.

Otsu, K., Toya, Y., Oshikawa, J., Kurotani, R., Yazawa, T., Sato, M., Yokoyama, U., Umemura, S., Minamisawa, S., Okumura, S., et al. (2010). Caveolin gene transfer improves glucose metabolism in diabetic mice. 450–456.

Palacios-Ortega, S., Varela-Guruceaga, M., Milagro, F.I.F.I., Mart??nez, J.A., De Miguel, C., Martínez, J.A., and De Miguel, C. (2014). Expression of caveolin 1 is enhanced by DNA demethylation during adipocyte differentiation. Status of insulin signaling. PLoS One *9*.

Palacios-Ortega, S., Varela-Guruceaga, M., Algarabel, M., Milagro, F.I.F.I., Martínez, J.A., De Miguel, C., Mart�nez, J.A., and De Miguel, C. (2015). Effect of TNF-Alpha on Caveolin-1 Expression and Insulin Signaling during Adipocyte Differentiation and in Mature Adipocytes. Cell. Physiol. Biochem. *36*, 1499–1516.

Parpal, S., Karlsson, M., Thorn, H., and Strålfors, P. (2001). Cholesterol Depletion Disrupts Caveolae and Insulin Receptor Signaling for Metabolic Control via Insulin Receptor Substrate-1, but Not for Mitogen-activated Protein Kinase Control. J. Biol. Chem. *276*, 9670–9678.

Parton, R.G., and del Pozo, M. a (2013). Caveolae as plasma membrane sensors, protectors and organizers. Nat. Rev. Mol. Cell Biol. *14*, 98–112.

Parton, R.G., and Simons, K. (2007). The multiple faces of caveolae. Nat. Rev. Mol. Cell Biol. *8*, 185–194.

Perl, A. (2015). MTOR activation is a biomarker and a central pathway to autoimmune disorders, cancer, obesity, and aging. Ann. N. Y. Acad. Sci. *1346*, 33–44.

Polotsky, V.Y., Li, J., Punjabi, N.M., Rubin, A.E., Smith, P.L., Schwartz, A.R., and O'Donnell, C.P. (2003). Intermittent hypoxia increases insulin resistance in genetically obese mice. J. Physiol. *552*, 253–264.

Poulain, L., Richard, V., Lévy, P., Dematteis, M., and Arnaud, C. (2015). Toll-like

receptor-4 mediated inflammation is involved in the cardiometabolic alterations induced by intermittent hypoxia. Mediators Inflamm. *2015*.

Qatanani, M., and Lazar, M.A. (2007). Mechanisms of obesity-associated insulin resistance: Many choices on the menu. Genes Dev. *21*, 1443–1455.

Rausch, M.E., Weisberg, S., Vardhana, P., and Tortoriello, D. V. (2008). Obesity in C57BL/6J mice is characterized by adipose tissue hypoxia and cytotoxic T-cell infiltration. Int. J. Obes. *32*, 451–463.

Razani, B., Engelman, J.A., Wang, X.B., Schubert, W., Zhang, X.L., Marks, C.B., Macaluso, F., Russell, R.G., Li, M., Pestell, R.G., et al. (2001). Caveolin-1 null mice are viable, but show evidence of hyper- proliferative and vascular abnormalities. J Biol Chem *16*, 16.

Razani, B., Combs, T.P., Wang, X.B., Frank, P.G., Park, D.S., Russell, R.G., Li, M., Tang, B., Jelicks, L.A., Scherer, P.E., et al. (2002). Caveolin-1-deficient mice are lean, resistant to diet-induced obesity, and show hypertriglyceridemia with adipocyte abnormalities. J. Biol. Chem. *277*, 8635–8647.

Regazzetti, C., Peraldi, P., Gre, T., Najem-lendom, R., Ben-sahra, I., Cormont, M., and Marchand-brustel, Y. Le (2009). Hypoxia Decreases Insulin Signaling Pathways in. Diabetes *58*, 95–103.

Regazzetti, C., Dumas, K., Lacas-Gervais, S., Pastor, F., Peraldi, P., Bonnafous, S.S.S., Dugail, I., Le Lay, S., Valet, P., Le Marchand-Brustel, Y., et al. (2015). Hypoxia inhibits cavin-1 and cavin-2 expression and down-regulates caveolae in adipocytes. Endocrinology *156*, 789–801.

Rochford, J.J. (2014). Mouse models of lipodystrophy and their significance in understanding fat regulation (Elsevier Inc.).

Romero-Ramirez, L., Cao, H., Nelson, D., Hammond, E., Lee, A.H., Yoshida, H., Mori, K., Glimcher, L.H., Denko, N.C., Giaccia, A.J., et al. (2004). XBP1 is essential for survival under hypoxic conditions and is required for tumor growth. Cancer Res. *64*, 5943–5947.

Rose, D.R., and Clemmons, D.R. (2002). Growth hormone receptor antagonist improves insulin resistance in acromegaly. Growth Horm. IGF Res. *12*, 418–424.

Ruiz de Galarreta, M., Navarro, A., Ansorena, E., Garcia Garzón, A., Mòdol, T., López-Zabalza, M.J., Martínez-Irujo, J.J., and Iraburu, M.J. (2016). Unfolded protein response induced by Brefeldin A increases collagen type I levels in hepatic stellate cells through an IRE1α, p38 MAPK and Smad-dependent pathway. Biochim. Biophys. Acta - Mol. Cell Res. *1863*, 2115–2123.

Sakagami, H., Makino, Y., Mizumoto, K., Isoe, T., Takeda, Y., Watanabe, J., Fujita, Y., Takiyama, Y., Abiko, A., and Haneda, M. (2014). Loss of HIF-1α impairs GLUT4 translocation and glucose uptake by the skeletal muscle cells. Am. J. Physiol. Endocrinol. Metab. *306*, E1065-76.

Sakharova, A.A., Horowitz, J.F., Surya, S., Goldenberg, N., Harber, M.P., Symons, K., and Barkan, A. (2008). Role of growth hormone in regulating lipolysis, proteolysis, and hepatic glucose production during fasting. J. Clin. Endocrinol. Metab. *93*, 2755–2759.

Samuvel, D.J., Sundararaj, K.P., Nareika, A., Lopes-Virella, M.F., and Huang, Y. (2009). Lactate boosts TLR4 signaling and NF-kappaB pathway-mediated gene transcription in macrophages via monocarboxylate transporters and MD-2 up-regulation. J. Immunol. (Baltimore, Md. 1950) *182*, 2476–2484.

Sano, H. (2003). Insulin-stimulated Phosphorylation of a Rab GTPase-activating Protein Regulates GLUT4 Translocation. J. Biol. Chem. *278*, 14599–14602.

Scherer, P.E., Lisanti, M.P., Baldini, G., Sargiacomo, M., Mastick, C.C., and Lodish, H.F. (1994). Induction of caveolin during adipogenesis and association of GLUT4 with caveolin-rich vesicles. J. Cell Biol. *127*, 1233–1243.

Schrauwen, I., Szelinger, S., Siniard, A.L., Kurdoglu, A., Corneveaux, J.J., Malenica, I., Richholt, R., Van Camp, G., De Both, M., Swaminathan, S., et al. (2015). A frame-shift mutation in CAV1 is associated with a severe neonatal progeroid and lipodystrophy syndrome. PLoS One *10*, 1–13.

Schulz, R., Mahmoudi, S., Hattar, K., Sibelius, U.L.F., Olschewski, H., Mayer, K., Seeger, W., and Grimminger, F. (2000). Enhanced release of superoxide from

polymorphonuclear neutrophils in obstructive sleep apnea. Am J Resp Crit Care Med *162*, 566–570.

Schwencke, C., Braun-Dullaeus, R.C., Wunderlich, C., and Strasser, R.H. (2006). Caveolae and caveolin in transmembrane signaling: Implications for human disease. Cardiovasc. Res. *70*, 42–49.

Sekimoto, J., Kabayama, K., Gohara, K., and Inokuchi, J.I. (2012). Dissociation of the insulin receptor from caveolae during TNF??-induced insulin resistance and its recovery by d-PDMP. FEBS Lett. *586*, 191–195.

Sellayah, D., Cagampang, F.R., and Cox, R.D. (2014). On the evolutionary origins of obesity: A new hypothesis. Endocrinology *155*, 1573–1588.

Semenza, G.L. (2001). Hypoxia-inducible factor 1: control of oxygen homeostasis in health and disease. Pediatr.Res. *49*, 614–617.

Senju, Y., and Suetsugu, S. (2016). Possible regulation of caveolar endocytosis and flattening by phosphorylation of F-BAR domain protein PACSIN2/Syndapin II. Bioarchitecture *992*, 00–00.

Sesti, G. (2006). Pathophysiology of insulin resistance. Best Pract. Res. Clin. Endocrinol. Metab. *20*, 665–679.

Shen, J., Lee, W., Li, Y., Lau, C.F., Ng, K.M., Fung, M.L., and Liu, K.J. (2008). Interaction of caveolin-1, nitric oxide, and nitric oxide synthases in hypoxic human SK-N-MC neuroblastoma cells. J. Neurochem. *107*, 478–487.

Shi, J., and Kandror, K. V. (2005). Sortilin is essential and sufficient for the formation of glut4 storage vesicles in 3T3-L1 adipocytes. Dev. Cell *9*, 99–108.

Simard, J.R., Meshulam, T., and Pillai, B.K. (2010). Caveolins sequester FA on the cytoplasmic leaflet of the plasma membrane, augment triglyceride formation, and protect cells from lipotoxicity. J. Lipid Res. *51*, 914–922.

Sinha, B., Köster, D., Ruez, R., Gonnord, P., Bastiani, M., Abankwa, D., Stan, R. V., Butler-Browne, G., Vedie, B., Johannes, L., et al. (2011). Cells respond to mechanical stress by rapid disassembly of caveolae. Cell *144*, 402–413.

Smyth, G.K. (2004). Linear models and empirical bayes methods for assessing differential expression in microarray experiments. Stat. Appl. Genet. Mol. Biol. *3*, Article3.

Speakman, J.R. (2013). Evolutionary perspectives on the obesity epidemic: adaptive, maladaptive, and neutral viewpoints. Annu. Rev. Nutr. *33*, 289–317.

Talukder, M.A.H., Preda, M., Ryzhova, L., Prudovsky, I., and Pinz, I.M. (2016). Heterozygous caveolin-3 mice show increased susceptibility to palmitate-induced insulin resistance. Physiol. Rep. *4*, e12736.

Tan, S.-X., Ng, Y., Burchfield, J.G., Ramm, G., Lambright, D.G., Stöckli, J., and James, D.E. (2012). The Rab GTPase-activating protein TBC1D4/AS160 contains an atypical phosphotyrosine-binding domain that interacts with plasma membrane phospholipids to facilitate GLUT4 trafficking in adipocytes. Mol. Cell. Biol. *32*, 4946–4959.

Taylor, C.T. (2008). Mitochondria and cellular oxygen sensing in the HIF pathway. Biochem. J. *409*, 19–26.

Trayhurn, P. (2014). Hypoxia and Adipocyte Physiology : Implications for Adipose Tissue Dysfunction in Obesity.

Trayhurn, P., and Wood, I.S. (2004). Adipokines: inflammation and the pleiotropic role of white adipose tissue. Br. J. Nutr. *92*, 347–355.

Vlaminck, B., Toffoli, S., Ghislain, B., Demazy, C., Raes, M., and Michiels, C. (2007). Dual effect of echinomycin on hypoxia-inducible factor-1 activity under normoxic and hypoxic conditions. FEBS J. *274*, 5533–5542.

Walser, P.J., Ariotti, N., Howes, M., Ferguson, C., Webb, R., Schwudke, D., Leneva, N., Cho, K.J., Cooper, L., Rae, J., et al. (2012). Constitutive formation of caveolae in a bacterium. Cell *150*, 752–763.

Wang, B., Wood, I.S., and Trayhurn, P. (2007). Dysregulation of the expression and secretion of inflammation-related adipokines by hypoxia in human adipocytes. Pflugers Arch. Eur. J. Physiol. *455*, 479–492.

Wang, Y., Roche, O., Xu, C., Moriyama, E.H., Heir, P., Chung, J., Roos, F.C., Chen, Y.,

Finak, G., Milosevic, M., et al. (2012). Hypoxia promotes ligand-independent EGF receptor signaling via hypoxia-inducible factor-mediated upregulation of caveolin-1. Proc. Natl. Acad. Sci. U. S. A. *109*, 4892–4897.

Weiszenstein, M., Musutova, M., Plihalova, A., Westlake, K., Elkalaf, M., Koc, M., Prochazka, A., Pala, J., Gulati, S., Trnka, J., et al. (2016). Biochemical and Biophysical Research Communications Adipogenesis , lipogenesis and lipolysis is stimulated by mild but not severe hypoxia in 3T3-L1 cells. Biochem. Biophys. Res. Commun. *478*, 727–732.

Wells, J.C.K. (2012). The evolution of human adiposity and obesity: where did it all go wrong? Dis. Model. Mech. *5*, 595–607.

Wiechen, K., Diatchenko, L., Agoulnik, A., Scharff, K.M., Schober, H., Arlt, K., Zhumabayeva, B., Siebert, P.D., Dietel, M., Schäfer, R., et al. (2001). Caveolin-1 is down-regulated in human ovarian carcinoma and acts as a candidate tumor suppressor gene. Am. J. Pathol. *159*, 1635–1643.

Wilcox, G. (2005). Insulin and insulin resistance. Clin. Biochem. Rev. *26*, 19–39.

Williams, E.P., Mesidor, M., Winters, K., Dubbert, P.M., and Wyatt, S.B. (2015). Overweight and Obesity: Prevalence, Consequences, and Causes of a Growing Public Health Problem. Curr. Obes. Rep. *4*, 363–370.

Wood, I.S., Wang, B., Lorente-Cebrián, S., and Trayhurn, P. (2007). Hypoxia increases expression of selective facilitative glucose transporters (GLUT) and 2-deoxy-d-glucose uptake in human adipocytes. Biochem. Biophys. Res. Commun. *361*, 468–473.

Wood, I.S., de Heredia, F.P., Wang, B., and Trayhurn, P. (2009). Cellular hypoxia and adipose tissue dysfunction in obesity. Proc. Nutr. Soc. *68*, 370–377.

Wouters, B.G., and Koritzinsky, M. (2008). Hypoxia signalling through mTOR and the unfolded protein response in cancer. Nat. Rev. Cancer *8*, 851–864.

Wu, Z., Xie, Y., Bucher, N.L., and Farmer, S.R. (1995). Conditional ectopic expression of C/EBP beta in NIH-3T3 cells induces PPAR gamma and stimulates adipogenesis. Genes Dev. *9*, 2350–2363.

Wyatt, S.B., Winters, K.P., and Dubbert, P.M. (2006). Overweight and obesity:

prevalence, consequences, and causes of a growing public health problem. Am. J. Med. Sci. *331*, 166–174.

Xu, Y., Henning, R.H., van der Want, J.J.L., van Buiten, A., van Gilst, W.H., and Buikema, H. (2007). Disruption of endothelial caveolae is associated with impairment of both NO- as well as EDHF in acetylcholine-induced relaxation depending on their relative contribution in different vascular beds. Life Sci. *80*, 1678–1685.

Yamamoto, M., Toya, Y., Lisanti, M.P., Martin, G., Ishikawa, Y., Schwencke, C., and Myers, M.G. (1998). CELL BIOLOGY AND METABOLISM : Caveolin Is an Activator of Insulin Receptor Signaling Caveolin Is an Activator of Insulin Receptor Signaling *. J. Biol. Chem. *273*, 26962–26968.

Ye, J. (2009). Emerging role of adipose tissue hypoxia in obesity and insulin resistance. Int. J. Obes. *33*, 54–66.

Ye, J., Gao, Z., Yin, J., and He, Q. (2007). Hypoxia is a potential risk factor for chronic inflammation and adiponectin reduction in adipose tissue of ob/ob and dietary obese mice. Am. J. Physiol. Endocrinol. Metab. *293*, E1118–E1128.

Yin, J., Gao, Z., He, Q., Zhou, D., Guo, Z., and Ye, J. (2009). Role of hypoxia in obesity-induced disorders of glucose and lipid metabolism in adipose tissue. Am J Physiol Endocrinol Metab *296*, E333-342.

Yu, J., Bergaya, S., Murata, T., Alp, I.F., Bauer, M.P., Lin, M.I., Drab, M., Kurzchalia, T. V., Stan, R. V., and Sessa, W.C. (2006). Direct evidence for the role of caveolin-1 and caveolae in mechanotransduction and remodeling of blood vessels. J. Clin. Invest. *116*, 1284–1291.

Yu, J., Li, J., Zhang, S., Xu, X., Zheng, M., Jiang, G., and Li, F. (2012). IGF-1 induces hypoxia-inducible factor 1??-mediated GLUT3 expression through PI3K/Akt/mTOR dependent pathways in PC12 cells. Brain Res. *1430*, 18–24.

Yun, Z., Maecker, H.L., Johnson, R.S., and Giaccia, A.J. (2002). Inhibition of PPAR □ 2 Gene Expression by the HIF-1-Regulated Gene DEC1 / Stra13 : A Mechanism for Regulation of Adipogenesis by Hypoxia. *2*, 331–341.

Di Zazzo, E., Feola, A., Zuchegna, C., Romano, A., Donini, C.F., Bartollino, S., Costagliola, C., Frunzio, R., Laccetti, P., Di Domenico, M., et al. (2014). The p85 Regulatory Subunit of PI3K Mediates cAMP-PKA and Insulin Biological Effects on MCF-7 Cell Growth and Motility. Sci. World J. *2014*, 1–11.

Zepeda, A.B., Pessoa, A., Castillo, R.L., Figueroa, C.A., Pulgar, V.M., and Far??as, J.G. (2013). Cellular and molecular mechanisms in the hypoxic tissue: Role of HIF-1 and ROS. Cell Biochem. Funct. *31*, 451–459.

Zhang, H., Gao, P., Fukuda, R., Kumar, G., Krishnamachary, B., Zeller, K.I., Dang, C., and Semenza, G.L. (2007). HIF-1 Inhibits Mitochondrial Biogenesis and Cellular Respiration in VHL-Deficient Renal Cell Carcinoma by Repression of C-MYC Activity. Cancer Cell *11*, 407–420.

Zou, M.H., Hou, X.Y., Shi, C.M., Nagata, D., Walsh, K., and Cohen, R.A. (2002). Modulation by peroxynitrite of Akt- and AMP-activated kinase-dependent Ser1179 phosphorylation of endothelial nitric oxide synthase. J. Biol. Chem. *277*, 32552–32557.